LAND DEGRADATION DETECTION, MAPPING and MONITORING in the LAKE NAIVASHA BASIN, KENYA

Torrion, Jessica A.
February, 2002

Land Degradation Detection, Mapping and Monitoring in the Lake Naivasha Basin, Kenya

by

Torrion, Jessica A

Thesis submitted to the International Institute for Geoinformation Science and Earth Observation in partial fulfillment of the requirements for the degree of Master of Science in Natural Resource Management

Degree Assessment Board

Assoc.Prof. Dr. D.G. Rossiter (ITC)	(Chairman)
Prof. Dr. A. K. Breght (WAU)	(External Examiner)
Dr. D. P. Shrestha (ITC)	(Main Supervisor)
Mr. G. Huurneman (ITC)	(Internal Examiner)
Dr. A. Farshad (ITC)	(Specialization Advisor)

INTERNATIONAL INSTITUTE FOR GEO-INFORMATION SCIENCE AND EARTH OBERVATION
ENSCHEDE, THE NETHERLANDS

Disclaimer

This document describes work undertaken as part of a programme of study at the International Institute for Geo-information Science and Earth Observation. All views and opinions expressed therein remain the sole responsibility of the author, and do not necessarily represent those of the institute.

ABSTRACT

The study was conducted to map and monitor land degradation using multi- source and multi-temporal data. Arithmetic and color related image fusion techniques were employed to extract the complimentary information from Landsat TM, ASTER and ERS-2 SAR data. Digital elevation model (DEM) was also considered an added feature dimension to classifier. Gullies in association with abrasion/deposition areas were detected by Landsat TM at 51% and ASTER at 56% accuracies respectively as compared to the small format aerial photography (SFAP) with 5 meters spatial resolution. Fusion of ERS-2 SAR did not improve detection of gullies but rather helped mapping areas prone to land degradation. Fusion of ERS-2 SAR and thermal band (TM6) to the first 3 principal components improved the separability of the different degradation classes. With the PC1, 2, and 3, the classification accuracy is 0.48 khat. Same performance observed with fusion of SAR data. Fusion of thermal band together with SAR data to Landsat TM improved the accuracy to 0.53 khat. Inclusion of DEM with the remote sensing data as an added feature dimension improved the accuracy to 0.64 khat. Post classification smoothing includes masking by using conditional statements and running majority filter. This improves the over-all accuracy to 0.73 khat. The step faulted plateau is assessed as prone to water erosion. Gullying is associated with the volcanic plain and sheetwash in lacustrine plain.

ACKNOWLEDGEMENT

I would like to express my appreciation to a number of people who contributed in one way or another to my ITC life and in the realization of this output.

To D. Shrestha for his patience and valuable advise.
To R. Hennemann for the fieldwork support and advise.
To W. Siderius, for helping me to carry out photo interpretation.
To D. Rossiter, his own way of dealing technical problems is awesome. Thanks for the support and constructive criticisms.

The support we obtained from B. Krol and A. Farshad is great, thanks for being supportive to our needs. Thanks also to T. Hengl for the materials and techniques shared. M. Weir has also been friendly to us, the materials, technical knowledge shared and for being our postmaster. Sir, thanks.

I will never forget Sheps and Somia, SISLM colleagues known to have very fuzzy boundary on our professional and personal lives. We made extremely nice friendship.

To Ellen, Fe, Rosal, Daisy, Mike, Jerry, Vic, John, Bing, Stella, Leo, Gingging, Ana and among others too many to mention for making Enschede a home.

Special thanks goes to few friends for their help. V. Cuadrado, for all his help. Jose Miguel for being so kind. Thanks for being a friend. NRM friends and Scatman buddies are unforgettable. Gorgeous Monjia, Maura and Katrin…. I count on your friendship. To some party potatoes in ITC (Rolf, Elena B, Martin, and others), thanks for an added rhythm to my steps.

To my wonderful beautiful buddies and friends back to the Philippines; Fro, Kat, Fro, Cris, Ja and Pet, texts and emails have made me smile. Special mention goes to sister Jovette, you are a wonderful friend.

To BSWM and Dr. Concepcion for the trust.

To the Dutch government for the scholarship granted.

To my God.

Dedicated to Nanay and late Tatay

My brothers, sisters and nieces

Table of Contents

List of Tables

List of Figures

Chapter 1

Introduction

Land degradation causes decline in productive capacity of the land. This in fact is the main reason for the dramatic decrease of prime lands where only 3% of the global surface is left prime or class I (Eswaran et al., 2001). Land degradation, causing the loss of productivity potential, receives a wide area of concern globally due to its significant negative impacts on production. Barrow (1994) affirmed land degradation causing productivity decline at an alarming rate. To mention a few, soil erosion caused yield reduction in Africa of about 2-40%, estimates of cereal loss in Asia as high as 7,200 million US Dollars (USD), as high as 44 billion USD $year^{-1}$ in USA and 400 billion USD $year^{-1}$ or 70 USD $person^{-1}$ $year^{-1}$ at a global scale (Lal, 1998a).

At the second International Conference on Land Degradation in Thailand, Eswaran et al. (2001) recommended 3 steps to address the issues and problems in land degradation; 1) assessment, 2) monitoring and 3) application of mitigating measures and/or technologies. The first 2 steps are pre-requisites to decide on the appropriate mitigating measures as a final step to combat the worsening degradation problems. Information on the extent, severity and location of degradation problems essentially will give paramount attention to planners and stakeholders in planning and implementing mitigation measures (Stewart, 1985; Barrow, 1994; Lal and Sujatha et al., 2000) and gain a collective effort in determining appropriate measures and land use strategies (Eswaran et al., 2001).

Remote sensing has long been recommended for its potential to detect, map and monitor degradation problems (Hellden and Stern, 1980; Sabins, 1987; Pickup, 1989; Frederiksen, 1993; Mohammed, 1993; Raina et al., 1993; Tripathy et al., 1996; Sujatha et al., 2000) including their spread and effects with time (Sommer et al., 1998). Use of remotely sensed imagery evolved on the basis that traditional survey became expensive and time-consuming. It is especially useful in areas that are not accessible.

Some attempts have been made to know if the degraded areas vary in space and time. The Global Assessment of Soil Degradation (GLASOD, 1988) and eventually regional, the Assessment of Soil Degradation in South East Asia, ASSOD (Lynden and Oldeman, 1997) have clear limitations in terms of scale relative to their use towards national and local level of planning. GLASOD in particular, is the product of different survey method/standards and expert judgments (Eswaran et al., 2001).

Land degradation features may not be well detected in a single sensor data. One sensor may provide high spectral resolution data with low spatial details. This does not allow the detection of some degraded features such as rills and gullies. In the other way around, some sensors having high spatial resolution data may have low spectral resolutions. In most cases, land degradation studies were carried out from the visible and thermal regions of the spectrum. Few studies include the microwave region of the spectrum. Microwave data being taken in an active sensor provides data in all weather conditions, a vital consideration to areas with frequent cloud cover. In addition, the backscattering signal of the radar is related to the surface roughness and moisture condition of the soil which helps discriminating land degradation classes. Fusion of data from the visible, thermal and the microwave regions of the spectrum will give complimentary information due to their differences in wavelength and physical characteristics (Pohl and Van Genderen, 1995).

Kenya like many African countries suffers from rural development problems such as land degradation accelerated by human activities. Example is soil erosion caused by overgrazing, over-cultivation, inappropriate farming practices, fuelwood demand, etc. Salinity and alkalinity are also considered land degradation problem. Only 20% of Kenya's land surface is arable which has the highest population density providing more than 70% of the Kenyan population-now standing between 25-30 million people (Omosa, 1999). Vital information such as spatial and temporal data on land degradation indeed becomes imperative. The challenge herein is on how these degradation features be mapped and visualize.

This study attempts at detecting study attempts at detecting and mapping soil degradation in the Lake Naivasha Basin by multi-source image fusion technique. In addition, the technique is also applied to monitor land degradation. Moreover, this study tests the adequacy of GLASOD legend framework to map soil degradation.

1.1. Research Questions

The study aims to answer the following research questions:

1. Which of the physical soil degradation types can be primarily identified by remote sensing techniques?
2. At what mapping scale can the different physical soil degradation types be best represented?
3. Which image fusion techniques are suitable to detect physical soil degradation types?
4. What is the trend of soil physical degradation in the area over time?
5. Are these land degradation types associated with soil landscape units?
6. Is the GLASOD legend framework sufficient to describe and classify such degradation types?

1.2. Objectives

The study aims to detect land degradation features with emphasis on soil physical degradation. Specifically it aims:

1. to determine the best image fusion technique to detect and map spatial distribution of physical soil degradation in the study area;
7. to relate land degradation to soil landscape units of the area
8. to determine the adequacy of GLASOD legend framework in the assessment and mapping on the degree of degradation; and
9. to detect changes on the spatial distribution and degree of soil degradation over time.

1.3. Hypotheses

The following hypothesis were drawn:

1. Some soil erosion features can be directly detected while other forms of land degradation are indirectly detectable by remote sensing techniques.
10. The mapping scale of the land degradation types identified vary depending on the mappability of degradation units.
11. Visual interpretation of multi-source and multi-temporal fusion of remotely sensed imagery is more applicable than automated classification.
12. The trend of change of soil degradation can be detected through a multi-temporal image fusion.
13. The GLASOD legend framework provides the mechanism to describe and classify land degradation at a large scale

Chapter 2

Literature Review

2.1. Some Perceptions of Land Degradation

Land degradation is a process which implies a reduction of potential productivity of the land (Hill et al., 1995b). Barrow (1994) pointed out land degradation as a reduction in rank or status of the land. Blaikie and Brookfield (1987) affirmed that land is degraded when it suffers from the loss of its intrinsic qualities and capabilities. Land degradation is also considered to be a collective degradation of different components of the land such as water, biotic and soil resources (Hennemann, 2001a). He further stressed out that the worsening biotic and water decline essentially will lead to a desertification process in susceptible climate zones. In a broader sense, Conacher and Sala (1998) cited land degradation as an "alteration to all aspects of the natural (or biophysical) environment by human actions to the detriment of vegetation, soils, landform, water (surface and sub-surface) and ecosystems".

Land degradation is closely associated with soil degradation. The loss of vegetation enhances soil erosion and reduces the productive value of the land (Hill et al., 1995a). In turn, soil degradation reduces biodiversity (Blum, 1998) and natural vegetation (De Jong, 1994). Lal and Stewart (1985) stressed that soil degradation undermines the productive capacity of the ecosystem resulting in alteration of water and energy balance.

Soil degradation is defined as a process that describes human-induced phenomenon which lowers the current and/or future capacity of the soil to support human life (GLASOD, 1988). This is in consonance with the definition made by Lal and Stewart (1985) as the decline in soil quality caused through its misuse by humans. They grouped soil degradation into 3 categories: 1) physical degradation, 2) biological degradation, and 3) chemical degradation. Besides vegetation degradation, soil degradation comprises the most degradation processes which are water erosion, wind erosion, salinization, soil fertility loss, soil compaction and crusting (Dregne, 1998).

2.2. Importance on the Availability of Land Degradation Information

Knowledge on the spatial distribution of land degradation is as relevant as knowing the availability of a resource base. Sujatha et al. (2000) claimed that the information on the nature, extent, severity and geographic distribution of degraded lands is of paramount importance for planning reclamation strategies and setting up preventive measures for sustainable agriculture

development. As such, they become a significant basis for planners in drafting and implementing development plans for sustainable use of land resources (Hill et al., 1995a) as well as for resource restoration and quality enhancement (Lal, 1998b). Particularly, reliable information on the nature, extent and magnitude of soil erosion is required in planning and implementation of soil conservation and management programs (Dwivedi et al., 1997a).

A satisfactory information on degradation changes provides satisfactory strategies for the prevention and mitigation of land degradation (Barrow, 1994). Degradation changes being monitored give a considerable attention to the planners. According to Eswaran et al. (2001) information which gives a warning indicator to degradation problems can gain a collective effort to determine mitigation measures.

2.3. Conventional Land Degradation Mapping and Monitoring Techniques

Hoosbeek et al. (1997) grouped methods of mapping land degradation into 2 broad categories. One of which is the Qualitative Extrapolation Model which includes delineation of degraded soils using topographic maps, remotely sensed imagery and selection of soil mapping unit. In this category, the Soil Survey Manual (USDA, 1993) and GLASOD framework (Oldeman et al. 1991) are recommended in describing and classifying soil degradation. The other method focused on the application of geostatistics.

The most accurate method for detection of land degradation is the direct measurement and observation at individual sites. This demands many observations as the area of mapping coverage becomes large. Consequently, stratification is done and examination of representative sites are employed which lead to subjective and non-rigorous selection (Pickup, 1989). In most cases, such a technique fail to produce detailed mapping outputs due to budget constraints, inaccessible areas, insufficient standardization and repeatability (Hill et al., 1995a). Impracticalities of the conventional survey mentioned by Sujatha et al. (2000) are reasonably due to rugged areas and inaccessible terrain.

With such a constraint, remote sensing becomes an alternative to map land degradation (King and Delpont, 1993; De Jong, 1994). Pickup (1989) stressed the importance of the spectral-temporal model of analysis in assessing land degradation. It is because of the differences of soil and vegetation reflectance at the different wavelengths and the temporal components giving a trend idea on the pattern at which land degradation occurs. Hill et al. (1995b) pointed out the importance of monitoring soil conditions including vegetation regime and recovery over time in understanding the process of land degradation from their spatial context. They claimed that the incorporation of terrain parameters improved the classification not only for the current degradation but also for erosion risk analysis. Temporal variation of eroded lands was investigated by Dwivedi et al. (1997b) using Landsat MSS and Landsat TM and reported the increase in land degradation units both in spatial context and severity.

2.4. Mapping Scale

The scale of the available information has been an important issue to regional and national land management planning strategy. Hoosbeek et al. (1997) stated that the scale at which the degradation needs to be assessed depends on the need of the problem and the purpose of assessment. Hill et al. (1995a) cited an example on the available information in Europe at 1:1,000,000 which does not allow an information on a level of spatial detail that is adequate for regional land management. Much of the generalized views, subjectivity and broad analysis are commented to the "World Map of the Human-induced Soil Degradation (GLASOD, 1988)" (Eswaran et al., 2001). For soil erosion in particular, the recommended working scales are 1:10,000 and 1:25,000 considering rills and gullies as parameters used in calculating soil losses (King and Delpont, 1993).

2.5. RS techniques to Land Degradation Detection and Monitoring

Remote sensing provides a convenient source of information but the data collected by these instruments do not directly correspond to the information we need (Hill et al., 1995b). They emphasized that changes in albedo and/or reflectance do not necessarily mean changes or worsening of degradation problems. This could be attributed to other changes in land surface characteristics such as clearing of woodlands, maturing cereals and dry vegetations. In a temporal aspect of analysis, Hill et al. (1995a) stressed that change detection should also be given extra care due to the radiometric effects that would mislead the analysis at different times of acquisition such as state of the atmosphere, illumination and drifts in sensor calibration. Singh (1989) considers soil moisture as an important factor affecting land degradation change detection analysis and thus proposes to be taken into account.

Remote Sensing has high potential for land degradation data collection due to large area coverage, regular time interval, spatial and spectral resolution and which facilitates detection of degraded areas (De Jong, 1994). For degradation mapping, features whether they are directly or indirectly visible on the ground should be considered. For this reason, signs of degradation features should be well considered (Metternicht and Zinck, 1997). Degradation features that must be checked in the field include 1) signs of degradation on bare ground, 2) signs of degradation provided by vegetation and land use, and 3) signs of degradation provided by the terrain morphology (King and Delpont, 1993).

Singh (1989) arrived at two basic approaches dealing with change detection; 1) the comparative analysis of independently produced classification for different dates, and 2) the simultaneous analysis of multi-temporal data. Different change detection techniques include univariate image differencing, vegetation index differencing, image regression, image ratioing, principal component analysis, post classification comparison, direct multi-date comparison, change vector analysis and background substraction. Various researchers use multi-sensor data in monitoring salt affected soils, water-logged and eroded soils, and desertification (Tripathy et al., 1996; Dwivedi et al., 1997b; Sujatha et al., 2000). Though researchers devised best techniques to serve their purpose,

these techniques seem to yield different levels of results for different environmental features and applications (Pohl and Van Genderen, 1998).

2.6. Image fusion for land degradation detection

Image fusion is defined as processing of time-series data acquired by the same sensor or different sensor (Wald, 1999). In a broader sense, image fusion is defined as combination and integration of multi source data using an algorithm with proper alignment into common coordinates. Image fusion can also be considered as the combination of two or more different images to form a new image by using certain algorithm(Van Genderen and Pohl, 1994). Pohl and Van Genderen (1998) summarized the advantages of image fusion such as image sharpening, improvement of registration accuracy, creation of stereo data sets, feature enhancement, improved classification, temporal aspect for change detection, and overcoming data gaps due to clouds. Fusion of images from different sources thus improves and yields more information than a single sensor data can provide (Mitiche and Aggarwal, 1986). Metternicht and Zinck (1997) found out the highest separability between erosion classes upon integration of 7 bands of the Landsat TM and JERS-1 SAR with an over-all classification accuracy of 87%. Dwivedi et al.(1997a) revealed that fusion of Landsat TM and SPOT MSS data provided an overall accuracy of 92% for erosion mapping.

2.7. Legend framework

Hoosbeek et al. (1997) recommended a legend for soil degradation mapping which consists of a description and classification of the soils and/or soil degradation features and a legend symbol. The soil survey manual of the U.S Department of Agriculture (USDA, 1993) is one of the few existing format in describing and classifying soil degradation applied at the level of soil horizons. The manual shows a legend for different erosion features and likewise changes of soil profile properties with different classes of erosion. FAO (1990) likewise offers a rule in describing soil degradation features and share similarities in terms of codes used in accelerated erosion with the former system.

A more standardized legend format is the GLASOD (1988) approach which grouped soil degradation into two categories: 1)the degradation by displacement of soil material including water and wind erosion, and 2) the in-situ soil degradation, which includes chemical (loss of nutrients, pollution and acidification, salinization, discontinuation of flood induced fertility, etc), physical (sealing and crusting, compaction, deterioration of soil structure, waterlogging, aridification and subsidence of organic soils) and biological deterioration. Its final legend is determined by two integral components of the framewok: 1) the degree of soil degradation, and 2) the frequency of occurrence within the mapping unit (Oldeman and Lynden, 1997). In table 1, the GLASOD's severity matrix is shown with the corresponding frequency occurrence class.

Table 1. The severity and frequency classes of soil degradation in GLASOD approach

Degree of Soil Degradation	Frequency of Soil Degradation				
	Infrequent (1-5%)	Common (6-10%)	Frequent (11-25 %)	Very frequent (26-50%)	Dominant (51-100 %)
Light	Slight	Slight	Medium	Medium	High
Moderate	Slight	Medium	High	High	Very High
Strong	Medium	High	High	Very High	Very High
Severe	Medium	High	Very High	Very High	Very High

The GLASOD framework is applied at a continental scale (Oldeman and Lynden, 1997) and has been applied at a large mapping scale. Nagelhout (2001) applied the GLASOD legend framework in his study in assessing status and trends of wind erosion using small format aerial photography in Naivasha, Kenya. The geopedologic map was used as a reference in the assessment but did not fully applied the GLASOD's principle of using mapping unit as a final degradation map.

Chapter 3

The Study Area

The study area is situated in the central Rift Valley, Nakuru Disitrict, Kenya about 100 km northwest from Nairobi (figures 1 and 2). Its geographic position lies between 36°15'E – 36°30'E longitude and 00°40'S-00°53'S latitude. The altitude range of the study area is 1800-2700 m.a.s.l.

Figure1.Location map of the study area (World Atlas, 1996)

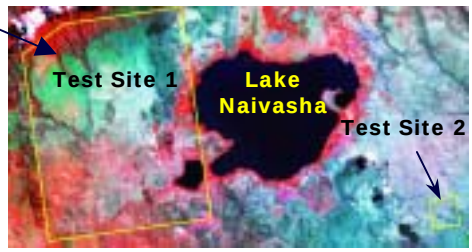

Figure 2. Location map of test site areas

The Lake Naivasha basin belongs to a semi-arid type of climate. It has a bimodal rainfall pattern shown in figure 3. March to May is described as a longer rainy season while October to November is the shorter rainy season (Kamoni, 1988). Obviously February, July and December are the driest months of the year. The average annual (1931-1960) precipitation is 608 mm which vary with elevation ranging from 600-1200mm from the Rift Valley bottom to the upper catchment (Becht, 1998).

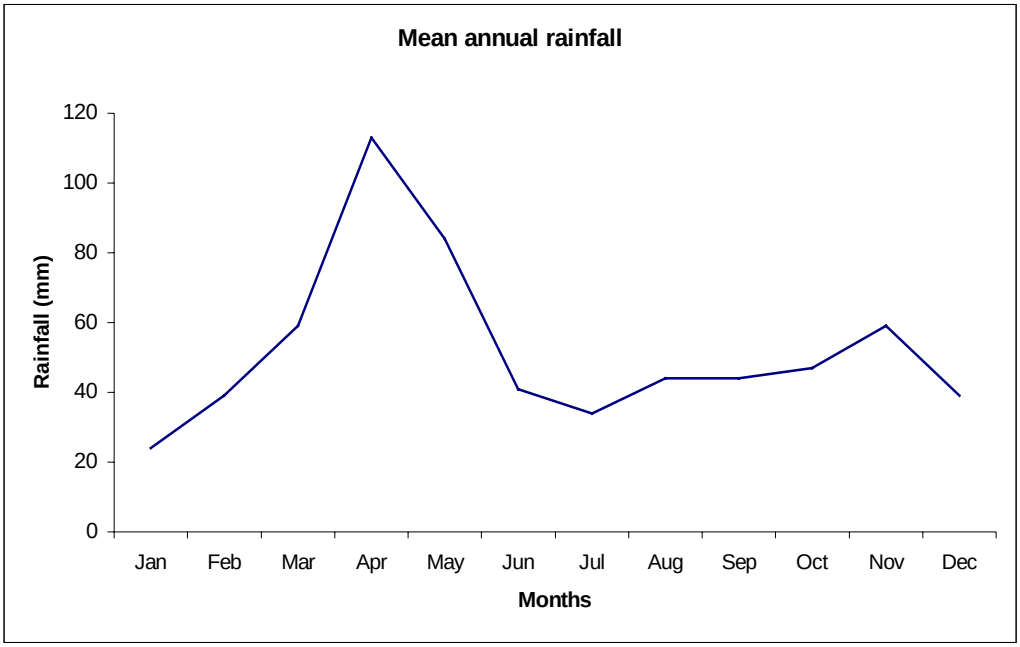

Figure 3. Mean annual rainfall in Lake Naivasha Kenya (1966-1980) Source: (Kamoni, 1988)

Soils in Naivasha is described as complex due to the influence of extensive relief variation, volcanic activity and underlying bedrocks (Sombroek et al., 1980). Based on studies conducted in the area (Sombroek et al., 1980, Siderius, 1998; Atkilt, 2001; and Nagelhout, 2001) soils can be grouped into 3 broad groups such as; 1) soils developed from lacustrine deposits; 2) volcanic and 3) lacustrine-volcanic.

The area consists of mountains, hillands, various types of plateaus and lacustrine plain. Parent materials found in these landscapes are influenced by quaternary deposits of lacustrine and volcanic in origin. Specifically, lithological composition is pantellerites and pantellerite trachytes (perkaline rhyolites and trachytes with high total iron and aluminum). The west of Naivasha is influenced by young volcanic activity from eastern Ebburru to the North and the Olkaria volcanic complex to the south with subsequent lacustrine sediment deposition. Ryolites occur mainly as domes, lava flow and pyroclastic cones (Clarke et al., 1990). Geological map of the area is shown in figure 4.

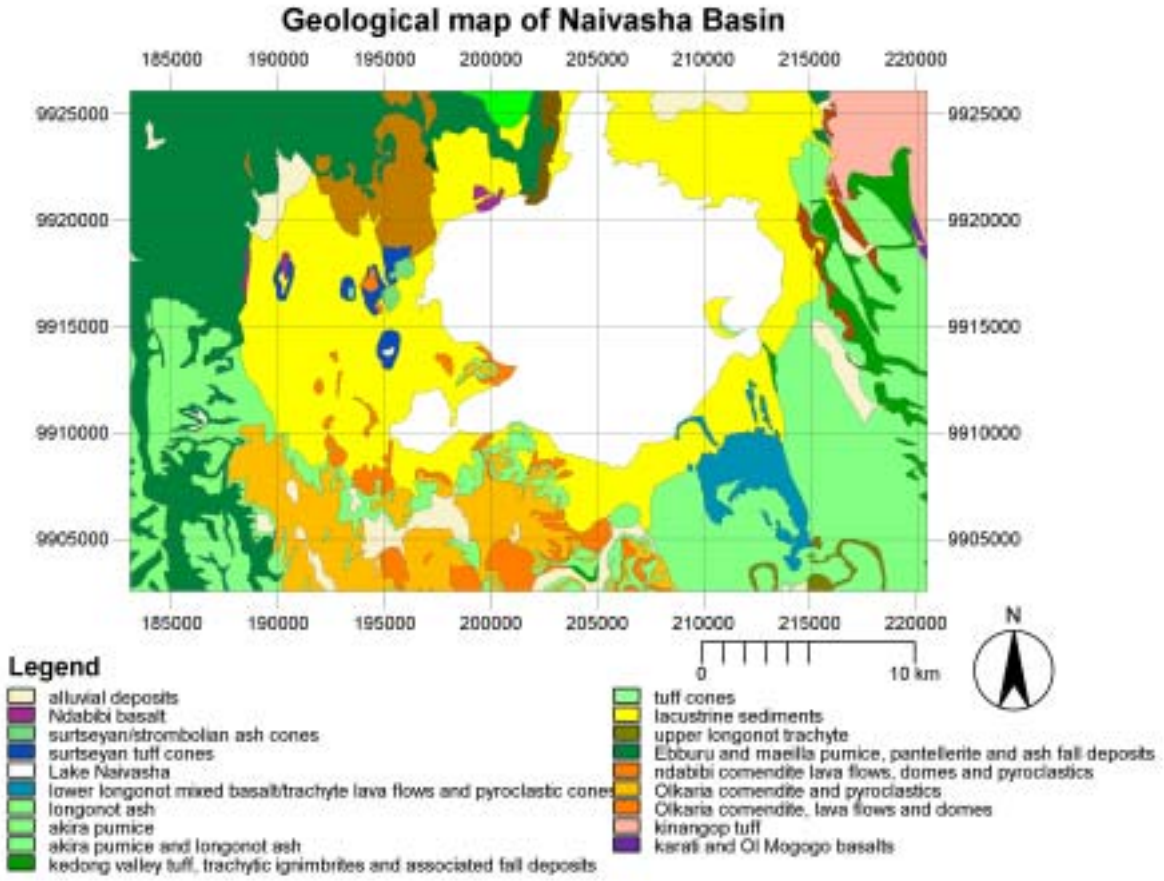

Figure 4. Geological map of Lake Naivasha (derived from Clarke, 1990)

The upper catchment have protected forest range, moor and bamboo zones. Subsistence farming with maize, pyrethrum and vegetable growing are found in the middle catchment. Rangeland is common due to small holder dairy production. Commercial farming for meat, dairy production and vegetables, citrus and flower cultivations are the major agricultural ventures in the area. Other establishments such as private game sanctuaries, national park and geothermal power plant which generates 20% of the total electricity in the country are located in Lake Naivasha basin.

Specifically, the Longonot area is abandoned and overgrazed while the Ndabibi Plain is used for grazing. The step-faulted plateau is used for commercial wheat production. The southwestern part (Moindabe area) is currently used for small farm holder for corn, castor oil and potato.

The area belongs to Zone V of the Agro-Ecological Zone (AEZ) in Kenya described as environmentally fragile and prone to land degradation. Soils are highly susceptible to both erosion and compaction (Kiai and Mailu, 1998). Prominent soil degradations in the area are due to wind erosion, water erosion, sealing and compaction (Nagelhout, 2001).The fragility of the area and various human activities seem to accelerate land degradation in the west and southeast area of the lake (Hennemann, 2001b).

Chapter 4

Materials and Methods

4.1. Materials Used

The study used a number of remote sensing, ancillary data and various softwares and tools.

4.1.1. Remote sensing data

Remote sensing data comprises aerial photographs as well as multi-sensor and multi-temporal data.

Aerial photos taken in 1972 at 1:50,000 nominal scale were made available covering the whole study area. Eight stereo pairs of aerial photos were selected in two runs from South to North flight direction.

Satellite data includes data from Landsat TM, ASTER and ERS-2 Synthetic Aperture Radar (SAR). Multi-temporal Landsat TM were from dates 25 February 1987, 21 January 1995 and 18 May 2000. In addition, ASTER image taken on September 2000 was obtained free of cost. Three bands were used in the visible spectral range such as bands 1, 2 and 3 with spatial resolution of 15 meters. Finally, ERS-2 (SAR) was used. It was taken on 26 September 2000 in C band, VV polarization and with 23 degree reference angle at midswath having ground resolution of 12.5 meters.

4.1.2. Ancillary data

The ancillary data consists of topographic maps, geological map, soil map, and digital elevation model. Four map sheets (133/1, 133/2, 133/3, 133/4) of topographic map at 1:50,000 nominal scale covering the whole Naivasha basin were used. Geological map at 1:100,000 nominal scale (Woodhall et al., 1988) was used in building the legend of the geomorphology. Soil map of Kenya (Sombroek et al., 1980) at 1:1M nominal scale was also used to gain idea on the general soil condition of the area, supplemented with the recent soil survery conducted in the area by (Sombroek et al., 1980; Siderius, 1998; Atkilt, 2001 and Nagelhout, 2001). Digital Elevation Model (DEM) was made available via the common database available at ITC. This was used in the orthophoto trasformation rectifying the aerial photos and the interpretation overlays (mylar).

4.1.3. Software packages

A number of softwares such as the Integrated Land and Water Information Systems (ILWIS) version 3.0, ERDAS Imagine version 8.4, Microsoft office processing tools (Excel, Word, Visio) and capture software. For processing SAR data, ERDAS was considered useful.

4.1.4. Field Equipment/Tools

The following field equipment and tools were used for fieldwork. Included are soil auger, geological hammer, hand penetrometer, soil knife, munsell color chart, 0.1 N hydrochloric acid, shovel, field bag, field stereoscope, mylar, digital camera ,Garmin 12 XL GPS receiver, slope meter, 30 meters and 2 meters measuring tapes, field record book, plastic wash bottle and a pH kit.

4.2. Fieldwork Planning Phase and Preparation

Fieldwork planning and preparation includes the following activities; 1) preparation of the fieldwork materials, tools equipment and the ancillary data. 2) printing of remote sensing images at 1:50,000 (i.e False Color Composite of Landsat TM 2000 and ASTER) which were used for navigation purposes to verify degradation related features, 3) aerial photo interpretation 4) sampling scheme and 4) building of field forms.

The aerial photo interpretation was carried out using the geopedologic approach developed by Zinck (1988/89). The mapping exercise was made as mapping unit of analysis to be used in degradation mapping in reference to the GLASOD framework. The initial interpretation lines were then prepared for verification in the field.

Due to the extensive relief variation in the area, sampling strategy was designed to facilitate field navigation and observations. Based on the initial output of the geopedologic interpretation, sampling was initialized by landscape position. Afterthat, the process was narrowed down to the vegetation types found, identification of land degradation surface features and finally the representativenes of the area for characterization. A 60 x 60 meters ground size was considered optimal for charaterization to cater the 30 x 30 meters gound resolution of Landsat data.

Building of field forms for degradation mapping legend and the surface description form followed. The soil degradation mapping legend was built based on the integration of three primary sources, namely: 1) the GLASOD framework (GLASOD, 1988) 2) the USDA survey manual (USDA, 1993) and 3) previous land degradation study conducted in the area (Nagelhout, 2001). For consistency in describing the surface features related to land degradation, building of a field form was carried out. Its development includes the components observable in space other than soil degradation features and attributes such as cover and/or vegetation types and their intensity and some soil data.

4.3. Field Survey and Data Collection

Field survey and data collection were subdivided into two phases; 1) the familiarization and recconnaissance survey, and 2) sample area survey, observation and data collection

1) Familiarization and Reconnaissance Field Survey

A two days exploratory field survey was conducted to get familiarized with the general conditions in the area such as geology, water resources and river systems, climate, vegetation, soils and accessibility. Verification of the API units and legend previously mentioned also formed part of the survey.

Reconnaissance field survey then followed and focused to areas affected by land degradation. This was done to identify sites for detailed study. Identification of affected/degraded sites followed according to King and Delpont (1993). In addition, information on how local people perceive the land degradation problem was also collected by talking to the farmers.

2) Sample area survey, observation and data collection

After the reconnaissance survey, the pre-identified areas for surface description were plotted on the geopedologic map and topographic map for direction-finding . The navigation plan was established based on the pre-identified areas and the landscape position. The landscape was considered in sampling to assure proper documentation of degradation types occur/observable in various geographic positions. In landscape positions were sample plots were not identified yet, a second round of reconnaissance was carried out in adjacent areas of the pre-identified sample plots already characterized. Sample plots were selected based on the representativeness of the landscape positions, vegetation types and degradation features.

Using the field form generated for land degradation feature description (appendix D), a 60 x 60 meters plot size was examined to represent the 30 meters spatial resolution of Landsat TM data. Elevation and geographic position were recorded using the Garmin GPS receiver set into ARC 1960 at zone 37 UTM. The slope was measured with the slope meter using a reference object with the same eyesight height of the recorder. Soil augering at most 1 meter deep was carried out in each sample plots and gathered some basic soil parameters at various depth.

Chemical soil properties were measured. Among which are the soil pH measured using the colorimetric test method and the calcareousness by effervescence test using 0.1N hydrochloric acid. Chemical testing was considered important to verify degradation types observed preventing wrong impression of dominating degradation types. Some soil physical properties were also measured. One of which is the soil color using the munsell color chart (USDA, 1994). Texture, plasticity and stickiness were also determined guided by (FAO, 1990). Penetration resistance of soil surface was measured randomly within the plot using the hand held penetrometer. The cylindrical rod of the penetrometer was pushed perpendicular to the ground surface. Values of

resistance in mega pascals (Mpa) were described according to (USDA, 1993). Soil loss was measured using the remaining soil surface at the base of the plant. For surface deformation, the depth, width and length of rills and gullies were measured.

Surface features were further examined. Within the sample plot, a representative 2 x 2 meters size was again characterised on its bareness and greenness (vegetation). The vegetation type was also roughly identified and characterized. Characterization of vegetation type was extrapolated to 200 meters radius and identified the land use. This was done as a background check of a possible pattern recognizable in remote sensing data. A total of 26 sample plots were characterized.

Summarizing the field data provided information on foreseen difficulties to pattern recognition in remote sensing data due to the interference of vegetation on the surface features. Thus, actual field mapping was carried out at a contiguous area of the Ndabibi escarpment where degradation classes are represented. This was done by walking through the boundaries of degradation feature classes and recorded the GPS readings forming a polygon.

4.4. Data Attribute Handling and Encoding

Observation points were downloaded from the GARMIN GPS receiver and imported to ILWIS format. They were seggregated into two sets, namely: 1) the field observations points which were later used as a training set, and 2) the GPS readings for the actual field mapping which was then polygonized by on-screen digitization. Elementary statistics of field data was calculated such as means and standard deviation of the topsoil loss and penetration resistance. Field observations were encoded.

4.5. Creating Geometrically Correct Orthophotos and Digitization of API

To compensate for possible error due to relief variation, an orthophoto transformation was carried out to rectify the photos and the mylar using the digital elevation model. The resulting rectified photos are called orthophotograph defined as an aerial photo photograph with nearly all the image displacement and scale errors removed (USDA, 1993).

Aerial photos were scanned at 1400 dots per inch (dpi) and the corresponding overlays (mylar) with the interpretation lines at 600 dpi. At least 8 ground control points were selected on the photos and coordinates were measured using the topographic map. Photos were then geometrically rectified by orthophoto transformation using DEM. Coordinate system followed the projection of the topographic map (ARC 1960 37 UTM, Clarke 1880). On-screen digitization of the interpretation lines followed. Afterwhich, polygonized and labelled. For the photos and the interpretation lines get north oriented, geocoding by resampling followed with the newly created georeference using the same coordinate system. A mosaic was created for both photos and digitized geopedologic lines. Edge matching followed by overlaying the lines onto the photo mosaic to check the fitness of the lines to the actual features.. This activity followed the guideline according to (Rossiter and Hengl, 2001).

4.6. Image Processing

Prior to image fusion analysis to detect and map degradation features, pre-processing of remote sensing data is required. Ideally, it must have started from the sensor induced error and radiometric correction (Van Genderen and Pohl, 1994) which is often hard to achieve due to the lack of sensor-calibration and atmospheric data. Since radiometric error caused by the sensor system is usually built-in with the data, it is however assumed to be minimal. Included in this section are: 1) the pre-processing phase 2) image fusion phase

4.6.1. Pre-processing of RS imagery

The pre-processing phase includes the radiometric correction of remote sensing data. The atmospheric correction in the visible range (the case of Landsat and ASTER) and speckle reduction of SAR data were carried out.

Remote sensing imagery taken from the optical region of the electromagnetic energy comprises energy reflected from the ground surface and the scattered energy emitted by the atmosphere (Brandt and Mather, 2001; Janssen et al., 2001). Thus, the DN values are composite of two factors mentioned. Atmospheric correction only includes a constant subtraction of haze effect derived from the lowest value of the shadow assumed to have a zero DN value. Haze is due to the particulates present in the atmosphere which interfere the spectral response of the object. It has an additive effect of the image brightness. Determination of such was done by using the lowest DN value of the shadow and/or dark object according to Richards and Jia (1999). The darkest shadow was supposed to have zero value and the spectral offset is actually haze effect. The haze effect included constant DN subtraction to the digital images within the visible to the near infrared regions.

Recommended techniques were not employed due to the demand of detailed data such as; 1) surface reflectance retrieval and aerosol optical depth Liang et al. (1997), and 2) model of the atmospheric scattering at the time of data acquisition Chavez (1988). A recommended data transformation for noise removal was not employed in this case because the technique was developed for imagery whose principal components transform do not show a decreasing image quality Green et al. (1988). Sun illumination angle correction was considered not applicable to the area due to the varying relief types understood to have a varying degree of illumination per pixel. This effect however was considered and assumed minimal since haze is usually the dominant atmospheric scattering component (Chavez, 1988) .

Speckle noise of radar data obscure image interpretation for various applications. Speckle noise is a variance of microwave backscattered signal due to interaction of varying terrain geometry, moisture, di-electric constant, wavelength, polarization and view angle resulting to a salt and pepper texture effect(Huang and Van Genderen, 1996; Lillesand and Kiefer, 2000). To reduce this effect, spatial averaging was employed. A 3 x 3 window size was considered to render localized filtering at various iterations.

Low pass spatial filtering was employed using linear averaging filter. Adaptive filters for radar were used. One of which is the Gamma MAP filter by which its development was based on the assumption of the image scene having a gamma distribution more suitable to realistic case. The filter is adaptive to radiometric statistics and geometric properties (Lopes, 1991). These are practically the reasons the Gamma MAP filter being selected among the available adaptive filters to remove the speckle of the ERS-2 SAR data. The Gamma MAP filter was likewise recommended by (Pohl, 1996) as it performed the best suited filter for speckle reduction of ERS-1 SAR data prior to image fusion of SAR and optical data for mapping applications among other adaptive filters tested. Local region filter was also used to re-filter the best filtered product of the previous filters mentioned. Basis of which is the remarkable improvement of despeckled image quality of SAR data in the work of (Feingersh, 2000).

In order to determine the best despeckled image, resulting despeckled images at varying iterations were tested using the following tests: 1) Speckle Index, 2) Speckled Image Ratio and 3) Visual assessment. Speckle index calculation was carried out using equation the following equation:

$$\text{Speckle Index, } SI = \left(\frac{\sqrt{\text{var}}}{\mu} \right) = \left(\frac{\sigma}{\mu} \right) \qquad [4.1]$$

After the each filtering process, histogram was displayed and computed the standard deviation, σ and the mean, μ. The resulting SI values were compared to the original ERS-2 SAR having a high SI value. It is believed that bigger the difference of the SI index from the original mean better result (Huang and Van Genderen, 1996). The limitation of such test was considered because too much difference could also mean too smooth image (Feingersh, 2000; Pohl and Van Genderen, 1995). Thus, the complimentary testing with visual test and the speckled image ratio was employed. The best despeckled product was then further tested with the speckled image ratio as shown below. In this test, the removal of feature/structure evidence means optimal speckle removal.

$$\text{Speckled Image Ratio, } SI_{ratio} = \left(\frac{Speckled_{image}}{Filtered_{image}} \right) \qquad [4.2]$$

Geometric alignment is considered crucial in image fusion (Van Genderen and Pohl, 1994;Pohl, 1996). The images were georeferenced and aligned into common coordinate system. The Landsat TM 2000 was georeferenced using the collected GPS ground control points and rectified using an affine transformation. Other optical data were georeferenced by image-to-image rectification using Landsat TM 2000 as master image. Same master image was used to rectify the ERS-2 SAR data using a third order polynomial transformation. The alignment of the different data sources were evaluated using at least 5 reference objects in the image and measured their coordinates. This was considered the first order alignment check.

To extract information from multi-source data through image processing (discussed in section 4.6.2), resampling of the data into common georeference and pixel size was performed. A 15 meters pixel size was considered optimum preserving the spatial details from the data with high

spatial resolution needed for the study. The second order alignment was checked after resampling simply by making a color composite display (RGB) of different data sources and fitness of the road lines, landscape edges, and other features were evaluated. Pre-processing step is shown in figure 5.

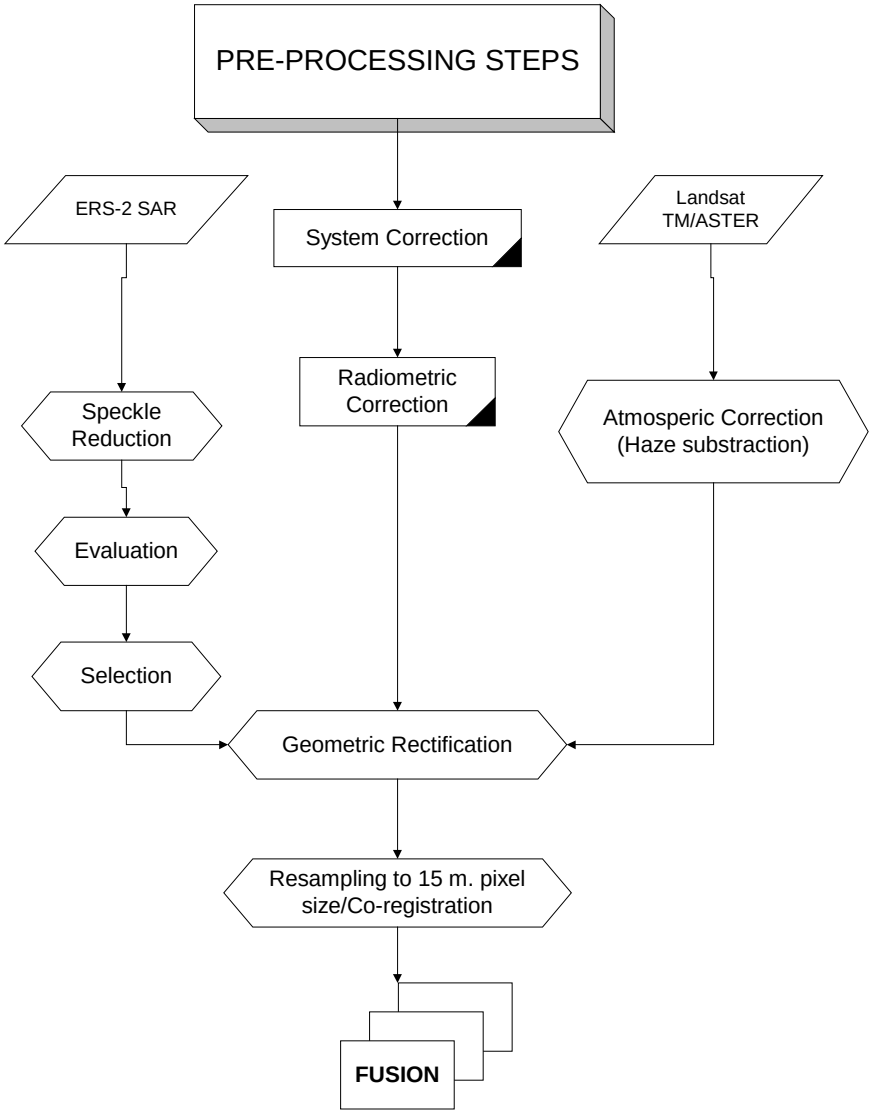

Figure 5. Schematic diagram showing the pre-processing steps prior to image fusion

4.7. Image Fusion

In this study, fusion of multi-source data was used to extract complimentary information from various sources. Primary objective was to improve detection of degradation features. Prior to image fusion processes, computation of the Optimum Index Factor (OIF) developed by (Chavez, 1982) was employed using the equation

$$OIF = \frac{\sum_{i=1}^{3} \sigma_i}{\sum_{j=1}^{3} |ccj|} \qquad [4.3]$$

σ_i= standard deviation of digital numbers for band, cc_j= correlation coefficient between any two of three bands.

This enabled to select three best band combinations with the highest variance and the least correlated bands and used as input to fusion techniques which used limited number of bands. This combination was assumed to have the highest amount of information.

Two groups of pixel based image fusion were employed in this study. They are 1) the statistical/arithmetic method (Principal Component Transformation, band ratio, division and multiplication and 2) the color related (RGB-HIS-RGB Transformation and the simple color composite (RGB) of multi-source images). The application of image fusion in this study are grouped into three categories, namely 1) Image fusion for degradation feature detection, 2) Image fusion for degradation feature monitoring and 3) Image fusion for classification improvement.

1) Image Fusion for degradation feature detection

An initial step was to normalize Landsat TM bands (1, 2, 3, 4, 5, & 7) and fused with the TM panchromatic band by multiplication using the algorithm described below. The scaling factor was used to spread the values in the histogram.

$$TM' = \left(\left[\frac{TM_i}{\sum TMi} \right] * TMPan \right) * f \qquad [4.4]$$

Where: TM' = new TM band; TM*i*= band number; f =scaling factor

The development of the algorithm was assumed to improve spatial resolution of the TM bands (the multiplication of the panchromatic band) while preserving the spectral integrity. This algorithm shared similarities with the Brovey transformation normalizing three bands to RGB display. OIF index [4.3] was then again calculated for the resulting fused TM bands.

Principal Component Analysis (PCA) using the fused TM bands was carried out. This image transformation technique was employed to reduce redundancy of spectral bands and to fuse SAR data with PC1 and PC2. They were transformed to RGB domain and visual interpretation followed. Exclusion of PC3 was due to its assumed low information content.

The color related image fusion technique (HIS-RGB) was carried out using the three band combination with the high OIF among the fused TM bands (TM bands 4, 3 and 7) using the algorithm shown below (equation 4.5). The transformation also visualized in figure 6. The flow chart for the image fusion by this transformation is given in figure 7.

$$\begin{pmatrix} I \\ v_1 \\ v_2 \end{pmatrix} = \begin{pmatrix} \frac{1}{\sqrt{3}} & \frac{1}{\sqrt{3}} & \frac{1}{\sqrt{3}} \\ \frac{1}{\sqrt{6}} & \frac{1}{\sqrt{6}} & -\frac{2}{\sqrt{6}} \\ \frac{1}{\sqrt{2}} - & \frac{1}{\sqrt{2}} & 0 \end{pmatrix} \begin{pmatrix} R \\ G \\ B \end{pmatrix} \quad \text{a.} \qquad [4.5]$$

$$H = \tan^{-1}\left(\frac{v_2}{v_1}\right) \quad \text{b.} \qquad S = \sqrt{v_1^2 + v_2^2} \quad \text{c.}$$

Where:

I= Intensity, H= Hue S= Saturation v_1 and v_2 = intermediate variable needed in the transformation

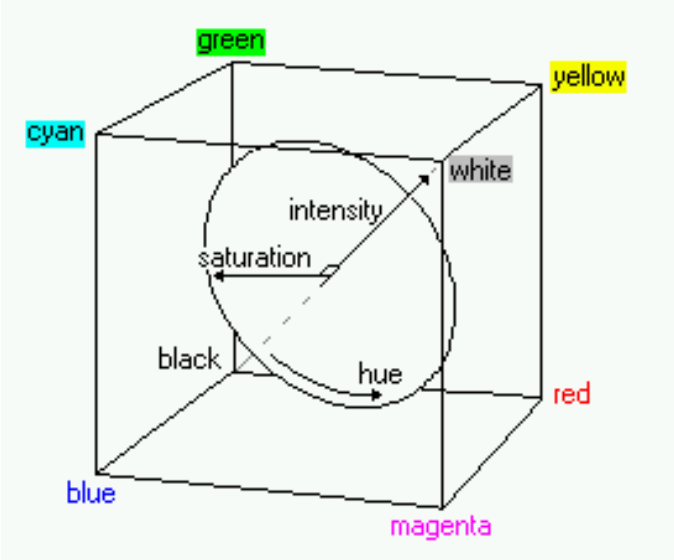

Figure 6. Color model showing the transformation of RGB-HIS color system

Intensity channel from HIS space was substituted with SAR data and then transformed back to RGB space. This results in fusion of TM bands with SAR data.

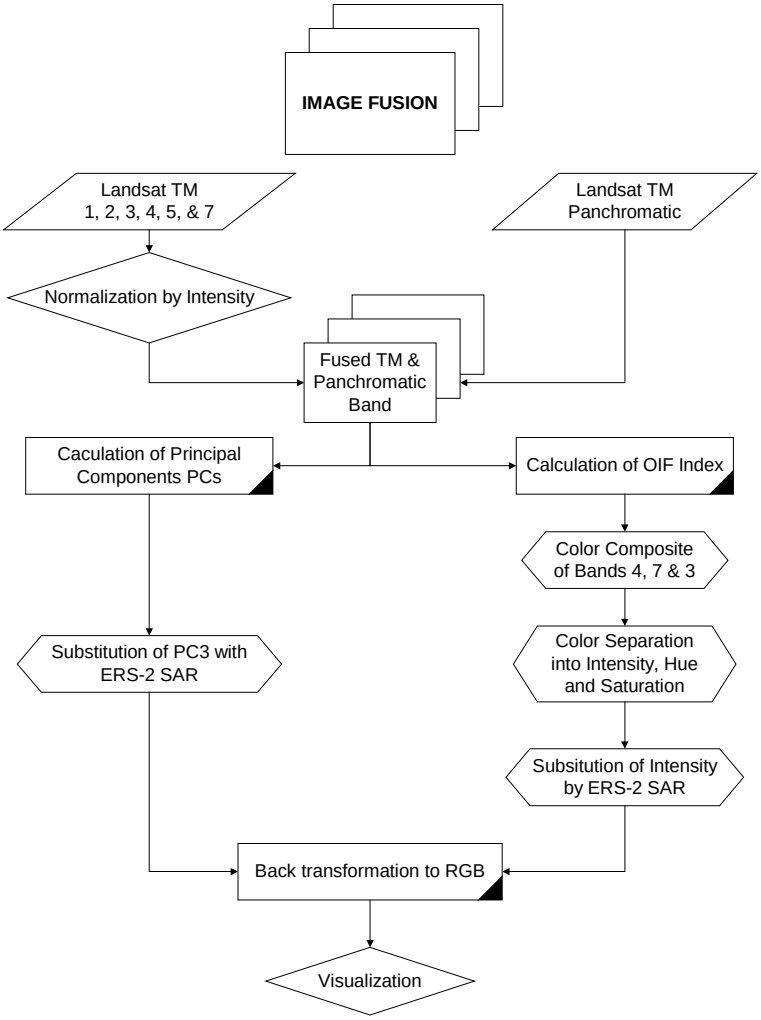

Figure 7. Flow chart of image fusion analysis in detecting land degradation in test site 1

In Test site 2 where gullies are directly observable, band ratio technique was employed. Band ratio is the process of dividing image band to another image band bringing out/emphasizing the object of interest (Pohl and Van Genderen, 1998; Sierra-Correa, 2001) and suitable for change detection (Zobrist et al al., 1979 cited in (Pohl, 1996)). This technique is also recommended by (Singh, 1989) being fast and simple. Landsat TM bands 5 and 3 were inputs to band ratio shown below.

Band ratio= TM band5/TM band 3 [4.6]

Because spectral response of the gullied areas in the optical bands are very low, resulting color composite was assumed not to emphasize the affected area. The choice of Band 5 and 3 was based on its subtle difference of the spectral response to gullies while taking into account non-degraded areas. Thus, resulting ratio for gullies presumed as 1 while more than 1 for the non degraded areas. Subsequent image inversion was done to highlight the gullies by the formula

Highlighted_gullies= 255-Band ratio of TM5 and 3 [4.7]

Inputs to image fusion through RGB needs three bands. PCA transformation was then generated. The ratio image, ERS-2 SAR and PC1 were displayed to RGB domain.

With ASTER data, only the visible bands were used with 15 meter resolution. The infrared region was not used because it has the same spatial resolution of the Landsat TM. The purpose of investigating ASTER data to the detection of gullies is due to its higher spatial resolution. Image band 3 was directly inverted to highlight the gullied area shown below

$$Highlighted\_gullies_{aster}=255\text{-ASTER Band 3} \quad [4.8]$$

To visualize through RGB, principal component transformation was carried out for ASTER bands 1, 2 &3. PC1, Inverted band 3 and SAR data was displayed through RGB domain.

2) Image fusion to monitor degradation features

Band ratio technique was also employed to monitor the gullies using the same bands. Temporal data were used, namely 1) Landsat TM 2000 2) Landsat TM 1995 and 3) Landsat TM 1987. Band ratios for Landsat TM 1995 and T 1987 were again calculated (refer to 4.6 and 4.7 formulas). Temporal fusion was carried out by passing band ratio 2000, band ratio 1995 and band ratio 1987 to RGB respectively. Process flow diagram is presented in figure 8.

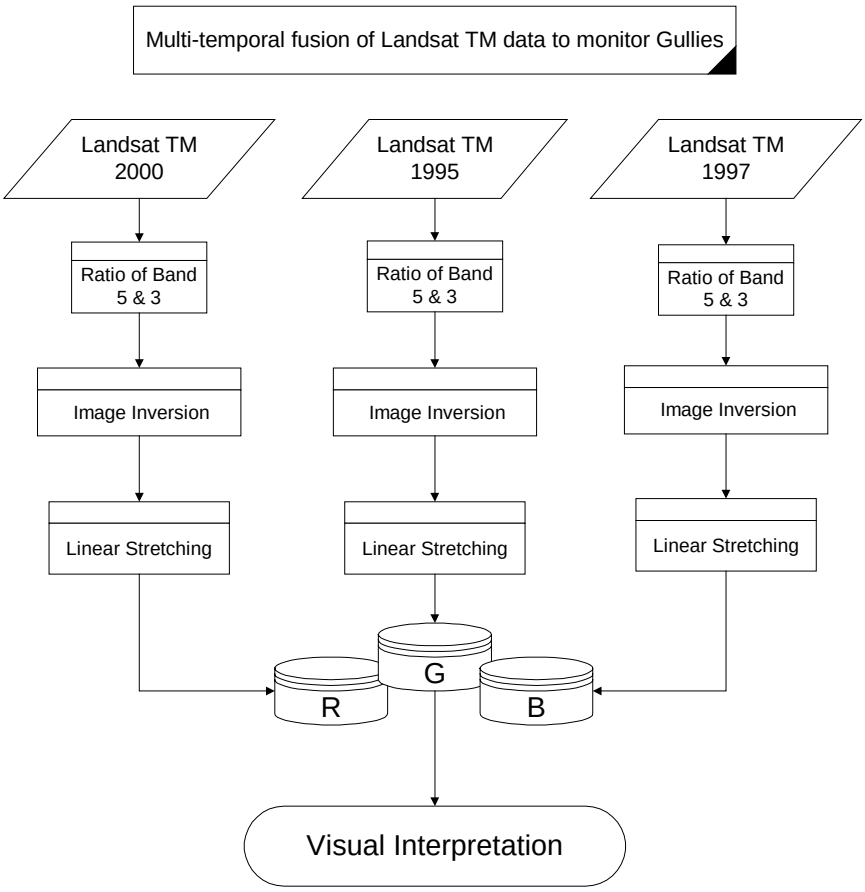

Figure 8. Process flow chart of multi-temporal image fusion of Landsat TM in detecting and monitoring gullies.

3) Image fusion for classification improvement

Image fusion are also recommended to improve classification accuracy (Metternicht and Zinck,1997;). In the next section (4.6.3), a univariate measure of spectral separability was measured. Since it only quantifies separability of a single band, fusion by multiplication of two data sources was carried out by multiplication. Principal components 1, 2 and 3 were multiplied with other data nature and sources such as ERS-2 SAR, thermal band (TM Band 6). Algorithm is shown below. Fused bands were assumed useful in investigating the advantage of an added feature dimension (different data nature) to the classifier.

Image Band'= (Image band 1 x Image band 2)/255 [4.9]

Where: Image Band'= new image fused band, Image band 1 and 2 = input bands

To visualize the fused products, the fused PC1 and ERS, fused PC2 and thermal band, and PC3 were displayed into RGB domain respectively. Visual interpretation followed.

4.7.1. Classification

Evaluation of the spectral separability among the bands was considered vital to reduce the dimensionality of the input bands to the classifier. A univariate measure of spectral separability was used, the 'normalized difference between the means', dnorm (Swain and Davis, 1978). The absolute value of the difference between the means (μ_1-μ_2) of two spectral classes divided by the sum of their standard deviation (σ_1- σ_2) was calculated as shown below

$$d_{norm} = \frac{|\mu_1 - \mu_2|}{\sigma_1 + \sigma_2} \quad [4.10]$$

The higher the d_{norm} value of a particular band, the higher the separabilty of the classes. The median, considered not sensitive to extreme values was calculated among the d_{norm} values in each band. The resulting median values were then compared in each band. Because only the median statistical parameter used quantifying the overall separability of the individual band, a 2-dimensional feature space was also visualized. This was carried out to see how well the quantitative measure of separability performed separates various classes in a feature space. The selection of the bands as inputs to the classifier followed.

Supervised classification was employed for the test site 1. Gathering of the training samples was done by recognizing patterns similar to the pattern of ground truth data. In some cases where the ground truth data has more than 2 representative samples, training samples were then derived using the reference data. Unsupervised classification or clustering was employed to the test site 2. Primary reason was that the areas affected by gullies are distinct and further emphasized with fusion technique. Therefore, clusters can be easily be distinguished.

4.7.2. Accuracy Assessment

Prior to accuracy assessment, filtering was carried out using the averaging filter and class merging /masking by conditional statement using the API units based on the priori knowledge of the area. In order to measure the goodness of the technique, accuracy assessment was done with the reference data using the following statistical procedures:

User-Producer Error Matrix

This was obtained by using a GIS 'cross operation' in ILWIS of the training samples and the reference data. Error of commission and omission was computed according to (Congalton and Green, 1999). The error matrix was used as an input the Khat statistical error computations as described below.

Kappa (KHAT) Statistics, a measure of actual agreement of in the error matrix for the remotely sensed classification and the reference data. Calculation was guided by the equation below.

$$K = \frac{N\sum_{i=1}^{r} x_{ii} - \sum_{i=1}^{r}(x_{i+} * x_{+i})}{N^2 - \sum_{i=1}^{r}(x_{i+} * x_{+i})} \qquad [4.11]$$

Where:

r is the number of rows in the matrix, x_{ii} is the number of observations in row *i* and column *i* ,

x_{i+} and x_{+i} are the marginal total row *i* and column *i* respectively

N is the total number of observations

4.8. Mapping Exercise using with the GLASOD matrix

The first step to applying the GLASOD legend framewok was to associate the classified land degradation map into the landscape units. API units for geopedologic mapping used was used as a mapping unit for degradation mapping using GLASOD approach. Since geopedologic units occur in more than one polygon, it is not eligible to be called a 'unique identifier' for the resulting database of the landscape units. Instead area numbering was employed and used as a unique identifier. The geopedologic map was resampled into the same pixel size and coordinate system of the land degradation map. Map crossing was employed followed by calculations of areas affected by land degradation classes and types and its relative frequency of occurrence in the map units.

Severity was assigned in each polygon based on their relative frequency and degree of degradation (see table 1) according to (GLASOD, 1988).

Chapter 5

Results and Discussion

5.1. The landscape units through geopedologic approach

The geopedologic approach was developed by Zinck (1988/89) to carry out a meaningful soil survey and mapping. The resulting API units shown in figure 9 were used to associate land degradation to landscape position. Moreover, the primary purpose of its usage was to be a mapping unit delved on the applicability of GLASOD's legend framework in mapping soil degradation at a large scale. Thus, detailed soil survey to describe the soils in each unit was not rendered in this study.

There are 5 major landscape units identified in the west of Naivasha basin shown in figure 9. They are; 1) Mountain 2) Hilland 3) Lava flow Plateau 4) Step-faulted Plateau and 5) Lacustrine Plain. The landscape units were further subdivided into relief, lithology and landforms resulted to 60 mapping units delineated. Details of which is presented at the geopedologic legend as shown in Table 2.

The Step-faulted plateau is the largest landscape unit with a surface area of 10, 163 hectares (ha). This unit is located at the foot of the Mau escarpment and subdivided at the relief level into mesa, escarpment and the V-shaped incision valley. Mesa has sloping and undulating topography. A unique lithology of the landscape is found at the escarpment (Pf231) due to basalt intrusion forming an elongated "dike-like" scarp.

The Lacustrine Plain (Lp) is second to the Step faulted plateau where it occupies 7, 211 hectares. The soils are product of both volcanic and lacustrine sediments. Surface soil texture ranges from sandy loam to sandy clay loam. Surface soil color is brownish to reddish and is acidic (pH 4.5-5.5) in reaction.

The Hilland (Hi) covers 3,612 hectares and described as a product of the volcanic activity in Ndabibi where most of the ryholitic activities were formed into volcanic cones (Clarke et al., 1990). They are categorized into low hills, high hills and depression. Though lava flow is described as product of this Hilland fomation, it is considered a landscape because of its size and the plateau formation This is the smallest landscape unit identified in the area occupying 848 hectares.

The Mountain landscape (Mo) is second from the smallest delineation (Lava flow plateau) because the delineation covered only a part of the footslope which extends between the Step faulted plateau (Pf) and the Lacustrine Plain (Lp). This covers 1062 has.

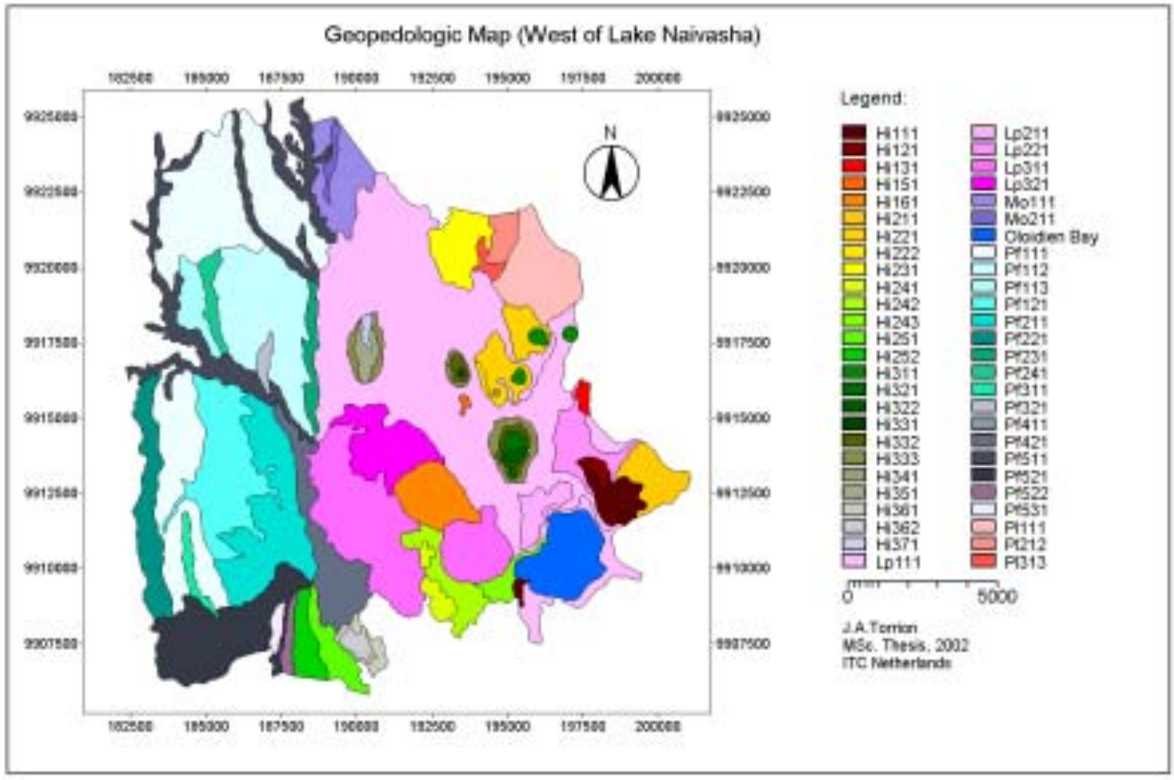

Figure 9. API for geopedologic map in west of Lake Naivasha Basin

Table 2. The geopedologic photo interpretation legend in the west of Naivasha basin

LANDSCAPE	RELIEF	LITHOLOGY	MU_ID	LANDFORM
Mountain Mo	1 Glacis	1 eastern Eburru pumice, lava flows and pyroclastic cones	Mo111	1 undifferentiated
	2 ridge	1 –do-	Mo211	1 summit
Hilland (Hi)	1 Low hills	1 Olkaria comendite pyroclastics (includes lacustrine sediments and re-worked pyroclastic)	Hi111	1 slope complex
		2 pantellerite	Hi121	1Lava flow
		3 Surtseyan/strombolian ash	Hi131	1 footslope
		5 Surtseyan/strombolian ash, Ndabibi comendite lava flow, domes and pyroclastic cones	Hi151	1 ash cone
		6 Basalt and hawaiite lava flows	Hi161	1 lava flow
	2 High hills	1 pantellerite	Hi211	1 Lava flow
		2 surtseyan/strombolian ash	Hi221	1 Ash cone
			Hi222	2 Footslope
		3 eastern Eburru pantellerite, lava flows and pyroclastic cones	Hi231	1 Lava flow
		4 pyroclastic cone	Hi241	1 ash cone
			Hi242	2 moderately steep footslope
			Hi243	3 gently sloping footslope
		5 Maeilla pumice, pantellerite pumice trachyte and ash fall deposits	Hi251	1 footslope
			Hi252	2 backslope
	3 Depression	1 Volcanic tuff	Hi311	1 Conical
		2 Surtseyan tuff	Hi321	1 summit
			Hi322	2 crater lake
		3 Surtseyan/Strobolian ash	Hi331	1 summit
			Hi332	2 backslope
			Hi333	3 footslope

LANDSCAPE	RELIEF	LITHOLOGY	MU_ID	LANDFORM
Hilland (Hi)	3 Depression	4 Ndabibi comendite	Hi341	1 summit
		6 old lacustrine sediments	Hi351	1 bottom depression
		6 Akira pumice	Hi361	1 footslope
			Hi362	2 slope complex
		7 basalt, hawaiite lava flows and pyroclastic cones	Hi371	1 graben floor
Step-faulted Plateau Pf	1 Mesa	1 Eburru pumice, pantellerite and trachyte pumice and ash fall	Pf111	1 sloping mesa
			Pf112	2 undulating surface
			Pf113	3 undulating higher surface
		2 maeilla and akira pumice, trachyte and pantellerite pumice and ash fall deposits	Pf121	1 undulating mesa
	2 Escarpment	1 maeilla and akira pumice, trachyte and pantellerite pumice and ash fall deposits	Pf211	1 Scarp
		2 eburru and akira pumice, pantellerite and trachyte pumice and ash fall	Pf221	1 dissected scarp
		3 basalt and hawaiite lava flows and pyroclatic cones	Pf231	1 elongated scarp
		4 eburru pumice, pantellerite and trachyte pumice and ash fall	Pf241	1 high scarp
	3 Low ridge	1 maeilla and akira pumice, trachyte and pantellerite pumice and ash fall deposits	Pf311	1 slope complex
		2 eburru pumice, pantellerite and trachyte pumice and ash fall	Pf321	1 scarp
	4 Footslope	1 akira pumice, olkaria comendite and pyroclastics (includes re-worked lacustrine sediments and pyroclastics)	Pf411	1 footslope
	5 V-shaped incision Valley	1 ebburu pumice, pantellerite and trachyte pumice and ash fall	Pf511	1 slopes
		2 maeilla and akira pumice, trachyte and pantellerite pumice and ash fall	Pf521	1 valley slopes
		3 basalt and hawaittee lava flows and pyroclastic cones	Pf522	2 steep slopes
			Pf631	1 almost flat

LANDSCAPE	RELIEF	LITHOLOGY	MU_ID	LANDFORM
Lava Flow Plateau Pl	1 Mesa	1 eastern eburru pantellerite, lava flows and pyroclastic cones	Pl111	1 sloping
	2 Escarpment		Pl212	2 scarp
	3 swale		Pl313	3 bottom
Lacustrine Plain LP	1 low terrace	1 Lacustrine sediments	LP111	1 undifferentiated flats
	2 middle terrace	1 Lacustrine sediments	LP211	1 undifferentiated flats
		2 Lacustrine sediments and volcanic tuff	LP221	1 undiferentiated flat
	3 higher terrace	1 lacustrine sediments with pantellerite lava flows and pyroclastic cones	LP311	1 rolling
		2 lacustrine sediments	LP321	1 shallow depression

5.2. Land degradation as observed in the field

In this study, the detection of erosion features are directly linked to the surface features as it is normally in remote sensing detection. Correlation of the soil erosion features with soil properties and/or understanding erosion process and soil erodibility are the limitations of this study. The study focused however on the detectability and mapping of land degradation by remote sensing with reference to surface features.

One of the observable indicators in the field is the sign of gullying which is very prominent in the southeastern part of the lake, near the Mt. Longonot and Kijabe Hill. Subsurface gray ashes are exposed in abrasion areas and deposited in a tail-like features which are considered to be the effects of to be the high wind speed, poor vegetation and the presence of micro-relief. Extensive study and detection of these features was studied by (Nagelhout, 2001) using small format aerial photography (SFAP), which was extensively used as a ground truth in this study. Individual gullies in the area are classified based on the field legend used as seen in table 3 from high to mostly severe classes. In table 4, dimensions of gullying are shown.

Gullying is not prominent at the west of the lake. It is always in association with sheet and rill erosion features. Sheet erosion and rill erosion were located and characterized due to the sign provided by bare soil surfaces. Though not very common in the study area, sign of erosion by piping and tunnelling was also found. The sign provided by the vegetation gave a considerable attention. Growth of natural vegetation such as grasses and shrubs dominated by Leleshwa (*Tarconanthus camphorates)* and thorned acacia (*Gleditsia triacanthos*) were observed at the eroded and/or degraded areas.

Sheetwash considered an association of wind and water action is found in the lacustrine plain. The overgrazing and drier environment makes the area prone to the wind action. The area is usually dusty. Also in the southern part of the lacustrine plain which is seasonally flooded area.

During heavy rain, overland flow from the upstream is moving down carrying sediments. Sediment deposition is worse that some of the buildings like schools and shops are half-buried.

Mass movement is also observable in the area. At the hilland, rock outcrops are evident and slumping and tunneling at the step-faulted plateau.

Table 3. Field legend describing the severity of the degradation classes

Major Type	Sub Type	Class	**Sub Class**	**Severity**	Symbol
Wind erosion (E)	Loss of top soil (t)	Sheet (s)	Loss of top soil <5cm	Slight	Ets1
			Loss of top soil 5-15cm	Moderate	Ets2
			Loss of top soil 15-25cm	High	Ets3
			Loss of top soil >25cm	Severe	Ets4
	Terrain deformation (d)	Deflation (f)	Deflation depth 25cm	Slight	Edf 1
			Deflation depth 25-50cm	Moderate	Edf2
			Deflation depth 50-100cm	High	Edf3
			Deflation depth >100cm	Severe	Edf4
		Deposition (n)	Depositional depth >5cm	Slight	Edn1
			Depositional depth between 5-25 cm	Moderate	Edn2
			Depositional depth 25-50 cm	High	Edn3
			Depositional depth <50cm	Severe	Edn4
Water erosion (W)	Loss of Topsoil (t)	Sheet erosion (s)	Loss of top soil <5cm	Slight	Wts-1
			Loss of top soil 5-15cm	Moderate	Wts-2
			Loss of top soil 15-25cm	High	Wts-3
			Loss of top soil >25cm	Severe	Wts-4
	Terrain deformation (d)	Rill erosion (r)	Shallow rill <3cm	Slight	Wdr1
			Incision rills which occurs in steep slope<10 cm	Moderate	Wdr2
			Wider braided rills 10-15 cm	High	Wdr3
			Wider braided rills 15- 20cm	Severe	Wdr4
		Gully (g)	Shallow gully 30 cm –1m	Slight	Wdg1
			Deep gully 1-5 m	Moderate	Wdg2
			Very deep gully >5 m	High	Wdg3
			V. V. deep >30 m	Severe	Wdg4

In contrary, characterization of land degradation in Longonot area was straightforward. Gullying due to the wind action is prominent. Sub-surface gray ashes are exposed (abrasion) and deposited into a "tail-like" feature. Orientation of the gullies was observed from east to west possibly influenced by wind direction. It was almost impossible to assess depth of deposition. However,

the deposition of dunes was used as a reference in which they are considered severe. In table 3, more than .5 meters deposition is considered severe.

Table 4. Gully size measurements at the wind erosion affected area in near Mt. Longonot

Gully no.	X coordinates	Ycoordinates	μWidth (m)	μ Depth (m)	Length (m)	Class, Symbol
1	219281	9903632	14.16	1.10	38.90	Severe, Edf4
2	219228	9903605	15.13	0.97	66.17	High, Edf3
3	219310	9903604	11.16	1.50	42.40	Severe, Edf4
4	219029	9903376	10.70	1.45	46.50	Severe, Edf4
5	219066	9903376	21.32	1.07	50.30	Severe, Edf4
6	219001	9903386	22.00	1.20	142.60	Severe, Edf4
7	219018	9903411	19.50	1.15	107.10	Severe, Edf4

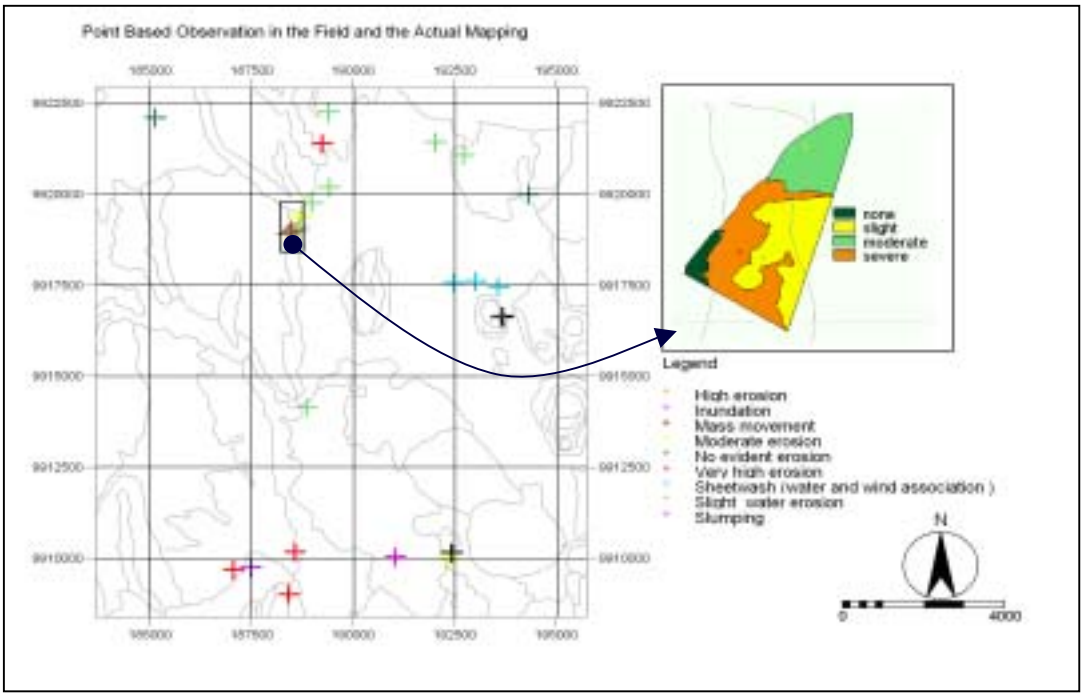

Figure 10.Showing the land degradation training samples gathered and the actual field mapping (background map: geomorphologic lines)

Figure 10 shows the collected sample observation in the field segregated into classes and a subset, actual mapping at the Ndabibi escarpment. The following classes of land degradation can be drawn based on the field observations.

1) None degraded areas. This is found at the wheat commercial farm and other cultivated areas where soil conservation measures are employed.

2) Slightly degraded. Surface soils are affected by sheet and rills.

3) Moderately degraded. Sheetwash is much pronounced with less vegetation.

4) Highly degraded. Sheetwash also pronounced but with few gullies and rills and located in steep slopes.

5) Severely degraded. This area is affected by rills, sheetwash and gullies.

6) Sheetwash. Thin topsoil removal due to the wind action during the dry season while sheet erosion on gentle slopes during rainy season

7) Mass movement. This class is dominated by rock outcrops and natural vegetation.

8) Inundation. An area seasonally flooded where soil sediments are deposited forming a crust. Thick soil depositions are common which led to destruction of infrastructures. Sand depositions at the waterways and road cuts are evident. Fallowing is common.

5.3. Pre-processing of Remote Sensing Data

Speckle noise is a variance of microwave backscattered signal due the interaction of varying terrain geometry, moisture, di-electic constant, wavelength, polarization and view angle that interferes image interpretation for various applications(Pohl and Van Genderen, 1995; Huang and Genderen, 1996, Xu, 1999; Feingersh, 2000; Lillesand and Kiefer, 2000). Speckle reduction was then considered a major activity.

Table 5 shows the result of speckle index and visual observation relating to the ERS-2 SAR data. Results on the use of non-adaptive filter (Linear averaging) showed an increase in despeckling ability of the filter with increasing iteration at a certain threshold level. The 6th filtering was chosen to have the optimum despeckled image because the 7th iteration resulted to a smoother image. Moreover, the image in its 6th filtering showed the least object pattern in the SI image ratio test, which means an advantage of speckle removal onto other iterations. The lower the speckle index, the less speckle noise left in the image (Huang and Van Genderen, 1996) does not hold true onto this image because it resulted to too smoothed image which led to losing some vital information. Thus, the integrative analysis and observation with the three tests mentioned (section 4.6.1).

The 7th iteration in Gamma MAP filter performed the optimum speckle removal. Though the SI index value continuously decreases at its 8th iteration, the resulting image is smoother. The 6th iterative process of the linear averaging resulted to a comparable product with the GMAP on its 7th iteration but some features are more distinct in Gamma Map filter. It could be due to the filter attribute which considers a Gamma distribution of the data more suitable to the real case (Huang and Van Genderen, 1996). Treating the 7th iteration image output of the Gamma Map filter to the Local region filter improved the quality of the image. In figure 11.b shows sharper edges of some features. The white spots in the image are the backscatter signals needed in this study.

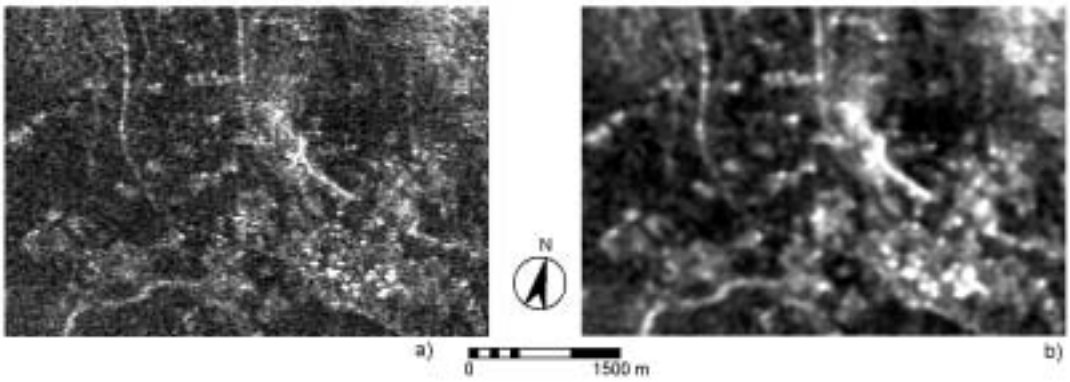

Figure 11. Showing the a) original ERS-2 SAR data and the b) despeckled ERS-2 SAR in Gamma MAP filter with 7 iteration and in Local Regional filter (1-pass) which performed the best results

Table 5.Speckle reduction of ERS-2 SAR using 3 Filtering techniques in 3x3 window size

Filter	Iteration	Mean,μ	SD,σ	Speckle Index, SI	Visual Observation
ERS-2 SAR		99.29	38.01	0.3800	speckled image (original image)
Linear averaging	1	103.25	36.31	0.3516	Speckled
	2	103.79	35.28	0.3399	Abundant speckles
	3	103.88	34.42	0.3313	Moderate speckles
	4	103.91	33.77	0.3249	Few speckles
	5	103.92	33.26	0.3201	Quite despeckled
	6	103.93	32.85	0.3161	Despeckled
	7	103.94	32.50	0.3127	Quiet Smooth
	8	103.94	32.20	0.3097	Smooth
	9	103.94	31.93	0.3072	Smooth
	10	103.94	31.69	0.3049	Smooth
	11	103.95	31.48	0.3028	Smooth
Gamma MAP	1	102.48	36.20	0.3532	Speckled
	2	101.69	34.83	0.3425	Abundant speckles
	3	100.38	33.57	0.3344	Moderate speckles
	4	98.99	32.50	0.3283	Few despeckled
	5	97.58	31.57	0.3235	Very few speckles
	6	96.17	30.74	0.3196	Quite despeckled
	7	94.78	29.98	0.3163	Despeckled
	8	93.40	29.28	0.3135	Quite smooth
	9	92.04	28.62	0.3109	Smooth
	10	90.69	28.0	0.3087	Smooth
Local regionUsing Gamma MAP filter output in its 7th itteration	1	94.75	30.06	0.3172	Performed the best output

5.4. Spectral Charateristics of the degradation classes

Figure 12 shows the spectral signatures of different degradation classes. In the optical range, the sheetwash (sheet erosion in association by water and wind) exhibits the highest reflectance of all the classes. Except in the near infrared region, it shows an absorption feature which indicate zone of vegetation stress. The inundated area is next to the sheetwash giving almost the same characteristics. Due to seasonal flooding, accumulations of sand and silt deposits are common which result in high spectral response.

The moderately degraded area follows in which the spectral response is an interaction between soil and little natural vegetation such as grasses and shrubs. The spectral response of the severe class is less compared to the above-mentioned classes. This is considered unique characteristics

of this class wherein the response is due to the exposed yellowish soil color and to the specific natural vegetation type common to this class. Leleshwa (*Tarconanthus camphorata*) shrub has a greenish broadleaf surface and shiny grayish at the bottom side of the leaf making it reflective.

The slight and highly degraded areas got almost the same pattern though the slightly degraded areas have higher DN values. Its response is due to the soil in infrared region and greener vegetation making reflective in the near infrared region. High class is dominated by dry unhealthy shrub species (i.e. thorned acacia, *Gleditsia triacanthos*).

In areas where there is no degradation, spectral response is the lowest. It has low near infrared response which means dry or stressed vegetation and relatively has a high response in the middle infrared regions. It is because the time of image acquisition coincides with the field preparation and planting time. The mass movement feature is considered unique because it has the lowest response in the infrared region. This zone is heavily covered with natural vegetation (*Euphorbia decaryi)* and few shrub species which has low leaf canopy cover.

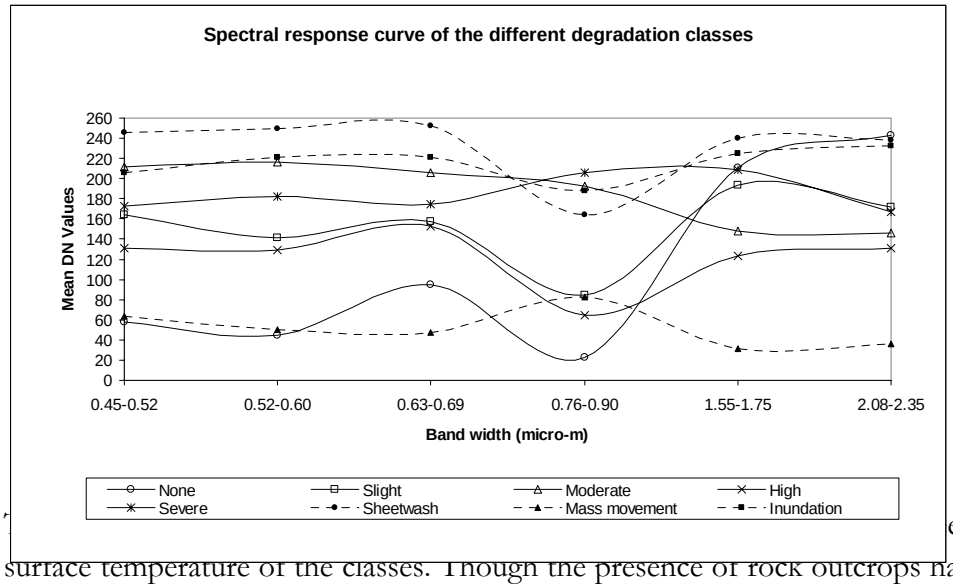

en differences of the surface temperature of the classes. Though the presence of rock outcrops has direct influence on the heat storage capacity of the soil surface (Metternicht, 1996), the succulent type of vegetation could be the attributing factor for a low surface temperature causing the lower digital number on the thermal band. In inundation area the cooler soil temperature could be attributed to the surface crusts layers slowing down evapotranspiration. The highest soil surface temperature is at the sheetwash zone where it suffers from vegetation stress (overgrazing and drier environment). The various spectral response of the thermal band indicates that its inclusion is quite promising. Further visualization of its usability is shown in the next section.

The microwave region of the spectrum (3.75-7.5 cm) showed relevance in its use since it showed differences on the surface roughness information. Roughness here is defined by the backscattering signal received by the radar sensor. The higher the backscattering, the more rough is the surface and the higher the DN values (Lopes et al., 1990; Metternicht, 1999; Feingersh, 2000; Lillesand and Kiefer, 2000). The vegetation type and the rock outcrops of the mass movement class had caused the high backscatter signal. The inundation area which is fallowed,

crusted soil surfaces, and with relatively higher soil moisture condition are the factors causing the high backscattering. Radar, sensitive to soil moisture (Janssen et al., 2001; Pohl and Van Genderen, 1995) is an important characteristic segregating the inundated areas over other classes.

5.5. Image fusion performances

Three categories were discussed on the usefulness of image fusion in this study, namely 1) detection of degradation features, 2) classification improvement and 3) land degradation monitoring.

5.5.1. Detection of degradation features by image fusion

The land degradation detection techniques used in this study are employed to find out how well the different combination of multi-source data can enhance degradation features. Fusion of TM panchromatic band to the multi-spectral band was carried out using the algorithm [4.4]. The algorithm shared similarities to Brovey transformation, which uses 3 bands in getting the intensity of the individual bands. Figure 13 shows the that the fused bands preserved the spectral integrity of the original bands while improving its spatial resolution from panchromatic band.

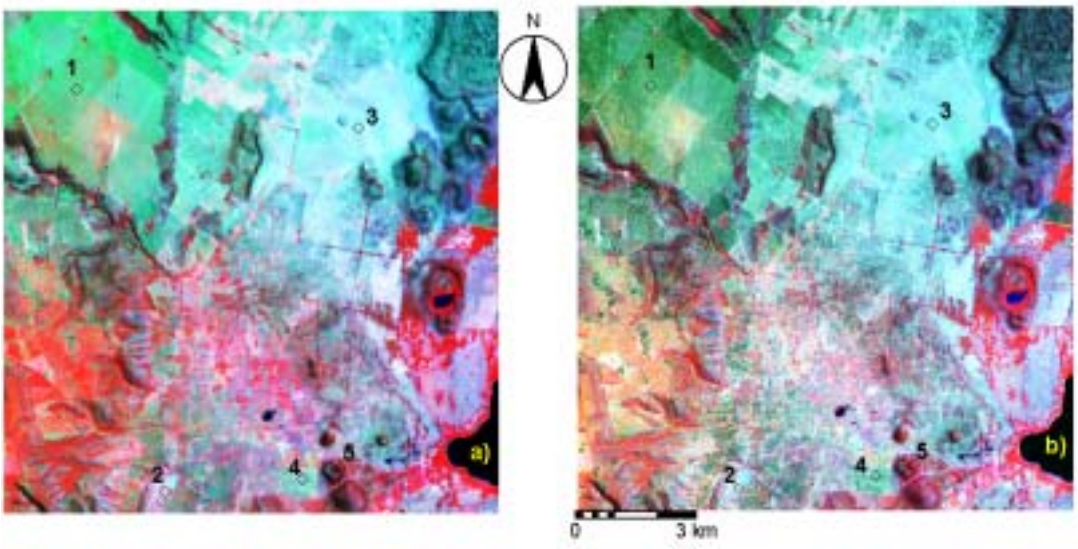

Legend: 1) Non degraded 2) Severely degraded 3) Sheetwash 4) Inundation 5) Mass movement
Image label: a) TM band 4, 7 , & 3 b) fused TM4, 7 &3 with TM pancromatic band as RGB respectively

Figure 13. Landsat TM bands 4, 7 &3 and fused product

Principal component substitution was also carried out. PC3 was substituted with SAR data. PC1, PC2 and SAR data were transformed to RGB domain. Figure 15 shows that this technique failed to highlight degradation areas.

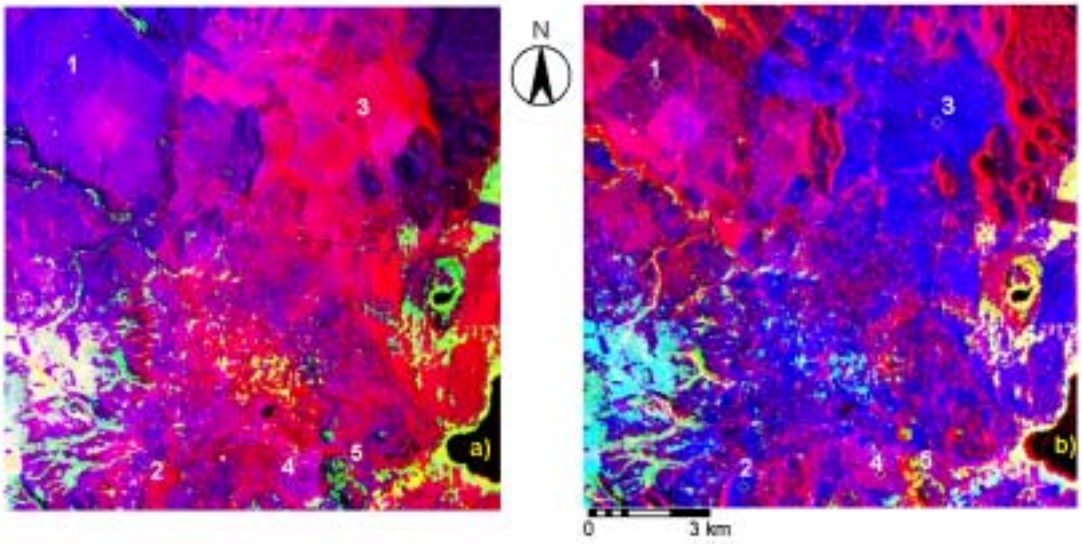

Legend: 1) Non degraded 2) Severely degraded 3) Sheetwash 4) Inundation 5) Mass movement
Image label: a) PC1, PC2 & PC3 b) SAR, PC2 & PC1 as RGB respectively

Figure 14. The PCA transformation of Landsat TM and fused product with SAR data

Figure 15 is the RGB to HIS transformation of TM bands 4, 7 & 3. Replacing the intensity channel with the ERS-2 SAR data and performed reverse transformation to RGB channel achieved the best fused product

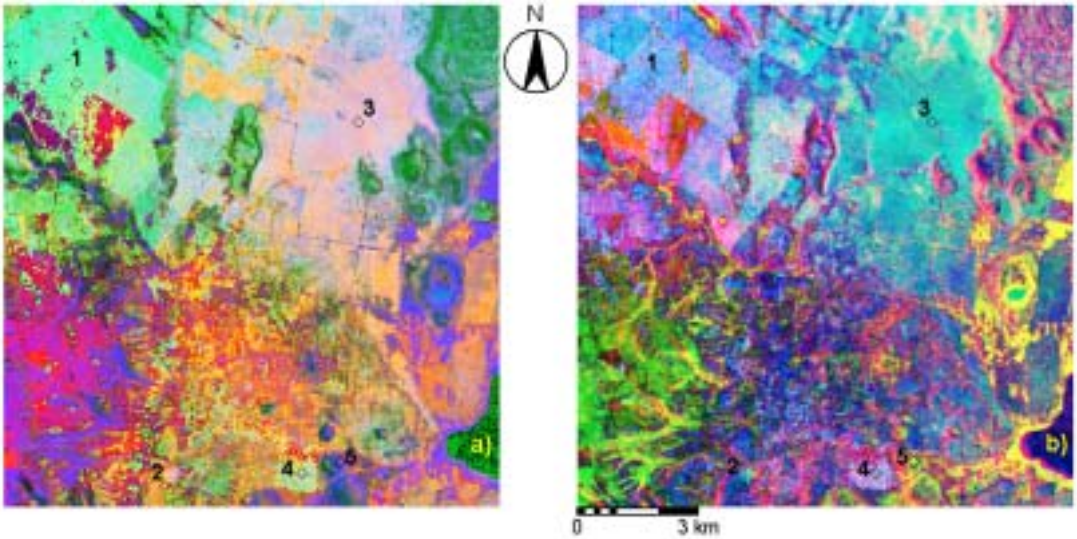

Legend: Non degraded 2) Severely degraded 3) Sheetwash 4) Inundation 5) Mass movement
Image label: a)Intensity, Hue and Saturation of TM Bands 4, 7 & 3 and b) SAR, Hue & Saturation of TM bands 473 into RGB respectively.

Figure 15. The HIS transformation of Landsat Band 4, 7, & 3 and the fused product with SAR data

Figure 15 (b) shows that it optimally represented the different degradation types identified in the area. As noticed, only broad classes are represented and not able to completely represent other erosion classes such as the slightly, moderately and highly degraded areas. The RGB back transformation of HIS bands shown in figure 15 (a) represented well the non-degraded areas.

HIS transformation changes the original spectral responses of the data into a different physical nature. The transformation and the intensity replacement by radar having different physical characteristics impaired the eligibility of the fused product for classification using the available algorithm (Pohl, 1996). Visual interpretation suggested optimal representation of the different degradation types and classes and was expected to yield high separability. However, samples gathered seemed not separable as displayed in a feature space. Researchers found out that such nature of fused product cannot be classified using a maximum likelihood classifier and recommended the Artificial Neural Network (ANN) technique (Yesou' et al., 1993; Huurneman et al., 1996; Pohl, 1996).

The increased spatial resolution of the data was found not sufficient in the detection of degradation features in test site 1. It failed to detect gullies where the dimension is far smaller than the lowest spatial resolution of the remote sensing data. However, it was noted that the boundaries of the degradation classes can be better identified than the original data. The technique was considered useful in test site 2 where the detection of gullies was associative of both the on-site and off-site effects (abrasion-deposition areas).

Figure 16 shows the color composite of ASTER bands and Landsat TM bands. The gullied shown in black color due to its low DN value caused by the subsurface dark gray ash exposure.

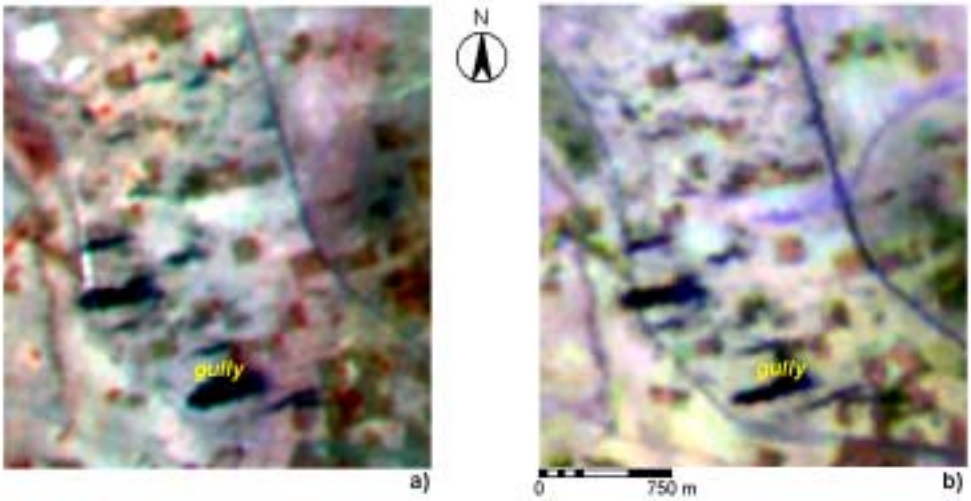

a) ASTER Bands 3, 2 &1 and b) Landsat 7, 5 & 3 , as RG respectively

Figure 16. Color composite of ASTER bands and Landsat TM bands

Figure 17 are products of bringing up the DN values by ratio and inversion of images. The red ones are the gullies, the greenish are the backscatter due to SAR and the bluish are the non-degraded areas. Arithmetic technique "ratio" fused with SAR data is considered the best image technique to map gullies. PC1 Substituting PC1 with band 7 yield the same result. This implies further that variance of PC1 come from the near infrared region as mentioned in section 5.6.

In figure 17 (b) gullies are well emphasized and boundaries are quite clear. In ratioing, similar response will have values close to 1 and un-like spectral response deviates further than 1. Thus

with image inversion, the target object having a close response from TM band 5 and 3 are highlighted.

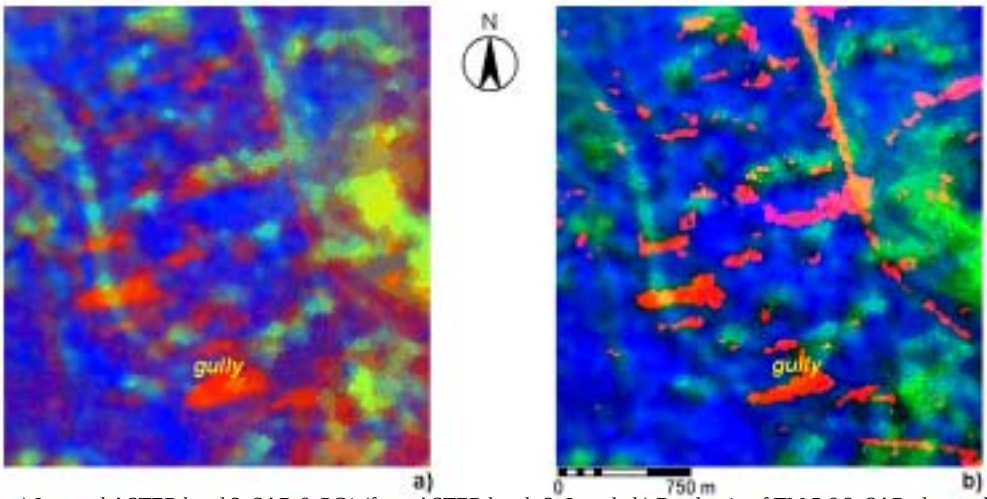

a) Inverted ASTER band 3, SAR & PC1 (from ASTER bands 3, 2, and b) Band ratio of TM 5 &3, SAR data and PC1 of TM bands as RGB resepctively

Figure 17. Fused products of ASTER and Landsat Bands with SAR data

5.5.2. Image fusion for improved classification

Image fusion was not only tested for improved visual detection but also to quantify separability of an added dimension to the classifier. Since the method used to quantify separabilty is a univariate measure according to (Swain and Davis, 1978) image fusion was done by multiplication to determine the advantage of complimentary information derived from different sources. A number of fused products are; 1) fused PC1 with SAR data 2) fused PC1 with thermal band 3) fused PC2 with SAR data and 3) fused PC3 with SAR data. Since visualization is indispensable to image fusion anlysis, figure 18 shows the fused product of PCs with SAR and thermal data. Results shows an optimal representation of the five classes indicated.

An advantage of fusion by multiplication is that RGB display is not only limited to three image sources but also additional data channels. Figure 18 is a composition of information derived from SAR, thermal band, PC1, PC2 and PC3.

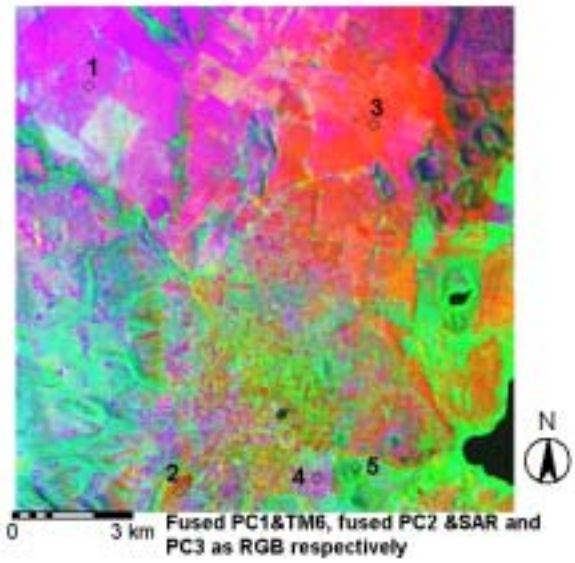

1)Non degraded 2) Severely degraded 3) Sheetwash 4) Inundation 5) Mass movement

Figure 18. Color composite of fused PCs with SAR and thermal data

5.5.3. Image fusion for land degradation monitoring

Changes of the area affected by gullying in Longonot are being monitored through temporal image fusion. The band ratios of TM bands 5 and 3 from TM 2000, TM1995 and TM1987 assigned to RGB respectively, shows temporal information. Figure 19 shows the temporal color assignment of the different features identified based on the pattern and the priori knowledge of the area. The white colored features implies degradation features present accross dates, orange in year 2000, yellow objects are present in years 1995 and 2000, green in 1995, magenta implies road cuts detected in 1987 and 2000, blue implies open areas detected in 1987, cyan could mean bare soil by cultivation detected in 1987 and 1995, and the dark green is the non-affected area.

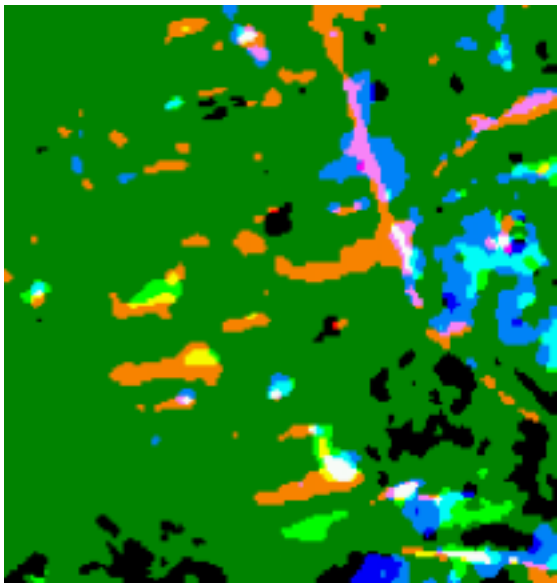

Features detected across time

Features detected in year 2000

Features detected in year 1995 and 2000

Features detected in year 1995

Road cuts detected in 1987 and 2000

Open areas detected in 1987

Exposed soil by cultivation detected in 1987 and 1995

?

Non-affected areas getting the spectral response from 1995

Figure 19 Resulting temporal image fusion of TM 2000, TM1995 and TM1987 to RGB respectively

5.6. Spectral separability of various land degradation classes in test site 1

'Spectral signatures' signifies a unique spectral characteristic to successfully identify an object. The purpose of this activity is to quantify the usefulness of the Landsat TM bands, transformed TM bands, the ERS-2 SAR, fused bands and the synthetic bands (i.e. DEM) using the normalized divergence matrix d_{norm} (Swain and Davis, 1978)(equation [4.6]). PCA transformation is found useful to reduce data layer but how well the PCs can separate the various classes is not known. This activity is considered useful in the choice of bands for visualization (color composite and feature space evaluation) and finally the choice of bands as input bands for classification.

Table 6 shows the elementary statistics of the spectral bands of Landsat TM. It reflects a high standard deviation of Bands 5 and 7 showing that the variability of the degradation classes is mostly contained in the infrared region. Correlation matrix shown in table 7 suggested that Bands 1 and 2 are highly correlated (values shown in **bold**) and while bands 3, 4, and 7 have low correlation values (values shown in ***bold italics*** form). This result is also reflected in the OIF factors shown in table 8 in which Band 3, 4 and 7 are the three band combination with the greatest amount of information.

Table 6. Elementary statistics of Landsat TM Bands

Bands	TM1	TM2	TM3	TM4	TM5	TM7
Mean	27.76	35.47	51.39	49.14	107.02	86.10
Standard deviation	10.70	12.62	21.44	17.41	32.41	31.44

Table 7. Correlation matrix of Landsat TM Bands

Bands	TM1	TM2	TM3	TM4	TM5	TM7
TM1	1.00					
TM2	0.96	1.00				
TM3	0.94	0.96	1.00			
TM4	***0.38***	0.50	***0.36***	1.00		
TM5	0.79	0.83	0.85	0.55	1.00	
TM7	0.78	0.80	0.88	***0.30***	0.94	1.00

Table 8. Optimum Index Factor (OIF) of three band combination of Landsat TM

Band combinations	347	457	345	147	247	145
OIF	45.59	45.34	40.43	40.42	38.43	35.0
Rank	1	2	3	4	5	6

The enormous amount of statistical information contains quite weak indication of the separability. Visualisation through a 2 dimensional feature space is time consuming especially when dealing with multi-band (multi-spectral, fused bands and synthetic bands) and limited to only 2-dimensions. Moreover, visualization through various combination of color composites with the data and other data sources is very much helpful yet become subjective for the following reasons; 1) color display is only limited to three bands 2) different degradation classes not fully represented. Usually 50% of the classes are represented while others are not distinguishable. Limitation of color perception of the human eye is a key factor.

Table 10 shows the ranking of the median d_{norm} values. Median value was used being less sensitive to extreme values. The higher the d_{norm} value, the higher the separability and the lower the d_{norm} values, the lower separability of the classes. PC2, ERS-2 SAR, TM Panchromatic, Landsat TM 1, 2 and 4 are bands with the low d_{norm} values. PC2 containing 9.26% variance (table 8) has low separability. It contains most of the information in the visible to near infrared region equally having low separability. Landsat TM band 7 possessed the highest separability. Band 5 likewise gained relatively high d_{norm} value. PC1 contains relatively higher d_{norm} values and its separability is improved by fusion of the radar data and thermal data through an arithmetic technique by multiplication.

Radar alone did not show good separability index. It however helped the optical range's performance owing to the increase of d_{norm} value of PC1. Similary, thermal band provided low d_{norm} but when fused with PC1, it showed the highest separability. Fusion of ERS-2 SAR to PC2 considerably decreases the d_{norm} value. The increase in the relative separability and the amount of information in PC3 when fused with higher resolution data is found similar to the findings of (Yesou' et al., 1993) in mapping geologic structures.

The synthetic band, digital elevation model revealed a high d_{norm} value second to the fused band of PC1 and TM Band 6. Though its matrix value could not be linked directly to the separability according to the spectral signatures, this implies a promising input to the classifier to improve the accuracy. This also suggests that the degradation features are related to the landscape positions which will be discussed in the next section.

To visualize the degree of separability mentioned, a two-dimensional feature space is shown in figure 20. The higher the degree of overlap perceived problematic in classifying the classes. The increase separability (d_{norm}) by fusion of PC1 and radar is visualized. Also the performance of TM band 7 and the radar is shown. Noticeably, the moderate and the slight classes are almost inseparable in most cases and become separable with the thermal band (TM 6). Separability of other classes are likewise improved. The complimentary information of Landsat TM band 6 indeed is useful in classifying land degradation classes.

Based on the visual and quantitative measures of separability, the following are the list of bands considered useful for classification, namely; 1) PC1 2) Landsat TM Band 6 3) 4) Landsat TM Band 7, 5) ERS-2 SAR data and 6) DEM.

Table 9. Percent variance of the Principal Components of Landsat TM

PC	PC1	PC2	PC3	PC4	PC5	PC6
Variance (%)	85.11	9.26	4.52	0.73	0.28	0.10

Table 10. Median value of the Normalized divergence (d_{norm}) matrix

Bands	d_{norm} value	Rank	Bands	d_{norm} value	Rank
Landsat TM Band 1	2.18	11	PC1	2.90	5
Landsat TM Band 2	2.12	14	PC2	1.71	12
Landsat TM Band 3	2.58	8	PC3	2.44	10
Landsat TM Band 4	2.13	13	Fused PC1 and ERS-2 SAR	3.15	4
Landsat TM Band 5	2.81	6	Fused PC1 and TM Band 6	3.78	1
Landsat TM Band 6	2.56	9	Fused PC2 and ERS-2 SAR	1.38	16
Landsat TM Band 7	3.48	3	Fused PC3 and ERS-2 SAR	2.67	7
Landsat Panchromatic	2.12	14	DEM	3.62	2
ERS-2 SAR	1.80	15			

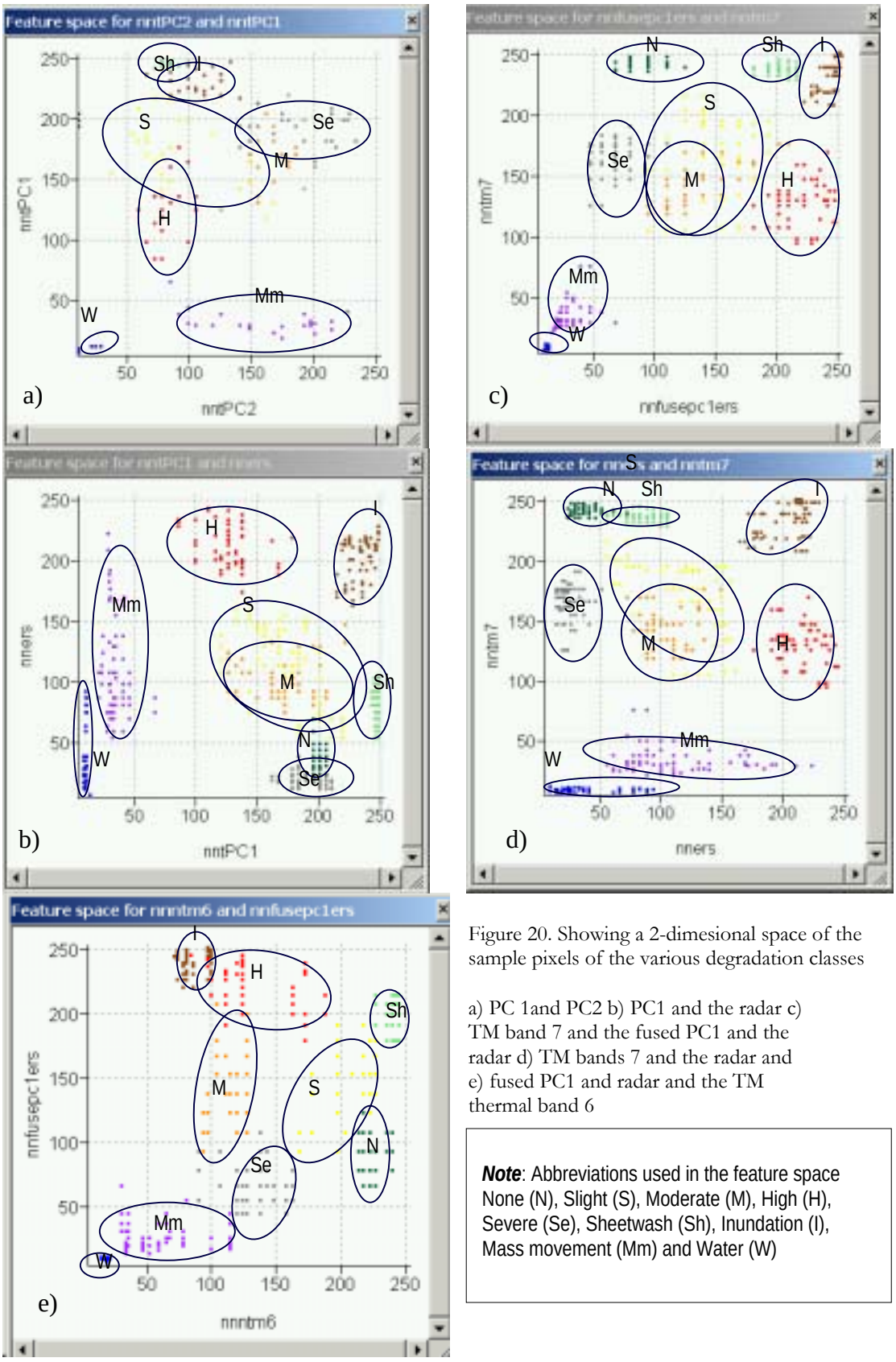

Figure 20. Showing a 2-dimesional space of the sample pixels of the various degradation classes

a) PC 1and PC2 b) PC1 and the radar c) TM band 7 and the fused PC1 and the radar d) TM bands 7 and the radar and e) fused PC1 and radar and the TM thermal band 6

Note: Abbreviations used in the feature space None (N), Slight (S), Moderate (M), High (H), Severe (Se), Sheetwash (Sh), Inundation (I), Mass movement (Mm) and Water (W)

5.7. Classification and accuracy assessment

Shown in table 12 is the summary of the error matrices using the minimum distance classifier. The first 3 principal components shows an accuracy of 0.48 (khat). The inclusion of the thermal band lowers the khat value by 8%. It fails to classify the 'none' degraded class. Its usefulness can be seen in classifying inundation area from .36 to 0.97 increase of producer's accuracy. In table 11, thermal band contributes to the increase of the overall producer and user accuracy by almost 50%. Likewise the inclusion of radar reduces khat value to 0.39 as it also fails to classify the 'none' class. However, radar showed accuracy increase of the inundation, and water. It improves the over-all producer user accuracy though thermal band performed better in this case. Among the remote sensing band combinations, the highest accuracy obtained is 0.53 khat in synergy of the VIR (Visible-Infrared), thermal and microwave region of the spectrum. Its producer and user accuracy increased by 60% than using the VIR data alone. The over-all highest accuracy was obtained when the DEM (considered as a synthetic image band) was used as added feature dimension to the classifier with the synergy of bands representing the VIR, thermal and the microwave regions. The highest over-all accuracy obtained is 0.64 khat. The post classification assessment based on the priori knowledge of the area, resulted to class merging. Based on the priori knowledge of the area, mass movement was merged to none degraded areas. It is because the study only deals with human induced degradation. Masking was also carried out in the Pf111 landscape unit (Figure 9) used as a commercial wheat farm. Post classification accuracy is 0.73 khat. Figure 18 shows the land degradation map in the west area of the lake naivasha.

Table 11. Elementary statistics of the producer / user accuracy

Band Combinations	ACCURACY	MEDIAN	STDEV
PC1, 2 & 3	Producer	0.42	0.30
	User	0.34	0.30
PC 1, 2, 3 & TM6	Producer	0.67	0.37
	User	0.63	0.37
PC1, 2, 3 & SAR	Producer	0.56	0.30
	User	0.49	0.35
PC1, TM6, SAR	Producer	0.70	0.26
	User	0.71	0.32
PC1, TM6, SAR &	Producer	0.54	0.29
	User	0.71	0.30
Post classification	Producer	0.71	0.28
	User	0.84	0.31

Table 12. Summary of accuracy matrix

BAND COMBINATIONS	ACCURAY	LAND DEGRADATION CLASSES								
		H	I	Mm	M	N	Se	Sh	S	W
PC1, 2 & 3	Producer	0.86	0.36	0.47	0.04	0.82	0.17	0.55	0.3	?
	User	0.57	0.34	0.77	0.03	0.73	0.24	0.74	0.29	0
	Overall Acc	50.83								
	Khat	0.48								
PC 1, 2, 3 & TM6	Producer	0.86	0.97	0.6	0.03	?	0.2	0.74	0.23	1
	User	0.63	0.38	0.75	0.03	0	0.31	0.86	0.92	1
	Overall Acc %	44.41								
	Khat	0.4								
PC1, 2, 3 & SAR	Producer	0.58	0.68	0.65	0	?	0.3	0.55	0.2	0.93
	User	0.49	0.37	0.53	0.01	0	0.24	0.62	0.92	1.0
	Overall Acc %	39.4								
	Khat	0.39								
PC1, TM6, SAR	Producer	0.6	1.0	0.62	0.54	0.7	0.83	0.92	0.2	1.0
	User	0.79	0.29	0.66	0.71	0.05	0.83	0.31	0.91	0.97
	Overall Acc %	52.7								
	Khat	.53								
PC1, TM6, SAR & DEM	Producer	0.51	1.0	0.54	0.43	0.91	0.76	0.5	0.16	1.0
	User	0.82	0.42	0.63	0.25	0.71	0.86	1.0	0.12	0.84
	Overall Acc %	64%								
	Khat	.64								
Post classification	Producer	0.71	1.0	0.57	0.47	0.94	0.94	0.51	0.19	1.0
	User	0.84	0.73	0.63	0.27	0.95	0.86	1.0	0.12	0.85
	Overall Acc %	73.05								
	Khat	.73								

Class symbols H= High, I=inundation, Mm=Mass movement , M= Moderate, N=None, Se=Severe, Sh=Sheetwash, S=Slight, W=Water

In test site 2, automated classification using Bands ERS-2 SAR, PC1 and a ratio of TM bands 5 and 3 was employed and PC1, Inveterd band 3 and SAR in case of ASTER data. Six possible clusters were made possible through visual interpretation. However, the area of gullying was not fully classified into one cluster. Number of clusters was increased to 10. Three classes resulted after masking the clustered product; 1) exposed subsoil 2) micro-relief and 3) non-affected areas.

Abrasion areas were not successfully classified using the radar data. It is because the backscattering signal received by the sensor is a composite of three types of surface roughness: 1) abrasion, 2) dunes and 3) micro-relief. The inclusion of the radar data to classification successfully mapped however, areas prone to degradation. Figures 23 (a,b) presented in section 5.8 having different input bands in the optical range consistently show the micro-relief areas. The degraded areas are contained in a miro-relief zone considered as a pre-cursor to wind erosion in the area (Ataya, 2000; Nagelhout, 2001). In the map, the exposed subsoil is referred to as degraded areas and described as an association between abrasion and deposition mainly by wind erosion.

Compared to its detection by small format aerial photography with 5 meters spatial resolution (Nagelhout, 2001), the detection accuracy using Landsat TM is 51%. ASTER improved the accuracy to 56%.

Shown in figure 19 (refer to section 5.5.3) classification of the resulting temporal fused product by clustering or unsupervised classification helped in discriminating unnecessary features creating noise in the interpretation. Some of them could be open areas caused by road cuts, cultivation, etc. The reference to the segregation of degraded features is due its pattern from east to west direction.

5.8. Land Degradation Mapping

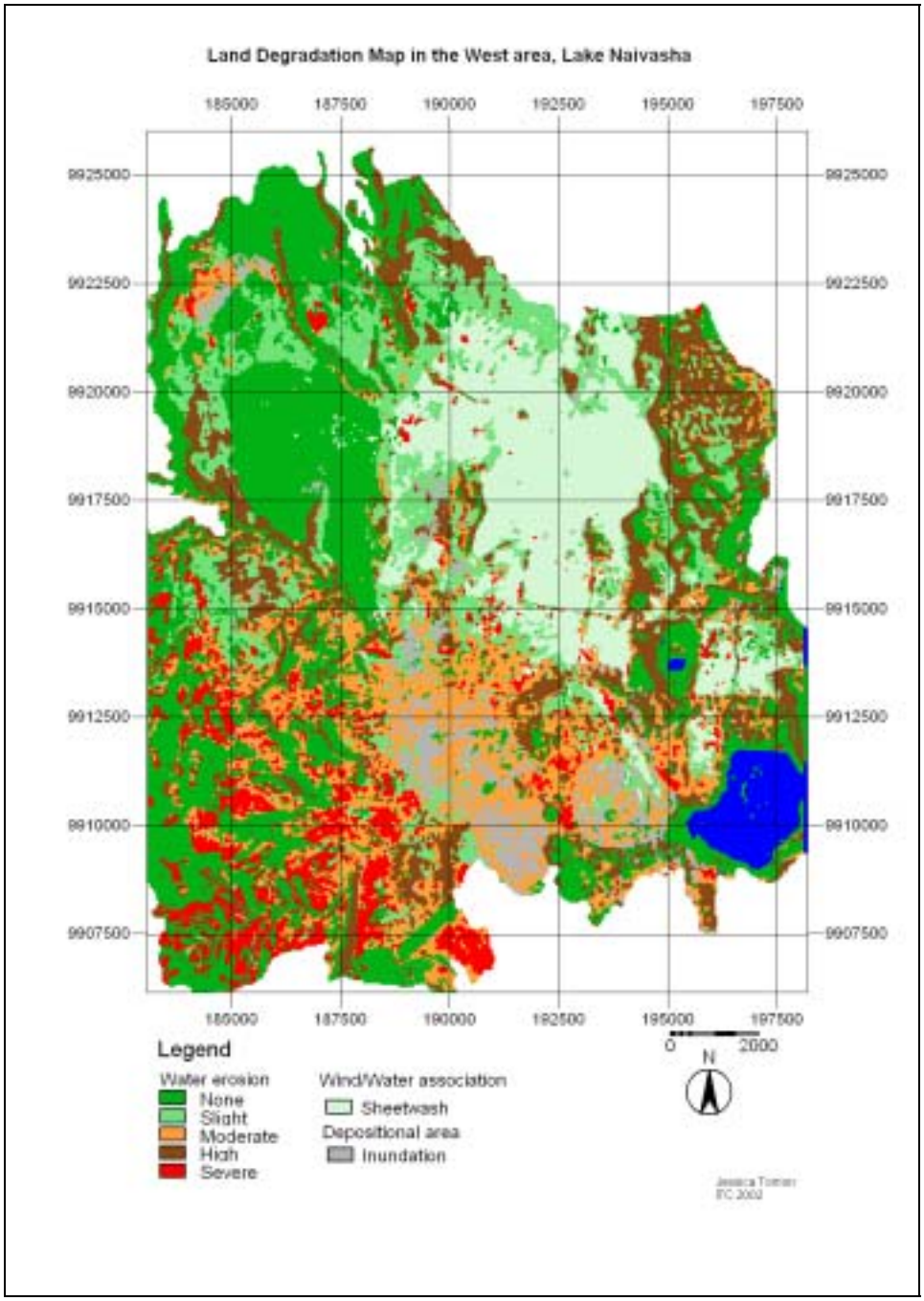

Figure 21. Land degradation map in the west area of Lake Naivasha

Figure 21 shows various land degradation classes and types in the west of Lake Naivasha. The map shows a contiguous vast area affected by sheetwash predominantly by wind erosion in association with water action. The inundated area is located to the adjacent areas affected by severely, highly and moderately degraded part of the area. Shown in figure 22, the highly degraded area is dominant affecting 3,328 hectares (refer table 13) while the moderate, slight and

sheetwash are affecting almost the same area. Affected by severe degradation covered 1,745 hectares. Five percent of the study area is affected by inundation.

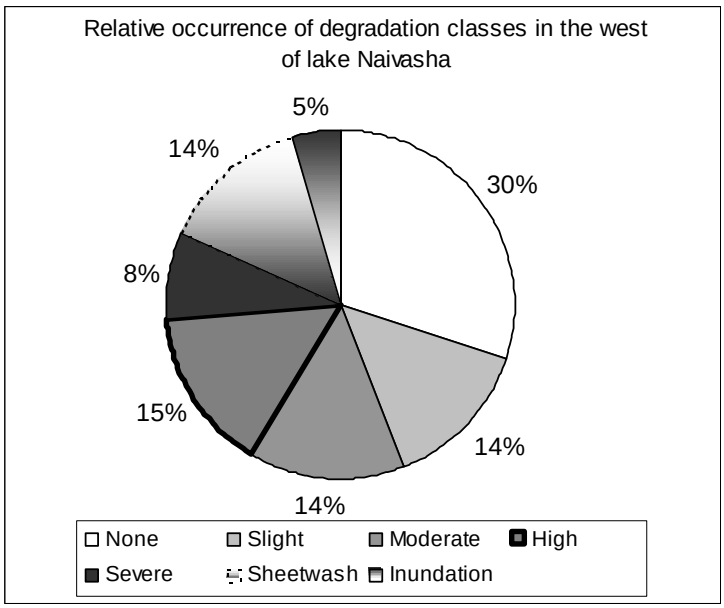

Figure 22. A pie chart showing the dominance of the various land degradation classes

Table 13 shows a summary of areas classified according to the land degradation types and classes associated with the major landscapes. The different severity classes of water erosion mostly occur in the step-faulted plateau (Pf) except for the moderate class. The severe class is concentrated within the landscape in the same way as the none degraded areas. Had it not with wheat farm situated at the Pf111 and Pf112 units of the landscape, degradation would have been worse. This landscape can be concluded as fragile and prone to soil erosion.

The sheetwash in association with water and wind factors are largely found in the Lacustrine Plain. Inundation areas are found in the Lacustrine Plain in Moindabe area(LP311). It serves as a depositional area of overland flow and sediments from the step faulted plateau.

An attempt to map degradation classes using the GLASOD legend framewok was carried out by calculating the degraded areas within the API interpretation for geopedologic mapping. As seen in table 14, the API mapping units usually contain more than 2 degradation classes. Difficulties were experienced in visualizing a final land degradation map using the GLASOD's legend framework.

Table 13. Summary of occurrence of various land degradation classes and types in the major landscapes

Land Degradation Classes	Major Landscape					Total
	Lacustrine plain	Lava flow plateau	Step-faulted plateau	Hilland	Mountain	
None	619.73 (9.45%)	123.50 (1.88%)	4,844.94 (**73.76**%)	871.29 (12.51%)	158.38 (2.41%)	6568.3 (100%
Slight	1,215.57 (**38.52**%)	163.16 (5.17%)	1,215.5 (**38.52**%)	408.76 (12.95%)	152.71 (4.84%)	3155.7 (100%)
Moderate	1,315.70 (**42.16%**)	76.41 (2.45%)	1,226.78 (39.31%)	498.37 (15.97%)	3.31 (0.11%)	3120.6 (100%)
High	693.24 (20.83%)	442.29 (13.29%)	1,245.88 (**37.44**%)	758.97 (22.81%)	187.43 (5.63%)	3327.8 (100%)
Severe	199.09 (11.41%)	13.59 (0.78%)	1,221.75 (**70.00**%)	300.80 (17.23%)	10.06 (0.58%)	1745.3 (100%)
Sheetwash	2,676.70 (**88.12**%)	21.83 (0.72%)	66.48 (2.19%)	266.62 (8.78)	6.03 (0.20%)	3037.7 (100%)
Inundation	818.80 (**81.64**%)	6.50 (0.65%)	111.56 (11.12%)	66.11 (6.59)	-	1003.0 (100%)

Table 14. Showing the relative frequency of occurrence of the different land degradation classes within API units

Units	N	%	S	%	M	%	H	%	Se	%	Sh	%	I	%	Total
Hi111	37.7	0.6	0.3	0.0	0.9	0.0	37.9	1.1		0.0	0.2	0.0	6.0	0.6	82.9
Hi121	23.8	0.4	0.7	0.0	5.2	0.2	10.4	0.3	0.6	0.0	0.7	0.0	1.1	0.1	42.4
Hi131	23.8	0.4	1.2	0.0	1.7	0.1	5.8	0.2		0.0	1.7	0.1	7.0	0.7	41.2
Hi151	0.3	0.0	9.8	0.3		0.0	1.9	0.1		0.0	3.6	0.1		0.0	15.6
Hi161	29.3	0.4	72.5	2.3	142.3	4.6	128.8	3.9	34.9	2.0	7.8	0.3	0.2	0.0	415.8
Hi221	103.0	1.6	89.5	2.8		0.0	156.8	4.7	5.6	0.3		0.0	0.1	0.0	354.9
Hi221		0.0		0.0	20.2	0.6		0.0		0.0	4.6	0.2		0.0	24.8
Hi222	0.2	0.0	2.2	0.1	0.1	0.0	16.8	0.5		0.0	0.1	0.0		0.0	19.3
Hi231	14.2	0.2	117.2	3.7	0.7	0.0	49.5	1.5	2.2	0.1	174.4	5.7	8.8	0.9	366.9
Hi241	81.4	1.2	0.4	0.0	14.2	0.5	27.9	0.8	2.0	0.1		0.0	2.0	0.2	127.8
Hi242	72.5	1.1	1.4	0.0	106.0	3.4	74.2	2.2	32.0	1.8		0.0	10.0	1.0	296.1
Hi243	51.9	0.8	0.1	0.0	11.5	0.4	32.4	1.0	2.1	0.1	3.9	0.1	13.9	1.4	115.9
Hi251	74.8	1.1	18.4	0.6	75.8	2.4	14.2	0.4	27.5	1.6		0.0	1.5	0.1	212.2
Hi252	88.1	1.3	6.3	0.2	26.0	0.8	5.7	0.2	80.1	4.6		0.0	0.8	0.1	206.9
Hi311	37.9	0.6	6.6	0.2	1.7	0.1	23.7	0.7	0.1	0.0		0.0	0.3	0.0	70.3
Hi321	64.2	1.0		0.0	1.5	0.0	4.1	0.1		0.0		0.0	0.1	0.0	69.9
Hi322	6.9	0.1		0.0		0.0		0.0		0.0		0.0		0.0	6.9
Hi331	0.8	0.0	2.2	0.1	1.3	0.0	1.5	0.0		0.0		0.0		0.0	5.8
Hi332	42.8	0.7	5.5	0.2	4.2	0.1	31.2	0.9	1.6	0.1	7.0	0.2	0.1	0.0	92.6
Hi333	12.6	0.2	37.8	1.2	16.1	0.5	94.1	2.8	13.7	0.8	59.8	2.0	11.3	1.1	245.4
Hi341	2.3	0.0		0.0		0.0	1.7	0.1	0.1	0.0		0.0		0.0	4.1
Hi351	13.6	0.2	29.9	0.9	22.6	0.7	19.8	0.6	7.4	0.4	0.5	0.0	1.5	0.1	95.3
Hi361	16.5	0.3		0.0		0.0		0.0		0.0		0.0	0.7	0.1	17.2
Hi361		0.0		0.0	26.4	0.8	8.0	0.2	45.3	2.6		0.0		0.0	79.7
Hi362	16.9	0.3		0.0	17.0	0.5		0.0	45.2	2.6		0.0	0.8	0.1	79.9
Hi371	6.3	0.1		0.0		0.0		0.0		0.0		0.0	0.1	0.0	6.5
Hi371		0.0	6.9	0.2	3.0	0.1	12.8	0.4	0.5	0.0	2.2	0.1		0.0	25.3
Lp111	452.3	6.9	824.6	26.1	333.1	10.7	553.0	16.6	125.8	7.2	2452.8	80.7	129.5	12.9	4871.0
Lp211	13.4	0.2	31.2	1.0	47.9	1.5	37.6	1.1	13.0	0.7	39.6	1.3	3.1	0.3	185.8
Lp221	41.9	0.6	55.9	1.8	13.8	0.4	54.1	1.6	4.0	0.2	80.6	2.7	7.8	0.8	258.0
Lp311	91.2	1.4	155.4	4.9	728.8	23.4	0.6	0.0	0.5	0.0	32.8	1.1	671.2	66.9	1680.4
Lp321	21.0	0.3	148.6	4.7	192.2	6.2	48.0	1.4	55.8	3.2	70.9	2.3	7.3	0.7	543.6
Mo111	135.6	2.1	142.8	4.5	2.5	0.1	170.6	5.1	7.7	0.4	6.0	0.2		0.0	465.2
Mo211	22.8	0.3	9.9	0.3	0.9	0.0	16.8	0.5	2.4	0.1		0.0		0.0	52.7
Pf111	1456.4	22.2	604.6	19.2	229.1	7.3	1.2	0.0	294.1	16.9	2.3	0.1	62.9	6.3	2650.6
Pf112	1145.0	17.4	0.5	0.0	9.0	0.3	0.7	0.0	1.9	0.1	21.3	0.7	9.9	1.0	1188.3
Pf113	5.8	0.1	104.5	3.3	1.6	0.0	102.5	3.1		0.0		0.0	2.6	0.3	216.9
Pf121	226.6	3.5	149.1	4.7	247.8	7.9	187.9	5.6	174.9	10.0	0.4	0.0	15.0	1.5	1001.8
Pf211	416.7	6.3	47.3	1.5	285.3	9.1	148.6	4.5	177.0	10.1	0.3	0.0	2.0	0.2	1077.1
Pf221	242.7	3.7	7.7	0.2	16.4	0.5	23.8	0.7	49.7	2.8		0.0		0.0	340.2
Pf231	14.5	0.2	75.1	2.4	23.9	0.8	22.4	0.7	4.7	0.3	35.9	1.2	0.4	0.0	176.9
Pf241	136.5	2.1	0.4	0.0		0.0	0.1	0.0		0.0		0.0		0.0	137.1
Pf311	64.1	1.0	0.7	0.0	7.4	0.2	0.6	0.0	27.0	1.5		0.0	0.8	0.1	100.5
Pf321	2.3	0.0	32.3	1.0	2.5	0.1	23.9	0.7	0.3	0.0	0.3	0.0	1.2	0.1	62.7
Pf421	40.9	0.6	98.6	3.1	193.3	6.2	176.4	5.3	93.2	5.3	2.2	0.1	5.8	0.6	610.4
Pf511	666.6	10.1	73.5	2.3	75.2	2.4	380.4	11.4	33.2	1.9	3.9	0.1	6.3	0.6	1239.1
Pf521	391.2	6.0	19.0	0.6	114.1	3.7	115.7	3.5	351.2	20.1		0.0	2.8	0.3	994.2
Pf522	17.4	0.3		0.0	3.2	0.1	52.5	1.6	6.6	0.4		0.0	1.9	0.2	81.4
Pf531	18.3	0.3	2.2	0.1	18.2	0.6	9.2	0.3	7.9	0.5		0.0		0.0	55.8
Pl111	94.5	1.4	119.1	3.8	72.1	2.3	349.9	10.5	11.7	0.7	0.3	0.0	2.4	0.2	649.9
Pl212	28.8	0.4	17.4	0.6	4.3	0.1	78.4	2.4	1.9	0.1	3.5	0.1	2.6	0.3	136.9
Pl313	0.2	0.0	26.7	0.8		0.0	14.0	0.4		0.0	18.1	0.6	1.5	0.2	60.5
Total	6568.3	100	3155.7	100	3120.6	100	3327.8	100	1745.3	100	3037.7	100	1003.0	100	21958.4

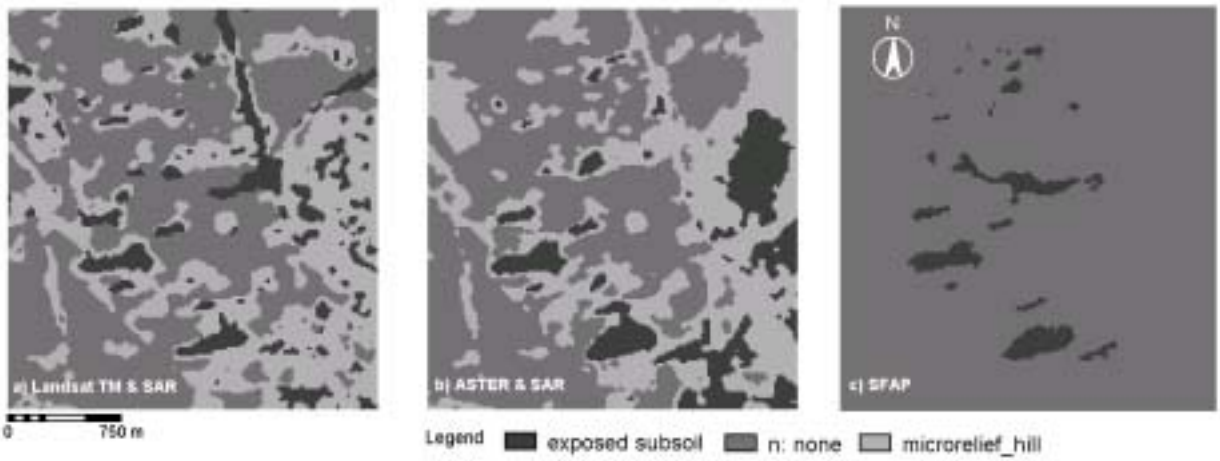

Figure 23.Land degradation map produced for the southeast area (Longonot) of Lake Navasha

Figure 23 shows the different performance of different data sources to detection of land degradation in the Longonot area. The first map (a) shows a classified map Landsat fused with SAR data. The second map (b) shows the performance of ASTER data fused with SAR data and the third (c) is the performance of the small format aerial photography (SFAP) (Nagelhout, 2001). The first two maps (a, b) show the performance of fusing radar data classifying areas prone to degradation. Micro-relief is considered precursor to wind erosion phenomenon in this area.

5.9. Land degradation monitoring

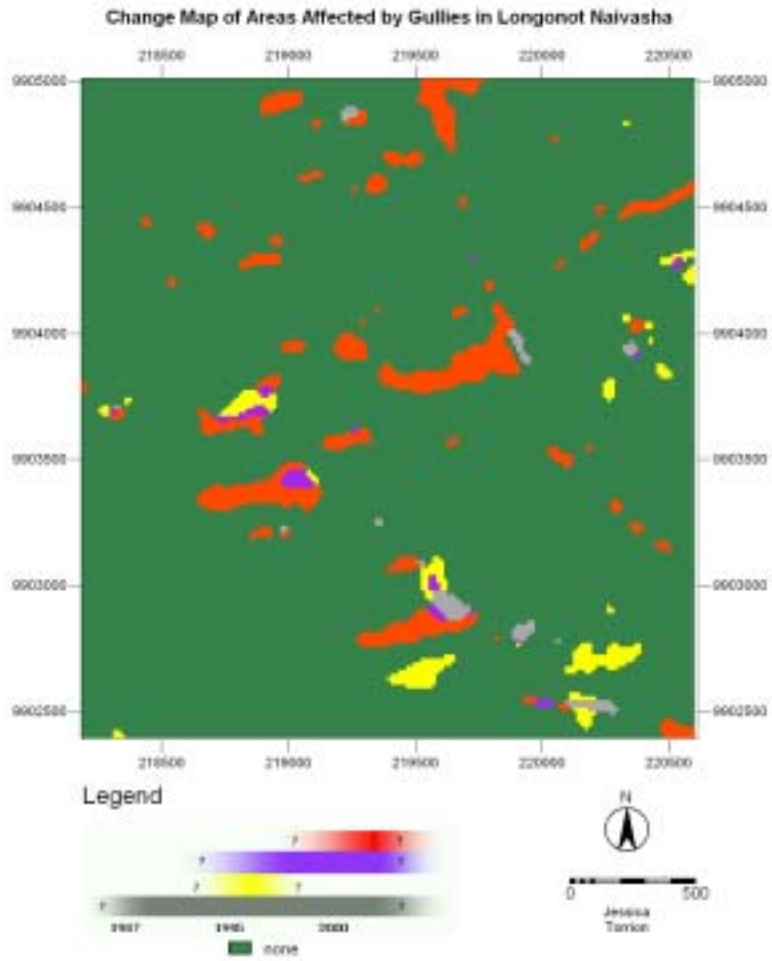

Figure 24. Temporal map of areas affected by gullies in Longonot area, Naivasha

Figure 24 shows the spatial changes of gullied area in Longonot. This is a product of fusing three temporal data, nanmely: 1) 2000 2) 1995 and 3) 1993. As to when these degraded features actually occurred is not known because the study only uses 3 temporal years. Actual occurrence of this features is not known. Time used in this study is "observation time" with which attributes and features are described at the moment when observations were made (Guptill, 1995). The "granularity" described as temporal resolution (Weir, 1999) increases the uncertainty to when they actually occur. Shown in the legend are uncertainties in between time. Some degradation features are observed in all dates (1987-2000), two dates (1995-2000) and in a single date (2000).

Degraded features observed in 1995 disappear in 2000. It can only be assumed that rehabilitation/growth of natural vegetation happen before the year 2000.

Degraded areas observed with time are shown in table 15 and trend data shown in table16. An exception to the cumulative calculation is the 1995 data, believed to get rehabilitated before the year 2000. Shown in figure 25, the trend of degradation is assumed linear.

Table 15. Temporal detection of areas affected by Gullies in Longonot area, Naivasha

Years	1987-2000	1995	1995-2000	2000
Area (hectares)	3.8	9.16	2.79	32.96

Table 16. Cumulative trend data affected by gullies

Years	1987	1995	2000
Area (hectares)	3.8	15.75	38.75

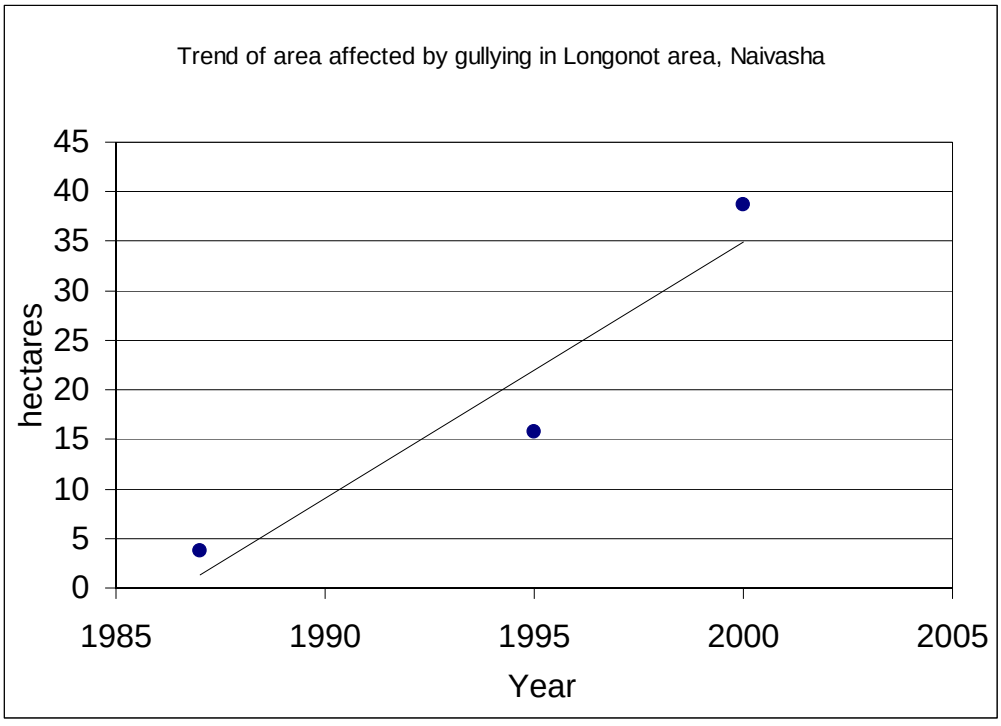

Chapter 6

Conclusion and Recommendation

6.1. Conclusion

The complimentary information of multi-source data proved to be useful in mapping land degradation not only with the remote sensing data but also considering the synthetic/ancillary image band. The digital elevation model added new dimension to classify degradation classes. The thermal and microwave data are also very useful in discriminating land degradation features. Radar data does not directly contributed to the detection of gullies. It mapped however, areas prone to degradation due to the contribution of micro relief to the backscatter signal of the Synthetic Aperture Radar.

Image fusion technique provides the means to maximize visualization of data from different sources through arithmetic fusion technique and subsequent transformation into color related fusion technique. Visual interpretation is indispensable to image fusion analysis. It includes evaluation of histogram for possible data re-scaling, pattern recognition, spectral integrity preservation and spatial improvement. The HIS transformation is an example where visual interpretation plays a key role. Due to the data transformation into intensity, hue and saturation domain, the spectral signature does changes. Therefore visual delineation of class boundaries is apparently valuable. In land degradation however, its detection is limited to broad degradation classes.

Multiplication of the transformed TM data such as the first three higher principal components to a different nature of data (thermal, microwave, and panchromatic) is found appropriate to quantify the separability advantage of an added feature dimension to classify various land degradation classes.

Multi-temporal image fusion to monitor land degradation improves the discrimination of superfluous features classified in single date imagery. The quantification of the degradation class is improved thus establishment of trend data is meaningful and reasonable.

Geopedologic mapping is vital when relating land degradation into landscape units. Landscape prone to water erosion is the step faulted plateau while the volcanic plain is prone to wind erosion. Using the geopedologic map, as a mapping unit to GLASOD legend framework seem

problematic. There are usually more than 2 degradation classes found per mapping unit and visualization becomes a constraint. Constraints to which generalizing spatial data forfeits the purpose of developing methods for an improved detection and mapping of land degradation useful for micro-scale planning.

6.2. Recommedation

Removing atmospheric effects is vital in optical remote sensing before any analysis of data is carried out. For change detection analysis, it will be better if data the data are acquired in the same season and preferably in the same month. Most of the available archived data do not satisfy this requirement. Usually, normalization of temporal data are employed.

Due to time constraint, the application of GLASOD legend framework was not carried out completely. This needs to be further studied.

Application of the image fusion techniques to other areas needs to be tested and verified. Success of image fusion is site specific.

References

ATAYA, C. O. (2000) Wind Erosion of Volcanic Soils: A reconnaissance study in the southern catchment of lake Naivasha Region, Kenya. MSc, ITC.

ATKILT, G. (2001) Soil survey to predict soil characteristics relevant to land management. MSc Thesis, ITC.

BARROW, C. J. (1994) *Land degradation : development and breakdown of terrestrial environments*. Cambridge University Press, Great Britain, 295 pp.

BECHT, R. (1998) Conflict and Trade-offs: The Lake Naivasha Case, pp. 8. ITC, Enschede, The Netherlands.

BLAIKIE, P. & BROOKFIELD, H. (1987) *Land degradation and society*, London, 296 pp.

BLUM, W. H. (1998) Foreward note. In: *Methods for Assessment of Soil Degradation* (Ed. by R. Lal, W. H. Blum, C. Valentine and B. A. Stewart). CRC Press, New York.

BRANDT, T. & MATHER, P. M. (2001) *Classification methods for remotely sensed data*. Taylor and Francis, New York etc, 332 pp.

CENTRAL INTELLIGENCE AGENCY MAP. (1988) Political Map, Kenya, *Vol. 2001*. Perry-Castañeda Library Map Collection, University of Texas at Austin.

CHAVEZ, G. L. (1982) Statistical method for selecting LANDSAT MSS ratios. *Journal of Applied Photographic Engineering*, **8**(1), 23-30.

CHAVEZ, P. (1988) An improved dark-object substraction technique for atmospheric scatterring correction of multi-spectral data. *Remote Sensing of Environment*, **24**, 459-479.

CLARKE, M. C. G., WOODHALL, D. G., ALLEN, D. & DARLING, G. (1990) Geological, volcanological and hydrogeological controls on the occurrence of geothermal activity in the area sorrounding Lake Naivasha, Kenya. British Geological Survey, Nairobe, Kenya, 138 pp.

CONACHER, A. J. & SALA, M. (1998) Land degradation in mediterranean environments of the world : nature and extent, causes and solutions. Wiley & Sons, 491 pp.

CONGALTON, G. R. & GREEN, K. (1999) *Assessing the accuracy of remotely sensed data : principles and practices*. Lewis Publishers, Boca Raton, 137 pp.

DE JONG, S. M. (1994) Applications of reflective remote sensing for land degradation studies in a mediterranean environment. Utrecht University, Utrecht, The Netherlands, 250 pp.

DREGNE, H. (1998) Land degradation: Assessment and Monitoring, pp. 32. International Task Force on Land Degradation.

DWIVEDI, R. S., KUMAR, A. B. & TEWARI, K. N. (1997a) The utility of multi-sensor data for mapping eroded lands. *International Journal of Remote Sensing*, **18**(11), 2303-2318.

Dwivedi, R. S., Ravi Sankar, T., Venkataratnam, L., Karale, R. L., Gawande, S. P., Seshagiri Rao, K. V., Senchaudhary, K. R., Bhaumik, K. R. & Mukharjee, K. K. (1997b) The Inventory and Monitoring of Eroded Lands Using Remote Sensing Data. *International Journal of Remote Sensing*, **18**(1), 109-119.

ESWARAN, H., LAL, R. & REICH, P. F. (2001) Land Degradation; An Overview. In: *Second International Conference on Land Degradation and Desertification* (Ed. by E. M. Bridges, I. D. Hannam, L. R. Oldeman, F. W. T. Pening de Vries and S. Sompatpanit). Oxford Press, Khon kaen, Thailand.

FAO. (1990) Guidelines for soil profile description. FAO, Rome, 70 pp.

FEINGERSH, T. (2000) Synergy of multi-temporal SAR and Optical imagery for crop mapping. MSc. Thesis, ITC.

FREDERIKSEN, P. (1993) Mapping and monitoring of soil degradation in semi-arid areas - satellite image methodology. *Geographica Hafniensia*, 49-52.

GLASOD. (1988) Guidelines for general assessment of the status of human induced soil degradation : Global Assessment of Soil Degradation GLASOD, pp. 25. ISRIC, Wageningen, The Netherlands.

GREEN, A. A., MARK, B., SWITZER, P. & CRAIG, M. (1988) A transformation for ordering multi-spectral data in tems of image quality with implications for noise removal. *IEEE Transactions on Geoscience and Remote Sensing*, **26**(1).

GUPTILL, S. C. (1995) Temporal Information. In: *Elements of spatial data quality* (Ed. by S. C. Guptill and J. L. Morrison), pp. 153-175. Elsevier on behalf of the International Cartographic Association, Oxford etc.

HELLDEN, U. L. F. & STERN, M. (1980) Monitoring land degradation in southern Tunisia: a test of Landsat imagery and digital data. *IAFHE RSL Research Report, Remote Sensing Laboratory, Institute of Agriculture Forestry and Home Economics, University of Minnesota*, **48**(42).

HENNEMANN, R. (2001a) Elective on Land Degradation, Assessment, Monitoring and Modelling. Soil Science Division, ITC, Enschede, The Netherlands.

HENNEMANN, R. (2001b) Some Notes About Soil and Land Degrafdation in the Naivasha Rangeland Zone, pp. 3. Soil Science Division, ITC, Enchede, The Netherlands.

HILL, J., MEGIER, J. & MEHL, W. (1995a) Land degradation, soil erosion and desertification monitoring in Mediterranean ecosystems. *Remote Sensing Reviews*, **12**(1-2), 107-130.

HILL, J., SOMMER, S., MEHL, W. & MEGIER, J. (1995b) Use of Earth observation satellite data for land degradation mapping and monitoring in Mediterranean ecosystems: towards a satellite-observatory. *Environmental Monitoring and Assessment*, **37**(1-3), 143-158.

HOOSBEEK, M. R., STEIN, A. & BRYANT, R. B. (1997) Mapping soil degradation. In: *Methods for assessment of soil degradation* (Ed. by R. Lal, W. H. Blum, C. Valentin and B. A. Stewart), pp. 407-423. CRC Press, Boca Raton. *Advances in Soil Science*.

HUANG, Y. & VAN GENDEREN, J. L. (1996) Evaluation of several speckle filtering techniques for ERS-1&2 imagery. *International Journal of Remote Sensing*, **31**(B2), 164-169.

HUURNEMAN, G. C., GENS, R. & BROEKEMA, L. (1996) Thematic information extraction in a neural network classification of multi sensor data including microwave phase information. *Internation Society of Photogrammetry and Remote Sensing*, **31**(B2), 170-175.

Janssen, L. L. F., Bakker, W. H., Reeves, C. V., Gorte, B. G. H., Pohl, C., Weir, M. J. C., Horn, J. A., Prakash, A. & Woldai, T. (2001) *Principles of remote sensing : an introductory textbook*. ITC, Enschede, 180 pp.

KAMONI, P. T. (1988) Detailed soil survey of a part of quarantine farm-National Husbandry Research Station, Naivasha, Nakuru District, pp. 24. Kenya Soil Survey, Nairobe.

KIAI, S. P. M. & MAILU, G. M. (1998) Wetland classification for agricultural development in Eastern and Southern Africa. FAO, Harare, Zimbabwe.

KING, C. & DELPONT, G. (1993) Spatial Assessment of Erosion: Contribution of Remote Sensing, a Review. *Remote Sensing Reviews*, **7**, 223-232.

LAL, R. (1998a) *Methods for assessment of soil degradation*. CRC Press, Boca Raton, New York, 558 pp.

LAL, R. (1998b) Preface note. In: *Methods for Assessment of Soil Degradation* (Ed. by R. Lal, W. H. Blum, C. Valentine and B. A. Stewart), New York.

LAL, R. & STEWART, B. A. (1985) Soil Degradation: A Global Threat. In: *Soil Degradation*, *Vol. 2* (Ed. by R. Lal and B. A. Stewart), pp. xiii-xvii. Springer-Verlag, New York. *Advances in Soil Science*.

LIANG, S., FALLAH-ADL, H., KALLURI, S., JA'JA', J., KAUFMAN, Y. J. & TOWNSHEND, R. G. (1997) An operational atmospherioc correction algorithm for LANDSAT thematic mapper imagery over the land. *Journal of Geophysical Research*, **102**(D14), 173-186.

LILLESAND, T. M. & KIEFER, R. W. (2000) *Remote sensing and image interpretation*. Wiley & Sons, New York etc, 724 pp.

LOPES, A., TOUZI, R. & NEZRY, E. (1990) Adaptive speckle filters and scene heterogeneity. *IEEE Transactions on Geoscience and Remote Sensing*, **28**(6), 992-1000.

LYNDEN, G. W. J. & OLDEMAN, L. R. (1997) The Assessment of the Status of Human-induced soil degradation in South and Southeast Asia, pp. 14. ISRIC, Wagenigen, The Netherlands.

METTERNICHT, G. I. (1996) Detecting and monitoring land degradation features and processes in Cochabamba Valleys,Bolivia: a synergistic approach. ITC, Enschede, The Netherlands, 390 pp.

METTERNICHT, G. I. (1999) Current status and future prospects of radar remote sensing for cartographic applications. *Cartography*, **28**(1), 1-17.

METTERNICHT, G. I. & ZINCK, J. A. (1997) Synergy of JERS-1 SAR and LANDSAT TM data for detecting and mapping soil erosion features. In: *SELPER meeting*, pp. 11, Merida, Venezuela.

MITICHE, A. & AGGARWAL, A. (1986) Multi Sensor Integration/Fusion Through Image Processing: A Review. *Optical Engineering*, **25**(3), 380-386.

MOHAMMED, S. O. (1993) Monitoring land degradation as indicator of desertification in North-Western Nigeria : an application of remote sensing and GIS. MSc, ITC.

NAGELHOUT, A. (2001) Performance Analysis of Small Format Aerial Photography (SFAP) in Assessing Current Status and Trends in Wind Erosion: A case study in the Longonot-Kijabe Hill Area, Naivasha District, Kenya. MSc thesis, ITC.

OLDEMAN, L. R., HAKKELING, R. T. A. & SOMBROEK, W. G. (1991) *World map of the status of human - induced soil degradation : an explanatory note*. ISRIC and UNEP, Wagenigen and Nairobi, 34 pp.

OLDEMAN, L. R. & LYNDEN, G. W. J. (1997) Revisiting the GLASOD Methodolgy. In: *Methods for assessment of soil degradation* (Ed. by R. Lal, W. H. Blum, C. Valentin and B. A. Stewart), pp. 423-440. CRC Press, Boca Raton. *Advances in Soil Science*.

OMOSA, E. (1999) Conflicts over forests as a shared natural resource: the case of Mau forest. Finnish NGO, Finland.

PICKUP, G. (1989) New land degradation survey techniques for arid Australia : problems and prospects. *Australian Rangeland Journal*, **11**(2), 74-82.

POHL, C. (1996) Geometric aspects of multisensor image fusion for topographic map updating in the humid tropcs. ITC, Enschede, The Netherlands, 159 pp.

POHL, C. & VAN GENDEREN, J. L. (1995) Multitemporal SAR and fused ERS-1 SAR - SPOT XS image maps of Indonesia. In: *2nd ERS applications workshop*, pp. 6, London, UK.

POHL, C. & VAN GENDEREN, J. L. (1998) Multisensor image fusion in remote sensing : concepts, methods and applications. *International Journal of Remote Sensing*, **19**(5), 823-854.

RAINA, P., JOSHI, D. C. & KOLARKAR, A. S. (1993) Mapping of soil degradation by using remote sensing on alluvial plain, Rajasthan, India. *Arid Soil Research and Rehabilitation*, **7**(2), 145-161.

RICHARDS, J. A. & JIA, X. (1999) *Remote sensing digital image analysis : an introduction*. Springer Verlag, Berlin, 363 pp.

ROSSITER, D. G. & HENGL, T. (2001) Creating geometrically-correct photo-interpretations, photomosaics, and base maps for a project GIS, *Vol. 2002*. http://www.itc.nl/~rossiter/teach/lecnotes.html#TN_Georef, Enschede.

SABINS, F. F. (1987) *Remote sensing : principles and interpretation*. W.H. Freeman, New York, 449 pp.

SIDERIUS, W. (1998) Soils of The Lake Naivasha Environs. In: *Contribution to the article in ITC journal*, pp. 8. Soil Science Division, ITC, Enshede, The Netherlands.

SIERRA-CORREA, P. C. (2001) Coastal landscape analysis using advanced remote sensing techniques for ICZM : case study in Cuapi - Iscuande, Pacific Coast, Colombia. MSc Thesis, ITC.

SINGH, A. (1989) Digital Change Detection Techniques Using Remotely-Sensed Data. *International Journal of Remote Sensing*, **10**(6), 989-1003.

SOMBROEK, W. G., BRAUN, H. M. H. & VAN DER POUW, B. J. A. (1980) *Exploratory soil map and agro - climatic zone map of Kenya*. Kenya Soil Survey, Ministry of Agriculture, National Agricultural Laboratories, Nairobi.

SOMMER, S., HILL, J. & MEGIER, J. (1998) The potential of remote sensing for monitoring rural land use changes and their effects on soil conditions. *Agriculture Ecosystems and Environment*, **67**(2-3), 197-209.

SUJATHA, G., DWIVEDI, R. S., SREENIVAS, K. & VENKATARATNAM, L. (2000) Mapping and monitoring of degraded lands in part of Jaunpur district of Uttar Pradesh using temporal spaceborne multispectral data. *International Journal of Remote Sensing*, **21**(3), 519-531.

SWAIN, P. H. & DAVIS, S. M. (1978) *Remote sensing : the quantitative approach*. McGraw-Hill, New York etc, 396 pp.

TRIPATHY, G. K., GHOSH, T. K. & SHAH, S. D. (1996) Monitoring of desertification process in Karnataka state of India using multi-temporal remote sensing and ancillary information using GIS. *International Journal of Remote Sensing*, **17**(12), 2243-2257.

USDA. (1993) *Soil survey manual*. Soil Conservation Service, Washington, D.C, 437 pp.

USDA. (1994) Munsell Soil Color Chart. In: *Soil Survey Handbook*, *Vol. 18*. USDA.

VAN GENDEREN, J. L. & POHL, C. (1994) Image fusion : issues, techniques and applications. In: *EARSeL workshop on intelligent image fusion*, pp. 2, Strasbourg, France.

WALD, L. (1999) Definitions and Terms of Reference in Data Fusion. *International Archives of Photogrammetry and Remote Sensing*, **32**(part 7-4-6 W6).

WEIR, M. J. C. (1999) Ensuring and maintaining data quality in geographical information systems for forest land management. Ph.D Dissertation, University of London.

WOODHALL, D. G., CLARKE, C. G., MWAGONGO, F. M., KORIO, R. & NDOGO, M. (1988) Geological Map of Longonot Vocano, the Greater Olkaria and Eburru Volcanic Complexes and Adjacent Areas. Ministry of Energy, Geothermal Section, Kenya.

WORLD ATLAS. (1996) African continent outline map, *Vol. 2002*. World Atlas.

XU, P. (1999) Despeckling SAR-type multiplicative noise. *International Journal of Remote Sensing*, **20**(13), 2577-2596.

YESOU', H., BESNUS & ROLET, J. (1993) Extraction of spectral information for Landsat TM data and merger with SPOT panchromatic imagery: a contribution to the study of geologic structures. *International Archives of Photogrammetry and Remote Sensing*, **48**, 23-36.

ZINCK, J. A. (1988/89) Physiography and Soils. ITC Lecture Notes SOL. 41. :, pp. 156. International Institute for Aerospace Survey & Earth Sciences (ITC), Enschede, The Netherlands.

Appendices

Appendix A. Orthophoto geometric erros

Category	Flight runs	Photo no.	control points	Sigma value	Pixel size (m)	Error (m)
Photo	Run 3	49	8	22.796	1.042	23.75
		50	9	23.860	1.056	25.20
		51	9	23.401	1.066	24.94
		52	10	35.006	1.055	36.93
	Run 4	60	10	22.280	1.087	24.22
		61	8	9.082	1.087	9.87
Mylar	Run 3	49	8	4.128	7.252	29.94
		50	8	10.80	2.456	26.52
		51	9	10.808	2.477	26.77
		52	10	15.041	2.451	36.86
	Run 4	60	9	2.798	7.523	21.05
		61	9	5.816	2.534	14.74

Appendix B. Typical land degradation features

Appendix C. Separability indices, d_{norm}

Landsat TM Band 5

Band	*Water*	*Slight*	*Sheetwash*	*Severe*	*None*	*Moderate*	*mass movement*	*Inundation*
Slight	7.94							
Sheetwash	52.50	1.86						
Severe	10.43	0.38	1.51					
None	27.92	0.60	3.26	0.08				
Moderate	5.32	0.97	3.28	1.41	2.01			
Mass	2.21	5.31	17.74	6.70	12.28	3.50		
Inundation	14.39	0.88	0.89	0.52	0.75	1.99	8.67	
High	4.63	1.55	4.40	2.06	2.96	0.52	2.88	2.74
MEDIAN	2.81							

Landsat TM Band 6

Band	*Water*	*Slight*	*Sheetwash*	*Severe*	*None*	*Moderate*	*mass movement*	*Inundation*
Slight	11.45							
Sheetwash	36.21	1.52						
Severe	6.94	2.43	5.21					
None	21.20	0.65	1.14	3.78				
Moderate	6.89	3.28	6.96	0.64	5.07			
Mass movement	1.55	3.22	5.13	1.54	4.23	1.20		
Inundation	5.74	4.66	9.78	1.80	7.15	1.22	0.54	
High	3.60	1.48	2.73	0.10	2.11	0.50	1.19	1.20
MEDIAN	2.98							

Landsat TM Band 7

Band	*Water*	*Slight*	*Sheetwash*	*Severe*	*None*	*Moderate*	*mass movement*	*Inundation*
Slight	5.09							
Sheetwash	42.31	1.95						
Severe	9.21	0.12	3.71					
None	44.81	2.09	0.59	3.98				
Moderate	7.42	0.55	4.48	0.64	4.74			
Mass	1.91	3.20	12.57	4.71	13.01	3.78		
Inundation	14.65	1.38	0.33	2.26	0.59	2.85	7.59	
High	6.37	0.85	5.02	1.08	5.28	0.43	3.20	3.26
MEDIAN	3.48							

Landsat TM Panchromatic

Band	*Water*	*Slight*	*Sheetwash*	*Severe*	*None*	*Moderate*	*mass movement*	*Inundation*
Slight	2.74							
Sheetwash	18.06	3.25						
Severe	7.25	1.81	1.00					
None	1.88	2.12	13.93	6.08				
Moderate	7.77	2.12	0.44	0.38	6.57			
Mass	1.75	0.80	5.17	2.98	1.09	3.32		
Inundation	7.72	1.98	0.78	0.17	6.48	0.22	3.18	
High	2.33	0.17	3.40	1.96	1.77	2.26	0.60	2.12
MEDIAN	2.12							

Prinicipal Component 1

Band	*Water*	*Slight*	*Sheetwash*	*Severe*	*None*	*Moderate*	*mass movement*	*Inundation*
Slight	5.85							
Sheetwash	78.60	2.60						
Severe	13.59	0.46	4.14					
None	34.83	0.82	8.83	0.47				
Moderate	6.03	0.07	2.86	0.57	0.98			
Mass	2.16	3.89	19.27	7.37	12.26	3.94		
Inundation	19.47	1.62	1.21	1.90	2.46	1.78	10.22	
High	5.00	1.00	5.21	1.96	2.85	0.95	2.95	3.38
MEDIAN	2.90							

Prinicipal Component 2

Band	*Water*	*Slight*	*Sheetwash*	*Severe*	*None*	*Moderate*	*mass movement*	*Inundation*
Slight	1.88							
Sheetwash	5.73	0.19						
Severe	4.82	1.41	2.75					
None	0.42	2.22	10.45	5.73				
Moderate	6.95	1.43	3.54	0.39	9.25			
Mass	2.88	0.83	1.46	0.35	3.27	0.13		
Inundation	3.82	0.33	1.00	1.50	4.94	1.55	0.75	
High	3.88	0.18	0.03	2.40	5.68	2.87	1.33	0.84
MEDIAN	1.71							

Principal Component 3

Band	*Water*	*Slight*	*Sheetwash*	*Severe*	*None*	*Moderate*	*mass movement*	*Inundation*
Slight	8.31							
Sheetwash	3.28	5.62						
Severe	4.05	0.53	2.94					
None	609.50	2.34	30.30	2.23				
Moderate	1.32	3.84	0.13	2.23	10.78			
Mass	2.53	3.65	0.87	2.03	11.38	0.47		
Inundation	4.06	0.76	2.87	0.16	2.72	2.14	1.92	
High	4.52	1.41	2.91	0.57	4.61	2.02	1.74	0.41
MEDIAN	2.44							

ERS-2 SAR

Band	*Water*	*Slight*	*Sheetwash*	*Severe*	*None*	*Moderate*	*mass movement*	*Inundation*
Slight	1.61							
Sheetwash	1.35	0.73						
Severe	0.26	2.45	2.54					
None	0.18	1.98	1.80	0.76				
Moderate	1.78	0.33	0.57	3.20	2.43			
Mass movement	1.21	0.15	0.42	1.77	1.41	0.09		
Inundation	4.26	1.81	3.64	7.10	6.05	3.01	1.71	
High	4.58	2.08	4.03	7.62	6.53	3.39	1.94	0.36
MEDIAN	1.80							

Fused PC 1 and ERS-2 SAR

Band	*Water*	*Slight*	*Sheetwash*	*Severe*	*None*	*Moderate*	*mass movement*	*Inundation*
Slight	5.88							
Sheetwash	15.83	1.42						
Severe	3.72	2.35	5.42					
None	5.47	1.69	4.46	0.90				
Moderate	4.80	0.36	1.83	1.80	1.17			
Mass movement	1.45	3.74	8.11	1.59	2.63	3.06		
Inundation	26.50	2.88	2.11	8.11	7.02	3.25	11.82	
High	11.31	1.65	0.63	4.90	4.14	1.99	6.90	0.87
MEDIAN	3.15							

Fused PC1 and TM Thermal Band (TM6)

Band	*Water*	*Slight*	*Sheetwash*	*Severe*	*None*	*Moderate*	*mass movement*	*Inundation*
Slight	4.91							
Sheetwash	49.70	2.64						
Severe	7.89	1.05	7.69					
None	23.58	0.87	4.75	3.77				
Moderate	4.46	1.42	7.07	0.74	3.96			
Mass movement	1.29	3.79	20.23	4.80	12.06	2.91		
Inundation	6.79	1.60	9.55	0.89	5.13	0.03	3.90	
High	2.90	1.41	5.77	0.85	3.42	0.30	2.01	0.27
MEDIAN	3.78							

Fused PC2 and ERS-2 SAR

Band	*Water*	*Slight*	*Sheetwash*	*Severe*	*None*	*Moderate*	*mass movement*	*Inundation*
Slight	2.10							
Sheetwash	5.78	0.29						
Severe	4.58	0.74	1.60					
None	0.00	2.10	5.78	4.58				
Moderate	8.59	1.17	2.78	0.33	8.59			
movement	3.19	0.74	1.35	0.17	3.19	0.05		
Inundation	5.11	0.79	1.74	0.01	5.11	0.34	0.16	
High	6.32	0.47	1.41	0.53	6.32	1.16	0.59	0.58
MEDIAN	1.38							

Fused PC3 and ERS-2 SAR

Band	*Water*	*Slight*	*Sheetwash*	*Severe*	*None*	*Moderate*	*mass movement*	*Inundation*
Slight	7.12							
Sheetwash	3.68	5.03						
Severe	3.35	1.45	2.16					
None	59.84	2.10	21.73	4.18				
Moderate	1.20	3.15	0.19	1.36	7.89			
movement	2.34	2.97	0.93	1.08	8.21	0.43		
Inundation	5.78	0.09	4.28	1.38	1.57	2.86	2.68	
High	5.94	0.03	4.33	1.31	1.85	2.84	2.65	0.10
MEDIAN	2.67							

Appendix D. Surface descriptions

LAND COVER/SURFACE DESCRIPTION FORM
Training Samples for Land Degradation Mapping

1. General

Observation ID	001
Date	September 25, 2001
Authors	J. Torrion
Location	Moindabe
GPS Code	021
Latitude (X)	188545
Longitude (Y)	9910210
Elevation	2092
Slope (%), form & length	30

2. Surface description

2.1 Land cover (natural vegetation/crops)

Land cover type(vegetation/crop/etc) in pixel area	Leleshwa shrubs and grasses
Percent Cover (%)	20-30
Average vegetation height (m)	1-2
Vegetation roughness(m)	1-2
Overall vegetation/crop type &^ status within 200 m radius, North	Leleshwa shrubs, grasses and yellow fever trees
East	Agricultural (corn/beans) and yellow fever
South	Leleshwa shrubs and grasses
West	Leleshwa shrubs, corn and grasses

2.2 Soil surface

Bareness (%)	>80
Roughness (plough ridges, cloddiness, etc)	
Graveliness/stoniness (%)	5 (15 cm diam.)
Crusting	-
Surface soil color	Dry 7.5YR 5/4 Moist 7.5YR 3/2
Surface soil texture	Sandy loam

Remarks

The soil is gravelly (pumice) and very loose. Augering was not possible

A gully like structure was observed with 90 cm top soil removal in

2.3 Land degradation features

LD type	water erosion, wind erosion, sealing and crusting, mass movements, subsoil compaction, sodification, salinization
LD sub-type	Sheet erosion, rill erosion, gully erosion, piping erosion, slumping, mudflows, deflation, abrasion, deposition, etc
LD intensity class	Slight, moderate, high, very high
% LD occurrence in pixel/map unit	
LD severity class	

	Depth of topsoil removal (cm)	Penetration resistance (kg/cm2)
1	11	4
2	20	>4.5
3	13	3.0
4	22	3.0
5	23	3.0
6	70	4.0
7	17	>4.5
8	29	>4.5
Mean	25.6	
Remarks		

Description of rills

Width (cm)	Depth (cm)	Length (m)	Shape
25	20	>10	U shape

Description of gullies

Width (m)	Depth (m)	Length (m)	Shape

Sketch

LAND COVER/SURFACE DESCRIPTION FORM
Training Samples for Land Degradation Mapping

1. General

Observation ID	02
Date	September 25, 2001
Authors	J. Torrion
Location	Gunyumu, side slope of the vale
GPS Code	026
Latitude (X)	187062
Longitude (Y)	9909705
Elevation	2190
Slope (%), form & length	100

2. Surface description

2.1 Land cover (natural vegetation/crops)

Land cover type(vegetation/crop/etc) in pixel area	Leleshwa shrubs and very few grasses
Percent Cover (%)	20
Average vegetation height (m)	<1
Vegetation roughness(m)	
Overall vegetation/crop type &^ status within 200 m radius, North	Grassland, heavily grazed
East	Corn fields
South	Saiso, grasses and corn fields
West	Leleshwa, grassland and corn fields

2.2 Soil surface

Bareness (%)	>80
Roughness (plough ridges, cloddiness, etc)	Saiso, trees and resistant spots from erosion
Graveliness/stoniness (%)	-
Crusting	-
Surface soil color	Dry 7.5YR 5/3 Moist 7.5YR 2.5/2
Surface soil texture	Gritty sandy loam

Remarks

- Erosion occur on the side slope of the vale
- Lower part are green
- Soils is very loose and friable
- overgrazed

2.3 Land degradation features

LD type	water erosion, wind erosion, sealing and crusting, mass movements, subsoil compaction, sodification, salinization	
LD sub-type	Sheet erosion, rill erosion, gully erosion, piping erosion, slumping, mudflows, deflation, abrasion, deposition, etc	
LD intensity class	Slight, moderate, high, very high	
% LD occurrence in pixel/map unit		
LD severity class		
	Depth of topsoil removal (cm)	Penetration resistance (kg/cm2)
1	80	>4.5
2	43	>4.5
3	100	3.0
4	52	2.0
5	32	2.5
6	33	>4.5
7	120	4.0
8	26	4.0
Mean	61	
Remarks		

Description of rills

Width (m)	Depth (m)	Length (m)	Shape
0.45	0.54	25.0	U shape
0.35	0.33	20.0	U shape

Description of gullies

Width (m)	Depth (m)	Length (m)	Shape
2.18	0.80	2.0	U shape
1.34	0.32	4.0	U shape
20.0	>2.0	25.0	V shape

Sketch

Soil depth (cm)	Color	pH	Texture	Plasticity	Stickiness
?	7.5YR 5/3	5.0	Gritty sandy loam	Non-plastic	Non-sticky

LAND COVER/SURFACE DESCRIPTION FORM
Training Samples for Land Degradation Mapping

1. General

Observation ID	003
Date	September 25, 2001
Authors	J. Torrion
Location	Gunyumu
GPS Code	028
Latitude (X)	187480
Longitude (Y)	9909775
Elevation	2138
Slope (%), form & length	2, gentle

2. Surface description

2.1 Land cover (natural vegetation/crops)

Land cover type(vegetation/crop/etc) in pixel area	Grasses (road side)
Percent Cover (%)	50
Average vegetation height (m)	.20
Vegetation roughness(m)	>4 m trees
Overall vegetation/crop type &^ status within 200 m radius, North	Corn field and grasses
East	Corn field
South	Corn field and grassland
West	Corn field, beans and few trees

2.2 Soil surface

Bareness (%)	50
Roughness (plough ridges, cloddiness, etc)	
Graveliness/stoniness (%)	-
Crusting	-
Surface soil color	Dry 10R 3/3 Moist 10R 2.5/1
Surface soil texture	Sandy clay loam

Remarks

- Very deep gully/collapse (suffotion)
- Very friable soil

2.3 Land degradation features

LD type	water erosion, wind erosion, sealing and crusting, mass movements, subsoil compaction, sodification, salinization	
LD sub-type	Sheet erosion, rill erosion, gully erosion, piping erosion, slumping, mudflows, deflation, abrasion, deposition, etc	
LD intensity class	Slilght, moderate, high, very high	
% LD occurrence in pixel/map unit		
LD severity class		
	Depth of topsoil removal (cm)	Penetration resistance (kg/cm2)
1	>500	2.5
2	70 cm	3.5
3		
4		
5		
6		
7		
8		
Mean		
Remarks		

Description of rills

Width (m)	Depth (m)	Length (m)	Shape

Description of gullies

Width (m)	Depth (m)	Length (m)	Shape
19.1	>5.0	49	?

Sketch

Soil depth (cm)	Color	pH	Texture	Plasticity	Stickiness
	10R 3/3	5.0	Sandy clay loam	Slightly plastic	Slightly sticky

LAND COVER/SURFACE DESCRIPTION FORM
Training Samples for Land Degradation Mapping

1. General

Observation ID	004
Date	September 25, 2001
Authors	J. Torrion
Location	Gunyumu (near the village)
GPS Code	029
Latitude (X)	188398
Longitude (Y)	9909043
Elevation	2099
Slope (%), form & length	35, concave

2. Surface description

2.1 Land cover (natural vegetation/crops)

Land cover type(vegetation/crop/etc) in pixel area	Grasses and thorny acacia
Percent Cover (%)	15
Average vegetation height (m)	1
Vegetation roughness(m)	
Overall vegetation/crop type &^ status within 200 m radius, North	Residential area, shops
East	Residential area, corn fields & few trees
South	Corn fields and grasses
West	Grassland

2.2 Soil surface

Bareness (%)	85
Roughness (plough ridges, cloddiness, etc)	Resistant spots to sediment trasport
Graveliness/stoniness (%)	90 (1-3 cm diam pumice)
Crusting	-
Surface soil color	Dry Moist
Surface soil texture	Sandy loam

Remarks

- Rills and sheetwash in the residential areas
- The area is affected by sheetwash with some gullying and rills occurrence
- The 85% bare is totally degraded
- Gullying (severe)

2.3 Land degradation features

LD type	water erosion, wind erosion, sealing and crusting, mass movements, subsoil compaction, sodification, salinization	
LD sub-type	Sheet erosion, rill erosion, gully erosion, piping erosion, slumping, mudflows, deflation, abrasion, deposition, etc	
LD intensity class	Slilght, moderate, high, very high	
% LD occurrence in pixel/map unit		
LD severity class		
	Depth of topsoil removal (cm)	Penetration resistance (kg/cm2)
1	28	3.5
2	32	2.5
3	33	3.0
4	40	1.0
5	40	1.0
6	50	1.5
7	35	3.5
8	33	1.0
Mean	36	2.1
Remarks		

Description of rills

Width (cm)	Depth (cm)	Length (cm)	Shape
40	24	>300	U shape

Description of gullies

Width (m)	Depth (m)	Length (m)	Shape
13.1	3-5	>30	V shape

Sketch

Soil depth (cm)	Color	pH	Texture	Plasticity	Stickiness
		5.5	Sandy loam		

LAND COVER/SURFACE DESCRIPTION FORM
Training Samples for Land Degradation Mapping

1. General

Observation ID	005
Date	September 26, 2001
Authors	J. Torrion & R. Hennemann
Location	Lacustrine plain of Ndabibi
GPS Code	031
Latitude (X)	0193541
Longitude (Y)	9917454
Elevation	1960
Slope (%), form & length	0.5

2. Surface description

2.1 Land cover (natural vegetation/crops)

Land cover type(vegetation/crop/etc) in pixel area	Grassland (herb-aporphai & alesegrai; grass – ngugit)
Percent Cover (%)	40-80
Average vegetation height (m)	
Vegetation roughness(m)	
Overall vegetation/crop type &^ status within 200 m radius, North	Grassland
East	Grassland
South	Grassland
West	Grassland

2.2 Soil surface

Bareness (%)	20-60
Roughness (plough ridges, cloddiness, etc)	
Graveliness/stoniness (%)	10 (1-2 cm pumice)
Crusting	-
Surface soil color	Dry 10YR 5/4 Moist 10YR 3/2
Surface soil texture	Fine sandy clay loam

Remarks

- 60% of the bareness affected by sheetwash

2.3 Land degradation features

LD type	water erosion, wind erosion, sealing and crusting, mass movements, subsoil compaction, sodification, salinization	
LD sub-type	Sheet erosion, rill erosion, gully erosion, piping erosion, slumping, mudflows, deflation, abrasion, deposition, etc	
LD intensity class	Slight, moderate, high, very high	
% LD occurrence in pixel/map unit		
LD severity class		
	Depth of topsoil removal (cm)	Penetration resistance (kg/cm2)
1	1	>4.5
2	1.5	>4.5
3		
4		
5		
6		
7		
8		
Mean		>4.5
Remarks		

Description of rills

Width (cm)	Depth (cm)	Length (cm)	Shape

Description of gullies

Width (m)	Depth (m)	Length (m)	Shape

Sketch

Soil depth (cm)	Color	pH	Texture	Plasticity	Stickiness
0-30	10YR 5/4	5.5	Fine sandy clay loam	Slightly plastic	Non-sticky
30-40	10YR 6/6	5.0	- (gravelly)	Non-plastic	Slightly sticky
40-80	10YR 6/6	5.0	-(gravelly)	Non-plastic	Slightly sticky
80+	10YR 6/6	5.5	-(gravelly)	Non-plastic	Slightly sticky

LAND COVER/SURFACE DESCRIPTION FORM
Training Samples for Land Degradation Mapping

1. General

Observation ID	006
Date	September 26, 2001
Authors	J. Torrion/R. Hennemann
Location	Lacustrine Plain
GPS Code	032
Latitude (X)	192980
Longitude (Y)	9917623
Elevation	1951
Slope (%), form & length	.5 (very gentle)

2. Surface description

2.1 Land cover (natural vegetation/crops)

Land cover type(vegetation/crop/etc) in pixel area	Dominated by grasses (ngugit) and some shrubs (Oloceda)
Percent Cover (%)	>80
Average vegetation height (m)	
Vegetation roughness(m)	
Overall vegetation/crop type &^ status within 200 m radius, North	Dominated by grasses (ngugit) and some shrubs (Oloceda)
East	Dominated by grasses (ngugit) and some shrubs (Oloceda)
South	Dominated by grasses (ngugit) and some shrubs (Oloceda)
West	Dominated by grasses (ngugit) and some shrubs (Oloceda)

2.2 Soil surface

Bareness (%)	10-20
Roughness (plough ridges, cloddiness, etc)	-
Graveliness/stoniness(%)	-
Crusting	-
Surface soil color	Dry 2.5 YR 5/4 Moist 2.5 YR 3/2
Surface soil texture	

Remarks

- Presence of burrowing animal activities
- Some micro-relief

2.3 Land degradation features

LD type	water erosion, wind erosion, sealing and crusting, mass movements, subsoil compaction, sodification, salinization	
LD sub-type	Sheet erosion, rill erosion, gully erosion, piping erosion, slumping, mudflows, deflation, abrasion, deposition, etc	
LD intensity class	Slight, moderate, high, very high	
% LD occurrence in pixel/map unit		
LD severity class		
	Depth of topsoil removal (cm)	Penetration resistance (kg/cm2)
1	5	>4.5
2		2.3
3		3.2
4		2.1
5		>4.5
6		
7		
8		
Mean		
Remarks		

Description of rills

Width (cm)	Depth (cm)	Length (cm)	Shape

Description of gullies

Width (m)	Depth (m)	Length (m)	Shape

Sketch

Soil depth (cm)	Color	pH	Texture	Plasticity	Stickiness
0-30	2.5Y 5/4	4.5	Sandy clay loam	Slightly plastic	Non-sticky
30-80	2.5Y 6/4	4.5	Sandy clay loam	Slightly plastic	Slightly sticky
80+	2.5Y 6/4	8.0	Sandy loam	Slightly plastic	Non-sticky

LAND COVER/SURFACE DESCRIPTION FORM
Training Samples for Land Degradation Mapping

1. General

Observation ID	007
Date	September 26, 2001
Authors	J. Torrion. H. Hennemann
Location	Lacustrine Plain
GPS Code	033
Latitude (X)	192440
Longitude (Y)	9917562
Elevation	1954
Slope (%), form & length	.2-.5

2. Surface description

2.1 Land cover (natural vegetation/crops)

Land cover type(vegetation/crop/etc) in pixel area	Grassland
Percent Cover (%)	80
Average vegetation height (m)	
Vegetation roughness(m)	
Overall vegetation/crop type &^ status within 200 m radius, North	Dominated by ngugit grass and some oloceda shrub
East	Dominated by ngugit grass and some oloceda shrub
South	Dominated by ngugit grass and some oloceda shrub
West	Dominated by ngugit grass and some oloceda shrub

2.2 Soil surface

Bareness (%)	20
Roughness (plough ridges, cloddiness, etc)	
Graveliness/stoniness (%)	
Crusting	
Surface soil color	Dry Moist
Surface soil texture	
Remarks	

2.3 Land degradation features

LD type	water erosion, wind erosion, sealing and crusting, mass movements, subsoil compaction, sodification, salinization
LD sub-type	Sheet erosion, rill erosion, gully erosion, piping erosion, slumping, mudflows, deflation, abrasion, deposition, etc
LD intensity class	Slight, moderate, high, very high
% LD occurrence in pixel/map unit	
LD severity class	

	Depth of topsoil removal (cm)	Penetration resistance (kg/cm2)
1	3	3
2		3.5
3		3.2
4		3.5
5		4.0
6		3.5
7		4.0
8		3.0
Mean		3.5
Remarks		

Description of rills

Width (cm)	Depth (cm)	Length (cm)	Shape

Description of gullies

Width (m)	Depth (m)	Length (m)	Shape

Sketch

Soil depth (cm)	Color	pH	Texture	Plasticity	Stickiness
0-30	2.5Y 5/4	4.5	Sandy clay loam	Slightly plastic	Non-sticky
30-80	2.5Y 6/4	4.5	Sandy clay loam	Slightly plastic	Slightly sticky
80+	2.5Y 6/4	8.0	Sandy loam	Slightly plastic	Non-sticky

LAND COVER/SURFACE DESCRIPTION FORM
Training Samples for Land Degradation Mapping

1. General

Observation ID	008
Date	September 27, 2001
Authors	J. Torrion
Location	Ndabibi escarpment
GPS Code	034
Latitude (X)	188657
Longitude (Y)	9919105
Elevation	2052
Slope (%), form & length	23

2. Surface description

2.1 Land cover (natural vegetation/crops)

Land cover type(vegetation/crop/etc) in pixel area	Grass (ngugit) and herbs (luceda and Luyavacea
Percent Cover (%)	>80
Average vegetation height (m)	
Vegetation roughness(m)	
Overall vegetation/crop type &^ status within 200 m radius, North	Grass (ngugit) and herbs (luceda and Luyavacea
East	Grassland (grazing)
South	Leleshwa and shrubs
West	Shrubs (Luyavacea)

2.2 Soil surface

Bareness (%)	10
Roughness (plough ridges, cloddiness, etc)	
Graveliness/stoniness (%)	
Crusting	
Surface soil color	Dry Moist
Surface soil texture	

Remarks

- Shrubs used for charcoal
- 50% of the bareness affected by sheetwash
- Ngugit grass predominate

2.3 Land degradation features

LD type	water erosion, wind erosion, sealing and crusting, mass movements, subsoil compaction, sodification, salinization	
LD sub-type	Sheet erosion, rill erosion, gully erosion, piping erosion, slumping, mudflows, deflation, abrasion, deposition, etc	
LD intensity class	Slight, moderate, high, very high	
% LD occurrence in pixel/map unit		
LD severity class		
	Depth of topsoil removal (cm)	Penetration resistance (kg/cm2)
1	2	>4.5
2	3	>4.5
3		>4.5
4		>4.5
5		
6		
7		
8		
Mean		>4.5
Remarks		

Description of rills

Width (cm)	Depth (cm)	Length (cm)	Shape

Description of gullies

Width (m)	Depth (m)	Length (m)	Shape

Sketch

Soil depth (cm)	Color	pH	Texture	Plasticity	Stickiness
0-30	2.5Y 5/2	5.0	Sandy clay loam	Slightly platic	Sticky
30-90	2.5Y 4/4	5.0	Sandy clay loam	Slightly plastic	Slightly sticky
90+	2.5Y 5/6	5.0	Loamy sand	Non-plastic	Non-sticky

LAND COVER/SURFACE DESCRIPTION FORM
Training Samples for Land Degradation Mapping

1. General

Observation ID	009
Date	September 27, 2001
Authors	J. Torrion
Location	Ndabibi escarpment
GPS Code	035
Latitude (X)	188571
Longitude (Y)	9918978
Elevation	2058
Slope (%), form & length	24

2. Surface description

2.1 Land cover (natural vegetation/crops)

Land cover type(vegetation/crop/etc) in pixel area	Leleshwa and grasses
Percent Cover (%)	50
Average vegetation height (m)	1
Vegetation roughness(m)	1
Overall vegetation/crop type &^ status within 200 m radius, North	Leleshwa and grasses
East	Leleshwa and grasses
South	Leleshwa and grasses
West	Leleshwa and grasses

2.2 Soil surface

Bareness (%)	50
Roughness (plough ridges, cloddiness, etc)	
Graveliness/stoniness (%)	
Crusting	
Surface soil color	Dry 2.5Y 5/4 Moist 2.5Y 3/2
Surface soil texture	

Remarks

- Grasses predominates in the area, followed by leleshwa shrubs and some herbs (oloceda)
- Very few rills observed

2.3 Land degradation features

LD type	water erosion, wind erosion, sealing and crusting, mass movements, subsoil compaction, sodification, salinization	
LD sub-type	Sheet erosion, rill erosion, gully erosion, piping erosion, slumping, mudflows, deflation, abrasion, deposition, etc	
LD intensity class	Slight, moderate, high, very high	
% LD occurrence in pixel/map unit		
LD severity class		
	Depth of topsoil removal (cm)	Penetration resistance (kg/cm2)
1	5	2.0
2	3	1.0
3	2	3.0
4	2	3.0
5	3	2.0
6	4	4.0
7	5	3.5
8	7	4.0
Mean	4	2.8
Remarks		

Description of rills

Width (cm)	Depth (cm)	Length (cm)	Shape

Description of gullies

Width (m)	Depth (m)	Length (m)	Shape
30	15		U shape

Sketch

Soil depth (cm)	Color	pH	Texture	Plasticity	Stickiness
0-30	2.5Y 5/4	5.0	Gritty sandy loam	Slightly plastic	Non-sticky
30-90	2.5Y 5/6	5.0	Sandy loam	Slightly plastic	Non-sticky
90+	2.5Y 5/4	5.0	Loamy sand	Slightly plastic	Non-sticky

LAND COVER/SURFACE DESCRIPTION FORM
Training Samples for Land Degradation Mapping

1. General

Observation ID	010
Date	September 27, 2001
Authors	J. Torrion
Location	Ndabibi escarpment
GPS Code	036
Latitude (X)	188491
Longitude (Y)	9919001
Elevation	2075
Slope (%), form & length	30

2. Surface description

2.1 Land cover (natural vegetation/crops)

Land cover type(vegetation/crop/etc) in pixel area	Leleshwa and thorned acacia
Percent Cover (%)	40
Average vegetation height (m)	2
Vegetation roughness(m)	
Overall vegetation/crop type &^ status within 200 m radius, North	Leleshwa and thorned acacia
East	Leleshwa and thorned acacia
South	Leleshwa and thorned acacia
West	Leleshwa and thorned acacia

2.2 Soil surface

Bareness (%)	60
Roughness (plough ridges, cloddiness, etc)	
Graveliness/stoniness (%)	80 (1 cm diam. Pumice)
Crusting	
Surface soil color	Dry2.5Y 5/3 Moist 2.5Y 3/3
Surface soil texture	Sandy loam
Remarks	

2.3 Land degradation features

LD type	water erosion, wind erosion, sealing and crusting, mass movements, subsoil compaction, sodification, salinization	
LD sub-type	Sheet erosion, rill erosion, gully erosion, piping erosion, slumping, mudflows, deflation, abrasion, deposition, etc	
LD intensity class	Slight, moderate, high, very high	
% LD occurrence in pixel/map unit		
LD severity class		
	Depth of topsoil removal (cm)	Penetration resistance (kg/cm2)
1	44	1.5
2	67	2.0
3	120	3.0
4		2.5
5		3.0
6		1.5
7		
8		
Mean		2.25
Remarks		

Description of rills

Width (cm)	Depth (cm)	Length (cm)	Shape

Description of gullies

Width (m)	Depth (m)	Length (m)	Shape
1.05	0.44	?	U shape
0.85	0.67	?	U Shape

Sketch

Soil depth (cm)	Color	pH	Texture	Plasticity	Stickiness
0-30	2.5Y 5/3	5.0	Sandy loam	Slightly plastic	Slightly sticky
30+	2.5Y 3/3	4.5	Sandy loam	Slightly plastic	Slightly sticky

LAND COVER/SURFACE DESCRIPTION FORM
Training Samples for Land Degradation Mapping

1. General

Observation ID	011
Date	September 27, 2001
Authors	J. Torrion
Location	Riverside of the Lava flow plateau
GPS Code	037
Latitude (X)	194281
Longitude (Y)	9919989
Elevation	1968
Slope (%), form & length	8

2. Surface description

2.1 Land cover (natural vegetation/crops)

Land cover type(vegetation/crop/etc) in pixel area	Corn
Percent Cover (%)	40
Average vegetation height (m)	1
Vegetation roughness(m)	
Overall vegetation/crop type &^ status within 200 m radius, North	Corn and grasses
East	Corn and grasses
South	Corn and grasses
West	Corn, grasses and shrubs

2.2 Soil surface

Bareness (%)	60
Roughness (plough ridges, cloddiness, etc)	Plough ridges
Graveliness/stoniness (%)	40 (1-2 cm diam. Pumice)
Crusting	
Surface soil color	Dry Moist
Surface soil texture	

Remarks

- No observable erosion features

2.3 Land degradation features

LD type	water erosion, wind erosion, sealing and crusting, mass movements, subsoil compaction, sodification, salinization	
LD sub-type	Sheet erosion, rill erosion, gully erosion, piping erosion, slumping, mudflows, deflation, abrasion, deposition, etc	
LD intensity class	Slight, moderate, high, very high	
% LD occurrence in pixel/map unit		
LD severity class		
	Depth of topsoil removal (cm)	Penetration resistance (kg/cm2)
1		1.0
2		1.5
3		0.5
4		1.0
5		0.5
6		1.0
7		
8		
Mean		0.92
Remarks		

Description of rills

Width (cm)	Depth (cm)	Length (cm)	Shape

Description of gullies

Width (m)	Depth (m)	Length (m)	Shape

Sketch

Soil depth (cm)	Color	pH	Texture	Plasticity	Stickiness
0-30	7.5YR 6/3	5.5	Sandy loam	Slightly plastic	Non-sticky
30.80	7.5YR 5/3	5.0	Sandy loam	Slightly plastic	Non-sticky
80+	7.5YR 4/3	5.0	Sandy loam	Slightly plastic	Non-sticky

LAND COVER/SURFACE DESCRIPTION FORM
Training Samples for Land Degradation Mapping

1. General

Observation ID	012
Date	September 27, 2001
Authors	J. Torrion
Location	midslope of Eburru
GPS Code	038
Latitude (X)	189380
Longitude (Y)	9922252
Elevation	2138
Slope (%), form & length	

2. Surface description

2.1 Land cover (natural vegetation/crops)

Land cover type(vegetation/crop/etc) in pixel area	Leleshwa and grasses (heavily vegetated)
Percent Cover (%)	>80
Average vegetation height (m)	
Vegetation roughness(m)	
Overall vegetation/crop type &^ status within 200 m radius, North	Leleshwa and grasses (heavily vegetated)
East	Leleshwa and grasses (heavily vegetated)
South	Leleshwa and grasses (heavily vegetated)
West	Leleshwa and grasses (heavily vegetated)

2.2 Soil surface

Bareness (%)	10
Roughness (plough ridges, cloddiness, etc)	
Graveliness/stoniness (%)	
Crusting	
Surface soil color	Dry Moist
Surface soil texture	

Remarks

- Leleshwa area that is not eroded (maybe due to the ground cover (grasses)
- The lower slope has less vegetation and is severely affected by sheetwash and gully erosion

2.3 Land degradation features

LD type	water erosion, wind erosion, sealing and crusting, mass movements, subsoil compaction, sodification, salinization	
LD sub-type	Sheet erosion, rill erosion, gully erosion, piping erosion, slumping, mudflows, deflation, abrasion, deposition, etc	
LD intensity class	Slight, moderate, high, very high	
% LD occurrence in pixel/map unit		
LD severity class		
	Depth of topsoil removal (cm)	Penetration resistance (kg/cm2)
1	3.0	
2	4.0	
3		
4		
5		
6		
7		
8		
Mean		
Remarks		

Description of rills

Width (cm)	Depth (cm)	Length (cm)	Shape

Description of gullies

Width (m)	Depth (m)	Length (m)	Shape

Sketch

LAND COVER/SURFACE DESCRIPTION FORM
Training Samples for Land Degradation Mapping

1. General

Observation ID	013
Date	September 28, 2001
Authors	J. Torrion
Location	Mt. Longonot
GPS Code	013
Latitude (X)	
Longitude (Y)	
Elevation	
Slope (%), form & length	2

2. Surface description

2.1 Land cover (natural vegetation/crops)

Land cover type(vegetation/crop/etc) in pixel area	Ngugit grass
Percent Cover (%)	60
Average vegetation height (m)	
Vegetation roughness(m)	
Overall vegetation/crop type &^ status within 200 m radius, North	Ngugit grass
East	Ngugit grass
South	Ngugit grass
West	Ngugit grass

2.2 Soil surface

Bareness (%)	40
Roughness (plough ridges, cloddiness, etc)	Micro-relief and micro-sandunes
Graveliness/stoniness (%)	
Crusting	
Surface soil color	Dry Moist
Surface soil texture	

Remarks

2.3 Land degradation features

LD type	water erosion, wind erosion, sealing and crusting, mass movements, subsoil compaction, sodification, salinization	
LD sub-type	Sheet erosion, rill erosion, gully erosion, piping erosion, slumping, mudflows, deflation, abrasion, deposition, etc	
LD intensity class	Slight, moderate, high, very high	
% LD occurrence in pixel/map unit		
LD severity class		
	Depth of topsoil removal (cm)	Penetration resistance (kg/cm2)
1		
2		
3		
4		
5		
6		
7		
8		
Mean		
Remarks		

Description of rills

Width (cm)	Depth (cm)	Length (cm)	Shape

Description of gullies

Width (m)	Depth (m)	Length (m)	Shape
14.16	1.10	38.90	U shape
15.13	0.97	66.17	U shape
11.66	1.50	42.40	U shape
10.70	1.45	46.50	U shape
21.32	1.07	50.30	U shape
22.00	1.20	142.60	U shape

Sketch

LAND COVER/SURFACE DESCRIPTION FORM
Training Samples for Land Degradation Mapping

1. General

Observation ID	014
Date	September 30, 2001
Authors	J. Torrion
Location	Ndabibi escarpment
GPS Code	170
Latitude (X)	188360
Longitude (Y)	9918918
Elevation	2092
Slope (%), form & length	11 (straight)

2. Surface description

2.1 Land cover (natural vegetation/crops)

Land cover type(vegetation/crop/etc) in pixel area	Dominated by herd and some are leleshwa
Percent Cover (%)	>80
Average vegetation height (m)	0.70
Vegetation roughness(m)	2 m trees (few)
Overall vegetation/crop type &^ status within 200 m radius, North	Wheat farm
East	Leleshwa
South	Wheat and leleshwa
West	Wheat

2.2 Soil surface

Bareness (%)	10
Roughness (plough ridges, cloddiness, etc)	
Graveliness/stoniness (%)	
Crusting	
Surface soil color	Dry10YR 4/3 Moist 10YR 2/1
Surface soil texture	Sandy clay loam

Remarks

- No evidence of erosion

2.3 Land degradation features

LD type	water erosion, wind erosion, sealing and crusting, mass movements, subsoil compaction, sodification, salinization	
LD sub-type	Sheet erosion, rill erosion, gully erosion, piping erosion, slumping, mudflows, deflation, abrasion, deposition, etc	
LD intensity class	Slight, moderate, high, very high	
% LD occurrence in pixel/map unit		
LD severity class		
	Depth of topsoil removal (cm)	Penetration resistance (kg/cm2)
1		3.0
2		3.5
3		4.0
4		3.5
5		4.0
6		3.0
7		3.0
8		4.0
Mean		
Remarks		

Description of rills

Width (cm)	Depth (cm)	Length (cm)	Shape

Description of gullies

Width (m)	Depth (m)	Length (m)	Shape

Sketch

Soil depth (cm)	Color	pH	Texture	Plasticity	Stickiness
0-30	10YR 4/3	5.0	Sandy clay loam	Plastic	Sticky
30-80	10YR 4/4	4.5	Silty clay	Very plastic	Very sticky
80+	10YR 5/6	5.0	Sandy loam	Plastic	Sticky

LAND COVER/SURFACE DESCRIPTION FORM
Training Samples for Land Degradation Mapping

1. General

Observation ID	015
Date	September 30, 2001
Authors	J. Torrion
Location	Ndabibi Escarpment
GPS Code	172
Latitude (X)	188707
Longitude (Y)	9919386
Elevation	2054
Slope (%), form & length	10, straight and somewhat undulated

2. Surface description

2.1 Land cover (natural vegetation/crops)

Land cover type(vegetation/crop/etc) in pixel area	Overgrazed grassland, burned leleshwa for charcoal
Percent Cover (%)	30
Average vegetation height (m)	0.20
Vegetation roughness(m)	5m tree
Overall vegetation/crop type &^ status within 200 m radius, North	Agriculture (wheat)
East	Grassland
South	Protected leleshwa and shrubs
West	Over-grazed and leleshwa

2.2 Soil surface

Bareness (%)	70
Roughness (plough ridges, cloddiness, etc)	
Graveliness/stoniness (%)	20 (1 cm diam. Pumice)
Crusting	Evident
Surface soil color	Dry10YR 4/3 Moist 10YR 2/1
Surface soil texture	Sandy loam

Remarks

2.3 Land degradation features

LD type	water erosion, wind erosion, sealing and crusting, mass movements, subsoil compaction, sodification, salinization	
LD sub-type	Sheet erosion, rill erosion, gully erosion, piping erosion, slumping, mudflows, deflation, abrasion, deposition, etc	
LD intensity class	Slight, moderate, high, very high	
% LD occurrence in pixel/map unit		
LD severity class		
	Depth of topsoil removal (cm)	Penetration resistance (kg/cm2)
1	30	3.5
2	26	2.5
3	20	2.7
4	23	3.0
5	22	2.0
6	20	4.0
7	21	2.7
8	18	4.0
Mean	22	3.0
Remarks		

Description of rills

Width (cm)	Depth (cm)	Length (cm)	Shape

Description of gullies

Width (m)	Depth (m)	Length (m)	Shape

Sketch

Soil depth (cm)	Color	pH	Texture	Plasticity	Stickiness
0-30	10YR 4/3	5.0	Sandy loam	Moderately plastic	Slightly sticky
30-80	10YR 4/6	4.5	Sandy clay	Plastic	Sticky
80+	10YR 5/6	5.0	Sandy loam	Plastic	Sticky

LAND COVER/SURFACE DESCRIPTION FORM
Training Samples for Land Degradation Mapping

1. General

Observation ID	016
Date	September 30, 2001
Authors	J. Torrion
Location	Below the escarpment, Ndabibi
GPS Code	174
Latitude (X)	188983
Longitude (Y)	9919764
Elevation	2035
Slope (%), form & length	7, complex

2. Surface description

2.1 Land cover (natural vegetation/crops)

Land cover type(vegetation/crop/etc) in pixel area	Overgrazed grasses (i.e ngugit) and shrubs
Percent Cover (%)	10
Average vegetation height (%)	0.40
Vegetation roughness(m)	>5 m trees
Overall vegetation/crop type &^ status within 200 m radius, North	Plowed, quite bare
East	Corn field
South	Corn field and grasses
West	Grassland

2.2 Soil surface

Bareness (%)	90
Roughness (plough ridges, cloddiness, etc)	-
Graveliness/stoniness, %	10 (1 cm diam. Pumice)
Crusting	evident
Surface soil color	Dry. 10YR 5/4 Moist. 10YR 3/1
Surface soil texture	

Remarks

Over-grazed surfaces/abandoned

2.3 Land degradation features

LD type	water erosion, wind erosion, sealing and crusting, mass movements, subsoil compaction, sodification, salinization
LD sub-type	Sheet erosion, rill erosion, gully erosion, piping erosion, slumping, mudflows, deflation, abrasion, deposition, etc
LD intensity class	Slight, moderate, high, very high
% LD occurrence in pixel/map unit	
LD severity class	

	Depth of topsoil removal (cm)	Penetration resistance (kg/cm2)
1	4.0	2.0
2	2.0	2.5
3	3.0	2.7
4	4.5	2.5
5	2.0	3.5
6	4.5	3.7
7	4.0	3.5
8	3.5	3.5
Mean	3.4	2.9
Remarks		

Description of rills

Width (m)	Depth (m)	Length (m)	Shape

Description of gullies

Width (m)	Depth (m)	Length (m)	Shape

Sketch

Soil depth (cm)	Color	pH	Texture	Plasticity	Stickiness
0-30	10YR 5/4	4.5	sandy clay loam	plastic	sticky
30-80	10YR 4/4	5.0	Sandy loam	plastic	Slightly sticky
80+	10 YR 5/6	4.5	gritty sandy loam	plastic	Slightly sticky

LAND COVER / SURFACE DESCRIPTION FORM
Training Samples for Land Degradation Mapping

1. General

Observation ID	017
Date	September 30, 2001
Authors	J. Torrion
Location	Ndabibi
GPS Code	175
Latitude (X)	189408
Longitude (Y)	9920197
Elevation	2039
Slope (%), form & length	6, (concave, very gentle)

2. Surface description

2.1 Land cover (natural vegetation/crops)

Land cover type(vegetation/crop/etc) in pixel area	Yellowish grasses (dried and grazed)
Percent Cover (%)	40
Average vegetation height (m)	.2
Vegetation roughness(m)	>5m trees (few)
Overall vegetation/crop type &^ status within 200 m radius, North	Plowed plateau
East	>5 m trees
South	Dried grasses and shrubs
West	Dried grasses and corn

2.2 Soil surface

Bareness (%)	60
Roughness (plough ridges, cloddiness, etc)	
Graveliness/stoniness (%)	20, (1 cm diam. Pumice)
Crusting	Evident
Surface soil color	Dry 10YR 5/4 Moist 10YR 3/1
Surface soil texture	Sandy loam

Remarks

- Smooth and shiny surface (somewhat sealed)

2.3 Land degradation features

LD type	water erosion, wind erosion, sealing and crusting, mass movements, subsoil compaction, sodification, salinization	
LD sub-type	Sheet erosion, rill erosion, gully erosion, piping erosion, slumping, mudflows, deflation, abrasion, deposition, etc	
LD intensity class	Slight, moderate, high, very high	
% LD occurrence in pixel/map unit		
LD severity class		
	Depth of topsoil removal (cm)	Penetration resistance (kg/cm2)
1	<2	>4.5
2		>4.5
3		>4.5
4		>4.5
5		>4.5
6		>4.5
7		>4.5
8		>4.5
Mean		>4.5
Remarks		

Description of rills

Width (cm)	Depth (cm)	Length (cm)	Shape

Description of gullies

Width (m)	Depth (m)	Length (m)	Shape

Sketch

Soil depth (cm)	Color	pH	Texture	Plasticity	Stickiness
0-30	10YR 5/4	4.0	Sandy loam	Slightly plastic	Non-sticky
30-70	10YR 6/4	4.0	Loamy sand	Non-plastic	Non-sticky
70+	10YR 6/6	4.5	Sand and pebbles	Non-plastic	Non-sticky

LAND COVER/SURFACE DESCRIPTION FORM
Training Samples for Land Degradation Mapping

1. General

Observation ID	018
Date	September 30, 2001
Authors	J. Torrion
Location	Ndabibi (hill besides the vale of the plateau)
GPS Code	176
Latitude (X)	189228
Longitude (Y)	9921379
Elevation	2087
Slope (%), form & length	40 (concave, hills are terraced)

2. Surface description

2.1 Land cover (natural vegetation/crops)

Land cover type(vegetation/crop/etc) in pixel area	Leleshwa, thorned acacia and grasses
Percent Cover (%)	10
Average vegetation height (m)	2.5
Vegetation roughness(m)	
Overall vegetation/crop type &^ status within 200 m radius, North	Leleshwa and other srubs, grasses
East	Cultivation area (terraced)
South	Terraced (no crops)
West	Terraced (no crops)

2.2 Soil surface

Bareness (%)	90
Roughness (plough ridges, cloddiness, etc)	Plough ridges and contour lines
Graveliness/stoniness (%)	50, (1-2 cm diam pumice)
Crusting	Few (very thin)
Surface soil color	Dry 10YR 5/8 Moist 10YR ¾
Surface soil texture	gravelly

Remarks

- Exposed pumice layer

2.3 Land degradation features

LD type	water erosion, wind erosion, sealing and crusting, mass movements, subsoil compaction, sodification, salinization	
LD sub-type	Sheet erosion, rill erosion, gully erosion, piping erosion, slumping, mudflows, deflation, abrasion, deposition, etc	
LD intensity class	Slilght, moderate, high, very high	
% LD occurrence in pixel/map unit		
LD severity class		
	Depth of topsoil removal (cm)	Penetration resistance (kg/cm2)
1	40	>4.5
2	35	>4.5
3	55	>4.5
4	52	>4.5
5	53	>4.5
6	54	>4.5
7	32	>4.5
8	30	>4.5
Mean	44	>4.5
Remarks		

Description of rills

Width (cm)	Depth (cm)	Length (cm)	Shape

Description of gullies

Width (m)	Depth (m)	Length (m)	Shape

Sketch

Soil depth (cm)	Color	pH	Texture	Plasticity	Stickiness
0-30	10YR 5/8	5.0	Gravelly (pumice) sandy loam	Non-plastic	Non-sticky

LAND COVER/SURFACE DESCRIPTION FORM
Training Samples for Land Degradation Mapping

1. General

Observation ID	019
Date	September 30, 2001
Authors	J. Torrion
Location	Hill besides the lava flow plateau
GPS Code	177
Latitude (X)	192695
Longitude (Y)	9921056
Elevation	2007
Slope (%), form & length	15, concave

2. Surface description

2.1 Land cover (natural vegetation/crops)

Land cover type(vegetation/crop/etc) in pixel area	Ngugit grass and shrubs (some shrubs, few are wilted and dried)
Percent Cover (%)	70
Average vegetation height (m)	0.80
Vegetation roughness(m)	
Overall vegetation/crop type &^ status within 200 m radius, North	Corn field
East	Corn field
South	Corn field
West	Corn field

2.2 Soil surface

Bareness (%)	30
Roughness (plough ridges, cloddiness, etc)	Plough ridges
Graveliness/stoniness (%)	30, (1 cm diam. Pumice)
Crusting	Evident
Surface soil color	Dry 10YR 6/4 Moist 10YR 2/1
Surface soil texture	

Remarks

- Crusting not very pronounced
- Shiny surface (sealed)
- Abandoned corn field

2.3 Land degradation features

LD type	water erosion, wind erosion, sealing and crusting, mass movements, subsoil compaction, sodification, salinization
LD sub-type	Sheet erosion, rill erosion, gully erosion, piping erosion, slumping, mudflows, deflation, abrasion, deposition, etc
LD intensity class	Slight, moderate, high, very high
% LD occurrence in pixel/map unit	
LD severity class	

	Depth of topsoil removal (cm)	Penetration resistance (kg/cm2)
1	7	3.0
2	4	3.5
3	3	2.0
4	2	1.5
5	3	3.0
6	4	2.5
7	2	3.0
8	2	2.0
Mean	3.4	2.6
Remarks		

Description of rills

Width (cm)	Depth (cm)	Length (cm)	Shape

Description of gullies

Width (m)	Depth (m)	Length (m)	Shape

Sketch

Soil depth (cm)	Color	pH	Texture	Plasticity	Stickiness
0-40		4.8	Gravelly sandy loam	Slightly plastic	Slightly sticky
40-60	10YR 5/4	5.0	Gravelly sandy loam	Slightly plastic	Non-sticky
60+	10YR 4/6	5.0	Gravelly sandy loam	Slightly plastic	Slightly sticky

LAND COVER/SURFACE DESCRIPTION FORM
Training Samples for Land Degradation Mapping

1. General

Observation ID	020
Date	September 30, 2001
Authors	J. Torrion
Location	Njojo (below Eburru)
GPS Code	178
Latitude (X)	191988
Longitude (Y)	9921429
Elevation	1992
Slope (%), form & length	6 (undulating-complex)

2. Surface description

2.1 Land cover (natural vegetation/crops)

Land cover type(vegetation/crop/etc) in pixel area		Grassland(moigadyo, mbagi and ngugit)
Percent Cover (%)		20
Average vegetation height (m)		0.60
Vegetation roughness(m)		
Overall vegetation/crop type &^ status within 200 m radius,	North	Corn(vegetative stage)
	East	Corn (maturity)
	South	Grassland(moigadyo, mbagi and ngugit)
	West	Grassland(moigadyo, mbagi and ngugit)

2.2 Soil surface

Bareness (%)	80
Roughness (plough ridges, cloddiness, etc)	Plough ridges
Graveliness/stoniness (%)	40 (1 cm diam. Pumice)
Crusting	
Surface soil color	Dry 10YR 5/4 Moist 10YR 3/1
Surface soil texture	Gravelly loam

Remarks

- Abandoned (one year)
- Previously planted with corn and wheat

2.3 Land degradation features

LD type	water erosion, wind erosion, sealing and crusting, mass movements, subsoil compaction, sodification, salinization	
LD sub-type	Sheet erosion, rill erosion, gully erosion, piping erosion, slumping, mudflows, deflation, abrasion, deposition, etc	
LD intensity class	Slight, moderate, high, very high	
% LD occurrence in pixel/map unit		
LD severity class		
	Depth of topsoil removal (cm)	Penetration resistance (kg/cm2)
1	3.5	3.0
2	2.5	3.5
3	4.0	>4.5
4	2.0	4.0
5	1.5	3.0
6	3.0	>4.5
7	2.0	4.5
8	2.0	3.0
Mean	2.56	
Remarks		

Description of rills

Width (cm)	Depth (cm)	Length (cm)	Shape

Description of gullies

Width (m)	Depth (m)	Length (m)	Shape

Sketch

Soil depth (cm)	Color	pH	Texture	Plasticity	Stickiness
0-30	10YR 5/4	4.0	Gravelly loam	Non-platic	Non-sticky
30+	pumice				

LAND COVER/SURFACE DESCRIPTION FORM
Training Samples for Land Degradation Mapping

1. General

Observation ID	021
Date	October 2, 2001
Authors	J. Torrion
Location	Foot of Moindabe
GPS Code	179
Latitude (X)	192317
Longitude (Y)	9909982
Elevation	2014
Slope (%), form & length	6 (convex)

2. Surface description

2.1 Land cover (natural vegetation/crops)

Land cover type(vegetation/crop/etc) in pixel area	Grassland (ngugit and Oloceda)
Percent Cover (%)	45
Average vegetation height (m)	.30
Vegetation roughness(m)	
Overall vegetation/crop type &^ status within 200 m radius, North	Leleshwa and Euphorbia
East	Grasses and Shubs
South	Euphorbia and Leleshwa
West	Leleshwa and other shrubs

2.2 Soil surface

Bareness (%)	55
Roughness (plough ridges, cloddiness, etc)	
Graveliness/stoniness (%)	5
Crusting	Evident
Surface soil color	Dry 5Y 5/3 Moist 5Y 3/2
Surface soil texture	Loamy sand

Remarks

- Abandoned for three years

2.3 Land degradation features

LD type	water erosion, wind erosion, sealing and crusting, mass movements, subsoil compaction, sodification, salinization	
LD sub-type	Sheet erosion, rill erosion, gully erosion, piping erosion, slumping, mudflows, deflation, abrasion, deposition, etc	
LD intensity class	Slight, moderate, high, very high	
% LD occurrence in pixel/map unit		
LD severity class		
	Depth of topsoil removal (cm)	Penetration resistance (kg/cm2)
1	14	>4.5
2	16	>4.5
3	8	>4.5
4	15	>4.5
5	12	>4.5
6	14	>4.5
7	15	>4.5
8	10	>4.5
Mean	13	>4.5
Remarks		

Description of rills

Width (cm)	Depth (cm)	Length (cm)	Shape

Description of gullies

Width (m)	Depth (m)	Length (m)	Shape

Sketch

Soil depth (cm)	Color	pH	Texture	Plasticity	Stickiness
0-30	5Y 5/3	5.5	Loamy sand	Non-plastic	Non-sticky
30-80	5Y 6/3	5.5	Loamy sand	Non-plastic	Non-sticky
80+	5Y 6/3	7.0	Loamy sand	Non-plastic	Non-sticky

LAND COVER/SURFACE DESCRIPTION FORM
Training Samples for Land Degradation Mapping

1. General

Observation ID	022
Date	October 2, 2001
Authors	J. Torrion
Location	Hillslope
GPS Code	180
Latitude (X)	192382
Longitude (Y)	9910182
Elevation	2013
Slope (%), form & length	38 (straight)

2. Surface description

2.1 Land cover (natural vegetation/crops)

Land cover type(vegetation/crop/etc) in pixel area	Herbaceous tree (Euphorbia)
Percent Cover (%)	45 (30% green part)
Average vegetation height (m)	>10
Vegetation roughness(m)	
Overall vegetation/crop type &^ status within 200 m radius, North	Euphorbia and Shrubs
East	Grasses and herbs
South	Euphorbia and shrubs
West	Euphorbia and shrubs

2.2 Soil surface

Bareness (%)	55
Roughness (plough ridges, cloddiness, etc)	
Graveliness/stoniness (%)	15 (1 cm-12 inches diam gravels and rock fragments)
Crusting	
Surface soil color	Dry 2.5Y 4/2 Moist 2.5Y 3/1
Surface soil texture	

Remarks

- Comandite rocks are common

2.3 Land degradation features

LD type	water erosion, wind erosion, sealing and crusting, mass movements, subsoil compaction, sodification, salinization	
LD sub-type	Sheet erosion, rill erosion, gully erosion, piping erosion, slumping, mudflows, deflation, abrasion, deposition, etc	
LD intensity class	Slight, moderate, high, very high	
% LD occurrence in pixel/map unit		
LD severity class		
	Depth of topsoil removal (cm)	Penetration resistance (kg/cm2)
1	40	3.0
2	40	3.5
3	45	3.5
4		3.4
5		>4.5
6		4.0
7		2.5
8		3.0
Mean		
Remarks		

Description of rills

Width (cm)	Depth (cm)	Length (cm)	Shape

Description of gullies

Width (m)	Depth (m)	Length (m)	Shape

Sketch

Soil depth (cm)	Color	pH	Texture	Plasticity	Stickiness
Ac	2.5Y 4/2	5.5	Slightly gravelly sandy clay loam	Slightly plastic	Non-sticky
B	2.5Y 5/4	5.0	Slightly gravelly sandy clay loam	Slightly plastic	Non-sticky
BC	2.5Y 6/4	7.5	Gravelly sandy loam	Non-plastic	Non-sticky
B					

LAND COVER/SURFACE DESCRIPTION FORM
Training Samples for Land Degradation Mapping

1. General

Observation ID	023A
Date	October 2, 2001
Authors	J. Torrion
Location	Inundated area (near Moindabe primary school)
GPS Code	181
Latitude (X)	191006
Longitude (Y)	9910057
Elevation	2013
Slope (%), form & length	3 (very gentle)

2. Surface description

2.1 Land cover (natural vegetation/crops)

Land cover type(vegetation/crop/etc) in pixel area	Grasses and castro oil
Percent Cover (%)	55
Average vegetation height (m)	
Vegetation roughness(m)	Castro oil (1.5 m)
Overall vegetation/crop type &^ status within 200 m radius, North	Corn field
East	Fallow
South	Corn field
West	Fallow

2.2 Soil surface

Bareness (%)	45
Roughness (plough ridges, cloddiness, etc)	
Graveliness/stoniness (%)	5 (transported, 1 cm diam)
Crusting	Evident
Surface soil color	Dry 2.5Y 5/4 Moist 2.5Y 3/3
Surface soil texture	sand

Remarks

- Inundated area starting from el niño of 1998
- Previously utilized for corn
- Fallow; no season of planting
- Previous yield was 40 sacks/quartet of an acre, presently not even a sack

2.3 Land degradation features

LD type	water erosion, wind erosion, sealing and crusting, mass movements, subsoil compaction, sodification, salinization	
LD sub-type	Sheet erosion, rill erosion, gully erosion, piping erosion, slumping, mudflows, deflation, abrasion, deposition, etc	
LD intensity class	Slight, moderate, high, very high	
% LD occurrence in pixel/map unit		
LD severity class		
	Depth of topsoil removal (cm)	Penetration resistance (kg/cm2)
1		3.5
2		3.5
3		1.5
4		2.5
5		1.2
6		3.5
7		2.5
8		1.5
Mean		2.5
Remarks		

Description of rills

Width (cm)	Depth (cm)	Length (cm)	Shape

Description of gullies

Width (m)	Depth (m)	Length (m)	Shape

Sketch

Soil depth (cm)	Color	pH	Texture	Plasticity	Stickiness
0-70	2.5Y 3/3	7.0	Sand	Non-plastic	Non-plastic
70+	2.5Y 3/3	7.0	Sandy loam	Slightly plastic	Slightly plastic

LAND COVER/SURFACE DESCRIPTION FORM
Training Samples for Land Degradation Mapping

1. General

Observation ID	024
Date	October 3, 2001
Authors	J. Torrion
Location	Footslope(entrance to Ndabibi plain)
GPS Code	183
Latitude (X)	193660
Longitude (Y)	9916659
Elevation	1957
Slope (%), form & length	13 (straight)

2. Surface description

2.1 Land cover (natural vegetation/crops)

Land cover type(vegetation/crop/etc) in pixel area	Leleshwa and other shrubs (solanaceous shrubs)
Percent Cover (%)	10
Average vegetation height (m)	0.80
Vegetation roughness(m)	
Overall vegetation/crop type &^ status within 200 m radius, North	Grasses, herbs and solanaceae
East	Leleshwa and other shrubs (solanaceous shrubs)
South	Euphorbia, Leleshwa, herbs and shrubs
West	Leleshwa and other shrubs (solanaceous shrubs)

2.2 Soil surface

Bareness (%)	90
Roughness (plough ridges, cloddiness, etc)	
Graveliness/stoniness (%)	10(1cm diam. Pumice)
Crusting	
Surface soil color	Dry Moist
Surface soil texture	

Remarks

2.3 Land degradation features

LD type	water erosion, wind erosion, sealing and crusting, mass movements, subsoil compaction, sodification, salinization	
LD sub-type	Sheet erosion, rill erosion, gully erosion, piping erosion, slumping, mudflows, deflation, abrasion, deposition, etc	
LD intensity class	Slight, moderate, high, very high	
% LD occurrence in pixel/map unit		
LD severity class		
	Depth of topsoil removal (cm)	Penetration resistance (kg/cm2)
1		
2		
3		
4		
5		
6		
7		
8		
Mean		
Remarks		

Description of rills

Width (cm)	Depth (cm)	Length (cm)	Shape

Description of gullies

Width (m)	Depth (m)	Length (m)	Shape

Sketch

LAND COVER/SURFACE DESCRIPTION FORM
Training Samples for Land Degradation Mapping

1. General

Observation ID	025
Date	October 3, 2001
Authors	J. Torrion
Location	Hillslope of volcanic cone (Ndabibi)
GPS Code	184
Latitude (X)	193612
Longitude (Y)	9916633
Elevation	1972
Slope (%), form & length	5 (straight)

2. Surface description

2.1 Land cover (natural vegetation/crops)

Land cover type(vegetation/crop/etc) in pixel area	Euphorbia, Leleshwa and other shrubs and herbs
Percent Cover (%)	15
Average vegetation height (m)	>5 m Euphorbia 3 m Leleshwa
Vegetation roughness(m)	
Overall vegetation/crop type &^ status within 200 m radius, North	Grassland
East	Euphorbia
South	Euphorbia
West	Euphorbia, Leleshwa and other shrubs

2.2 Soil surface

Bareness (%)	>80
Roughness (plough ridges, cloddiness, etc)	
Graveliness/stoniness (%)	60 (1 cm diam.)
Crusting	
Surface soil color	Dry 10YR 4/3 Moist 10YR 3/2
Surface soil texture	Loamy sand

Remarks

2.3 Land degradation features

LD type	water erosion, wind erosion, sealing and crusting, mass movements, subsoil compaction, sodification, salinization	
LD sub-type	Sheet erosion, rill erosion, gully erosion, piping erosion, slumping, mudflows, deflation, abrasion, deposition, etc	
LD intensity class	Slight, moderate, high, very high	
% LD occurrence in pixel/map unit		
LD severity class		
	Depth of topsoil removal (cm)	Penetration resistance (kg/cm2)
1	29	
2	20	
3	23	
4	22	
5	25	
6	27	
7	28	
8	18	
Mean	24	
Remarks		

Description of rills

Width (cm)	Depth (cm)	Length (cm)	Shape

Description of gullies

Width (m)	Depth (m)	Length (m)	Shape

Sketch

Soil depth (cm)	Color	pH	Texture	Plasticity	Stickiness
0-30	10YR 4/3	6.5	Loamy sand	Non-plastic	Non-sticky
30+	10YR 5/3	6.5	Gravelly loamy sand	Non-plastic	Non-sticky

LAND COVER/SURFACE DESCRIPTION FORM
Training Samples for Land Degradation Mapping

1. General

Observation ID	026
Date	October 3, 2001
Authors	J. Torrion
Location	Foot of naibor adjick plateau
GPS Code	186
Latitude (X)	188849
Longitude (Y)	9914165
Elevation	2006
Slope (%), form & length	7 (complex, gentle)

2. Surface description

2.1 Land cover (natural vegetation/crops)

Land cover type(vegetation/crop/etc) in pixel area	Over-grazed, very low grasses with white flowers
Percent Cover (%)	15
Average vegetation height (m)	0.30
Vegetation roughness(m)	
Overall vegetation/crop type &^ status within 200 m radius, North	Grasses and shrubs
East	Over-grazed, very low grasses
South	Over-grazed, very low grasses
West	Over-grazed, very low grasses

2.2 Soil surface

Bareness (%)	>80
Roughness (plough ridges, cloddiness, etc)	
Graveliness/stoniness (%)	
Crusting	
Surface soil color	Dry 10YR 4/3 Moist 10YR 2/2
Surface soil texture	Sandy clay loam
Remarks	

2.3 Land degradation features

LD type	water erosion, wind erosion, sealing and crusting, mass movements, subsoil compaction, sodification, salinization	
LD sub-type	Sheet erosion, rill erosion, gully erosion, piping erosion, slumping, mudflows, deflation, abrasion, deposition, etc	
LD intensity class	Slight, moderate, high, very high	
% LD occurrence in pixel/map unit		
LD severity class		
	Depth of topsoil removal (cm)	Penetration resistance (kg/cm2)
1	5	2.5
2	4	3.0
3	3	2.0
4	10	1.5
5	5	2.0
6	6	3.0
7	4	2.5
8	4	2.2
Mean	5	2.3
Remarks		

Description of rills

Width (cm)	Depth (cm)	Length (cm)	Shape

Description of gullies

Width (m)	Depth (m)	Length (m)	Shape

Sketch

Soil depth (cm)	Color	pH	Texture	Plasticity	Stickiness
0-40	10YR 4/3	5.0	Sandy clay loam	Plastic	Slightly sticky
40-80	10YR 5/4	6.5	Sandy clay loam	Plastic	Slightly sticky
80+	10YR 5/4	8.0	Sandy clay loam	Plastic	Slightly sticky